Asynchronous Techniques for New Generation Variation-Tolerant FPGA

Hock Soon Low

A Thesis Submitted for the Degree of Doctor of Philosophy

at Newcastle University

School of Electrical and Electronic Engineering

Faculty of Science, Agriculture & Engineering

October 2015

Abstract

This thesis presents a practical scenario for asynchronous logic implementation that would benefit the modern Field-Programmable Gate Arrays (FPGAs) technology in improving reliability. A method based on Asynchronously-Assisted Logic (AAL) blocks is proposed here in order to provide the right degree of variation tolerance, preserve as much of the traditional FPGAs structure as possible, and make use of asynchrony only when necessary or beneficial for functionality. The newly proposed AAL introduces extra underlying hard-blocks that support asynchronous interaction only when needed and at minimum overhead. This has the potential to avoid the obstacles to the progress of asynchronous designs, particularly in terms of area and power overheads. The proposed approach provides a solution that is complementary to existing variation tolerance techniques such as the late-binding technique, but improves the reliability of the system as well as reducing the design's margin headroom when implemented on programmable logic devices (PLDs) or FPGAs. The proposed method suggests the deployment of configurable AAL blocks to reinforce only the variation-critical paths (VCPs) with the help of variation maps, rather than re-mapping and re-routing. The layout level results for this method's worst case increase in the CLB's overall size only of 6.3%. The proposed strategy retains the structure of the global interconnect resources that occupy the lion's share of the modern FPGA's soft fabric, and yet permits the dual-rail

completion-detection (DR-CD) protocol without the need to globally double the interconnect resources. Simulation results of global and interconnect voltage variations demonstrate the robustness of the method.

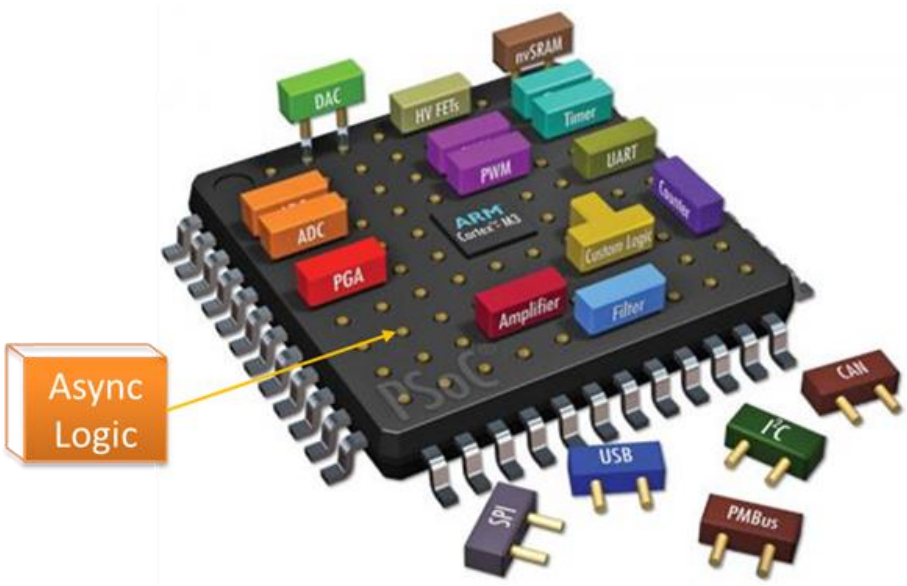

Acknowledgements

First of all, I would like express my profound thanks for my supervisors Prof Alex Yakovlev for his support through the course of my studies. His wisdom and vision were invaluable source of inspiration for me.

I would also like to express my gratitude to Dr Delong Shang and Dr Fei Xia for their guidance and advice throughout my PhD.

I am also grateful to colleagues and friends in the Microelectronics System Design research group at Newcastle University for their assistance and inspiring working atmosphere. Dr Danil Sokolov, Dr XueFu Zhang, Dr Maxim Rykunov, Dr James Docherty, Dr Graeme Coapes, Dr Nizar Dahir and Dr Ra'ed Aldujaily and Dr Ghaith Tarawneh. They made my PhD journey more enjoyable.

Finally, I wish to thanks my family for their love and unwavering support through the duration of my studies.

CONTENTS

FIGURES

TABLES

1 Introduction

1.1 Motivation and Objective

The effects of variability have become increasingly significant as a result of the scaling of technology. Static and dynamic variations affect the reliability of integrated circuits. Conservative approaches to increases the timing-margin/guard-band across the whole chip is imprudent and degrades performance. Figure 1 shows that excessive design margins to guarantee correct circuit operation over fix periods for both spatial and temporal variations are wasteful and reduced the circuit's efficiency in a synchronous system [1, 2]. (Note: the scale of the margins in Figure 1 and Figure 2 are for illustration only and may not scale accordingly).

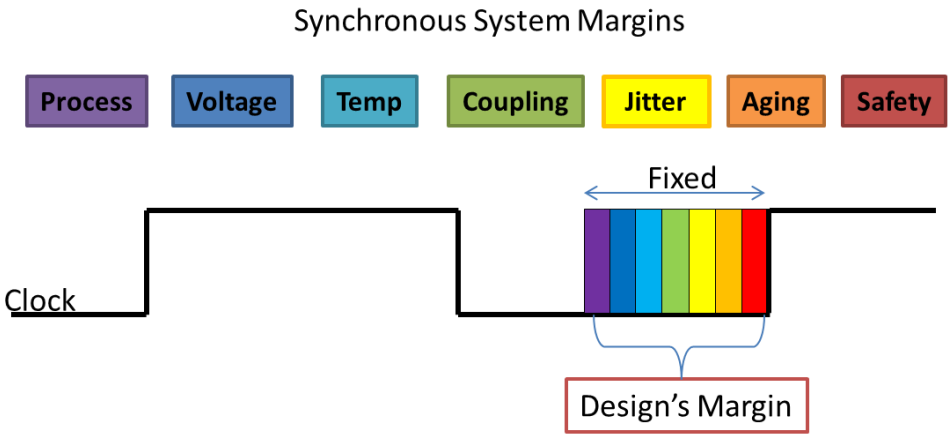

Figure 1: Design margin barriers to efficiency.

FPGAs may be more affected compared to Application-specific integrated circuit (ASIC) because the circuit mapping and critical path vary depending on

user design in post-fabrication [3]. Therefore various traditional variation tolerance techniques proposed for ASICs may not be directly applicable. Yet, due to its configurability, the FPGA presents a unique opportunity to address variability and reliability challenges [4, 5].

Asynchronous designs are highly tolerant to voltage and delay changes, and have been shown to be very robust in the present of variations [6, 7]. This also gives the potential for efficiency improvements in the margin headroom as shown in Figure 2. Therefore, applying asynchronous logic to FPGAs is an attractive idea.

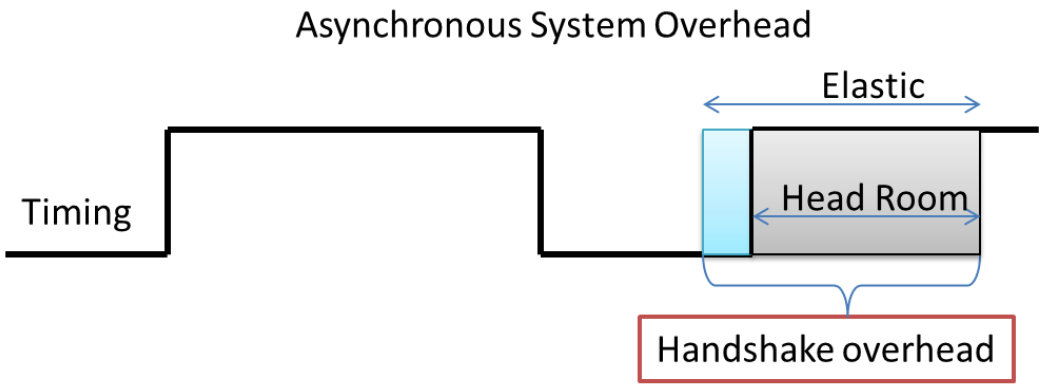

Figure 2: Asynchronous handshaking overhead and elastic margin's headroom.

However, there are three major challenges in applying asynchrony in balancing between the handshaking overhead and level of tolerances, as illustrated in Figure 2 . These challenges are as follows:

i. Asynchronous circuits are more difficult to design and test compare to synchronous ones because of the wide variety of possible signalling

protocols and a broad spectrum of the degree of delay insensitivity from bounded-delay to fully delay insensitive (DI). Partly because of this, asynchronous designs suffer from a lack of automatic design tools, especially those combining all possible techniques in a single suite. These issues have impeded the progress of asynchronous techniques in the FPGA, because the latter is intrinsically less customizable.

ii. Asynchronous circuit is normally higher in area and power overheads due to the extra circuitry needed for handshaking. This depends on the delay assumption made or the protocols used. For example, converting all of the communication to dual-rail will double the interconnect resources. This is not acceptable, since interconnects occupy the lion's share of the fabric.

iii. Depending on the timing assumptions made or handshaking protocols used, asynchronous logic can provide a range of improvements in power and speed/throughput efficiency in addition to its robustness toward variability. For instance, a single-rail delay-matching (SR-DM) protocol is more efficient in terms of power and area but more susceptible to variation compared to the 4-phase dual-rail (4P-DR) scheme which is more robust to variation but may require higher power and area as shown in theoretical graph in Figure 3 – relative cost of elasticity and handshaking protocols. Similar project of cost of elasticity using different asynchronous tools also presented in [8].

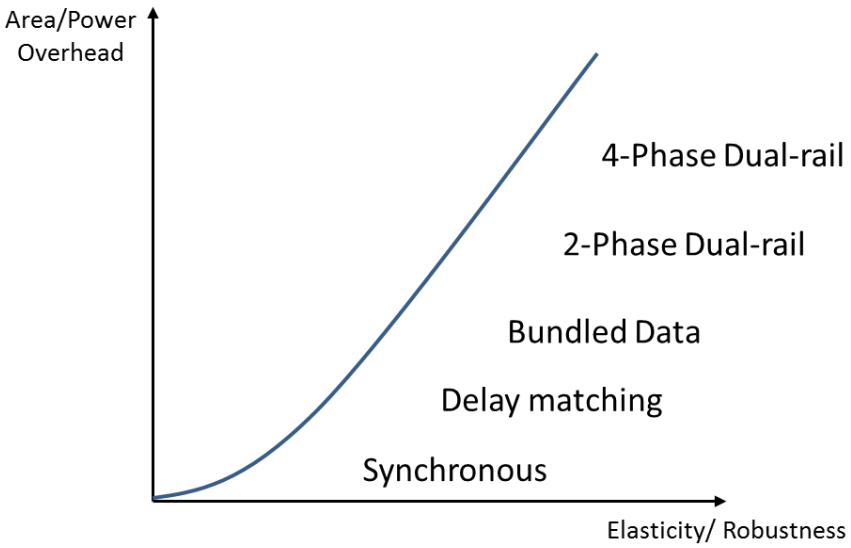

Figure 3: Theoretical graph of relative cost of elasticity and handshaking protocols.

Therefore the objective of this thesis is centred on strategies which can maximise the variation tolerance benefit and keep the overhead at a balance. The challenges mentioned above are addressed using the following approaches:

i. A wrapper-based asynchronous logic approach to communication and the preservation of the LUT-based computation block of modern FPGA architecture. This allows the re-use of the major part of the design tool flow, particularly the logic packing and mapping. It seeks to achieve *delay insensitive (DI)* in the large for long inter-cluster wires and *speed independence (SI)* in the small within clusters.

ii. Characterising the performance of the most popularly used handshaking protocols that are tailored for reconfigurable logics. The power, throughput, area and robustness are determined of protocols

such as 4-phase dual-rail (4P-DR), 2-phase dual-rail (2P-DR), and bundled-data (BD).

iii. A strategy to balance the use of asynchrony to tolerate the effects of variations and the minimization of the area and power overheads.

1.2 Overview of Chapters

Chapter 2 gives an introduction to the development of programmable logic devices (PLDs) and their evolution into today's modern FPGA architectures. The continued scaling of CMOS technology enables the development of many advanced technologies. However the associated challenges include increasing variability problems in the manufacturing process as well as the effects of degradation effects over time. The second part of the chapter classifies the sources of variability and reviews its impact on FPGA structure as well existing techniques which attempt to reduce the impact.

Chapter 3 presents a literature review of the use of asynchronous approaches. The fundamental theory and terminology of asynchronous design are also briefly introduced here to serve as a basis for further understanding of the following chapters.

Chapter 4 describes the distributed control architecture which retains the computational block of the traditional FPGA un-touched (single-rail) and proposes the asynchronous wrapper and David's cell control around it. The

result achieves a balance between the desire to use asynchrony for tolerate the effects of variations and retention of the major part of the current design flow.

Chapter 5 presents new concepts for addressing the overhead challenges with an on-demand strategy. This approach suggests the deployment of asynchronous logic only on variation-critical paths (VCPs) by leveraging the mature techniques in obtaining variation maps. The proposed integration of asynchronously assisted logic (AAL) with state of the art FPGA architecture involves a minimal increase in overhead. Furthermore, the AAL supports the use of multi-style asynchronous logic implementation to allow the exploration of asynchrony at different levels of variation.

Chapter 6 summarises the techniques presented and describes the outlook for future developments.

1.3 Contributions

- Classification of sources of the variability and its impact on FPGA architecture (chapter 2)
- Survey of asynchronous reconfiguration architectures based on the protocols and delay assumption used (Chapter 3)
- A detailed circuit realization at components level for the asynchronous wrapper using the distributed control approach for asynchronous components (Chapter 4)

- The proposal of a novel AAL architecture that applied Asynchrony only on the VCPs for the balancing of resource overhead and variation tolerance (Chapter 5)
- Summaries the work and proposed techniques for advancement. (Chapter 6)

1.4 Publications

The following papers have been published during the course of this work:

H. S. Low, D. Shang, F. Xia, and A. Yakovlev, "Variation tolerant asynchronous FPGA", poster presented at the 19th ACM/SIGDA International Symposium on Field-Programmable Gate Arrays (FPGA 2011) conference, Monterey, California, pp 282, 2011.

H. S. Low, D. Shang, F. Xia, and A. Yakovlev, "Variation tolerant AFPGA architecture", presented at the *17th IEEE International Symposium Asynchronous Circuits and Systems (ASYNC 2011)*, Ithaca, NY, pp 77–86, 2011.

X. Zhang, D. Shang, F. Xia, H. S. Low, and A. Yakovlev, "A hybrid power delivery method for asynchronous loads in energy harvesting systems", in *IEEE 10th International New Circuits and Systems (NEWCAS 2012) conference*, Montreal, Canada, pp 413-416, 2012.

H. S. Low, D. Shang, F. Xia, and A. Yakovlev, "Asynchronously Assisted FPGA for Variability", poster presented at the *Field Programmable Logic and Applications (FPL 2014)* conference, Munich, Germany, 2014.

Chapter 2. Background

2.1 Introduction

Field-programmable Gate Arrays (FPGAs) have become a popular technology for implementing digital electronic systems today due to their re-configurability nature and short design cycle. Continued technology scaling enables more and more features to be implemented in a same size form-factor. However, similar to other VLSI design, many new challenges emerged due to the continued scaling of CMOS process technology. Variability and reliability have become growing issues in the nanometre scale region.

In order to understand the impact of variation on FPGA architecture, this chapter first provides an overview of FPGA technology and its development in recent years. Variation can be from many sources due to imperfection of manufacturing process, environmental changes or ageing effect resulting in correlated and random behaviour. This chapter also serves to clarify the terms by classification of the variability sources and technique commonly used to characterise them. On-chip, off-chip and soft-sensing classification techniques will be reviewed.

With the understanding of the variability through the characterisation techniques available from industry as well as academic research, improvements of performance and yield can be achieved through variation aware techniques that are unique for reconfigurable architectures such as

FPGA. The remainder of the chapter is structured into the following subsections:

i. Introduction to FPGA Technology

ii. Classification of Variability Sources

iii. Sensing and Characterisation Techniques

iv. Variation-tolerant and Yield Improvement Techniques

2.2 Introduction to FPGA Technology

The FPGA is a hardware programmable device whose function can be defined after fabrication. The concept of the reconfigurable logic device was introduced in the electronic system design market in 1980s. The reason for the initial development of reconfigurable devices was mainly to ease the challenges faced by the traditional board-level design with standard components that increased in number with circuit complexity and size. The amount of components and layers of printed circuit boards (PCBs) grew drastically and thus the chance interconnection errors occurring increased together with the pressure on create a small form factor to fit the components into the enclosure.

Fuelled by the fast-moving market and evolving standards and rising of mask development costs in the manufacturing applications-specific integrated circuits (ASIC), the concept of the programmable logic device (PLD) that would

allow its functionality to be restructured was born and has served the basis for more advance in PLDs.

The programmable logic array (PLA) was one of the earliest types of PLD. Figure 4 (a) shows a typical structure of a PLA consisting of a matrix of programmable AND-gates and OR-gates in a plane used to implement the minimised standard forms of Boolean expressions, which are sum-of-products functions.

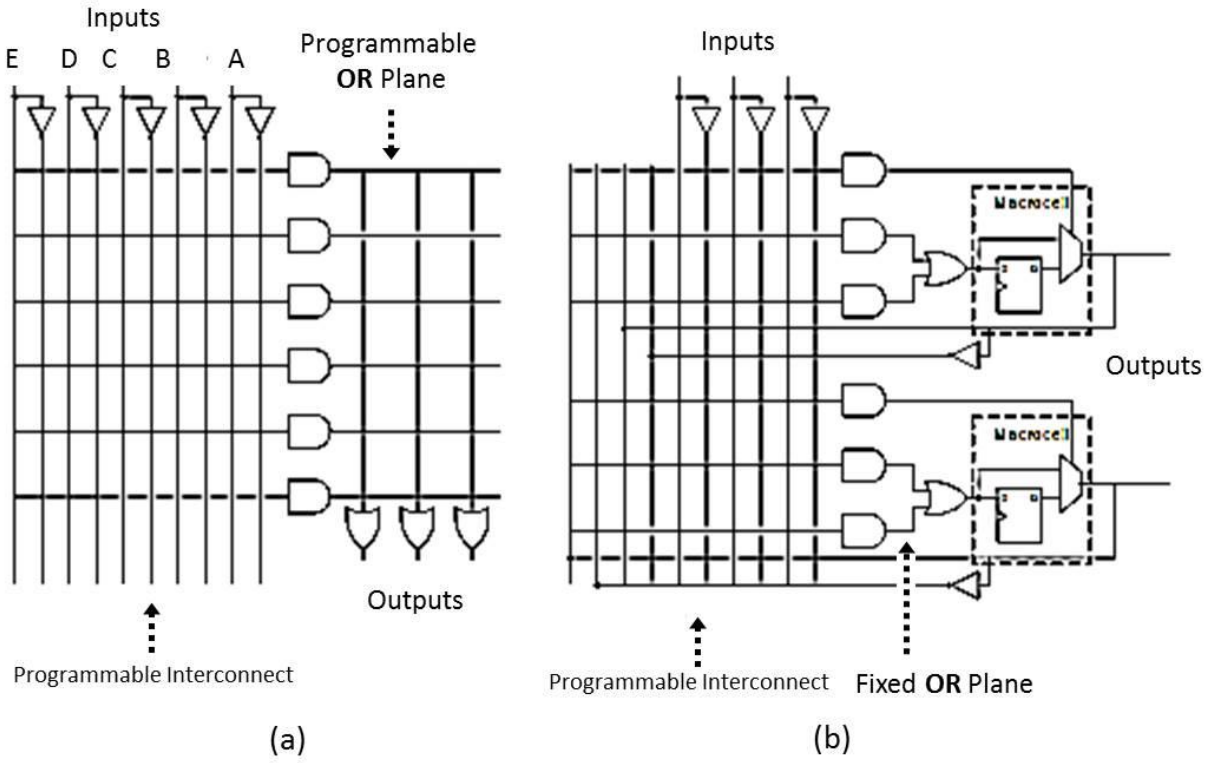

Figure 4: (a) PLA with programmable OR plane; (b) PAL with fixed OR plane [9].

With the realization that even with a fixed OR plane, the system would still be sufficient for logic implementation as a PLA, interconnect optimised programmable array logic (PAL) structures were introduced in 1978 [10], trademarked by Monolithic Memories, Inc. (MMI). As illustrated in Figure 4 (b), the architecture was evolved with the removal of the programmable OR-plane and the introduction of new macro-cells that contained registers and multiplier for optional combinational or sequential logic implementation. The concept of the PAL was then extended to offer more complex logic functionality, and was later succeeded in the market by a new family called complex PLDs (CPLDs).

Although the level of logic complexity has increased, yet the main market for CPLDs was still not able to go far beyond a glue-logic within large systems. FPGA architecture based on the Look-Up Table (LUT) then emerged, which offered more features rich solutions.

2.2.1 Moore's Law and Configuration Cells

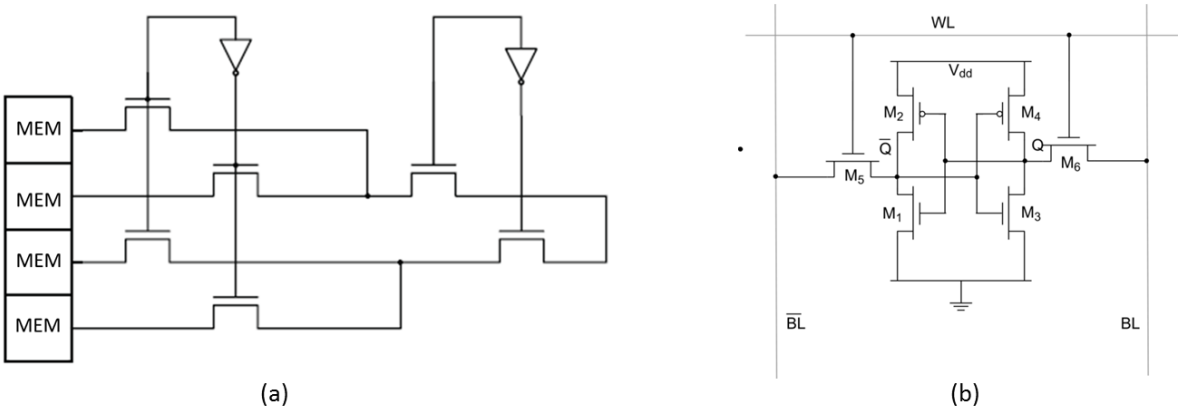

Figure 5: (a) Look-Up Table (LUT) Structure, (b) 6-Transistors SRAM Cell.

Gordon Moore, co-founder of Intel, forecast in his 1965 paper, "Cramming more components onto integrated circuits" [11] that the cost of transistors in a silicon chip would continue to fall with every advance of technology every two years or so, and later the prediction turned into a self-fulfilling prophecy. The doubling of numbers of transistors every 18 months following Moore's Law has stimulated drastic growth in the electronics industry. The doubling of transistor number at a rapid rate has also meant reductions in the cost per transistor with every new generation of smaller transistors. This benefited the advances in FPGA technology in the market in the mid-1980s. This is because the LUT-based FPGA, as in Figure 5 (a), used static-random-access-memory (SRAM) as the basis of the architecture and the typical SRAM circuit requires six transistors, as shown in Figure 5 (b), which means the configuration memory cell comes with a high overhead. However, with the growth indicated by Moore's Law, up to this point this has led the industry to exploit transistors

which are almost free, especially in programmable hardware devices. This validated the area and cost overhead issue on SRAM-based FPGA.

2.2.2 Programmable Memory

Programmable memory or the configuration cells are the underlying technology for hardware configurability. Earlier PLD devices used programmable read-only memory (PROM) where the programming could only be done once and was irreversible; namely the on-time-programmable (OTP) memory. Anti-fuse memory type, which is one, is more beneficial in terms of lower area, resistance and capacitance compared to others. Because it is a non-volatile memory, this means that the system can work instantly at power-up in contrast to SRAM. In addition, the prime advantage of the anti-fuse PLD and the FPGA are their susceptibility to faults in environment with heightened radiation. In particular, the Actel/Microsemi [12] PLDs dominated the military and aerospace markets for over fifteen years [13]. However, the main disadvantage of anti-fuse FPGAs is that it requires specialised manufacturing and programming mechanism. This make it not in-system programmable as opposed to SRAM, which can fit well within the standard CMOS manufacturing process, the anti-fuse technology cannot scale and advance at the same rate as CMOS devices, making it far behind the process geometry in many generation in comparison.

An alternative Non-volatile memory that supports multiple re-write cycles and is convenient for in-system programming is the EEPROM (electrically erasable programmable read-only-memory) or flash memory. Technically this is a type of EEPROM but offers higher speed when writing large amounts of data compared to non-flash EEPROM memory. In addition, flash memory also offers fast read access times similar to DRAM (dynamic RAM) but slower than SRAM. The key advantages of flash based FPGA over SRAM are its low power requirement, non-volatility and it is also more secure and reliable for IP (intellectual property) protection purposes from a security standpoint as no extra external configuration memory required upon start since SRAM is volatile and cannot hold the data at power lost. However, the disadvantages of flash memory are its limited write cycle and the fact that specific manufacturing processes are used which differ from standard CMOS technology.

SRAM is the most popular type of memory used in today's FPGAs for two primary reasons. First, it offers the unlimited in-system programming and second the standard CMOS process technology is used and therefore, it benefits from the advances of the latest scaling of CMOS technology. However, continuous technology scaling may also have adverse impacts, which are discuss later in this chapter.

Unlike flash-based non-volatile devices, the volatile SRAM-based FPGA cannot hold its configuration without power source. Therefore, a dedicated

programming circuity and sequence is needed to load the configuration bits at every system power-up. This also means that SRAM-based FPGA has a lead-time at power-up before live operation and requires extra board-level non-volatile components, which increase the overall cost. Since the configuration data are stored externally, this also opens up the potential for IP protection issues, although alternative encryption solutions may eliminate this. A summary and comparison of these three main types of memory are show in Table 1.

Table 1: Key configurable cells technology comparison[9].

Memory Type / Features	Anti-fuse	Flash	SRAM
Non-Volatile	Yes	Yes	No
Reconfigurable Cycle	one-time	Limited	Unlimited
Area (element size)	Low	Moderate	High
In-System programing	No	Yes	Yes
Manufacturing Process	Anti-fuse custom	Flash process	Standard CMOS
Speed	Fast read, slow write	Fast read, slow rewrite	Fast

2.2.3 Modern FPGA Fabric

The tradition basic FPGA architecture consisting only of reconfigurable logic, an interconnect block and the input/output (I/O) pad is call *s*oft fabric. Today's state-of-the-art PFGAs are packed with over a million LUTs. Also more and

more hard blocks have been included in the package to improve computation performance, including the digital-signal-processing (DSP) block, distributed memory, high-speed communication links, and an advanced clock management system together with mixed signal analogue functionality. This has made the architecture increasingly heterogeneous as illustrated in Figure 6. In hybrid structures, combinations of hard and soft microprocessor cores are also included. With the advances in FPGA technology, the use of mature intellectual property (IP) and computer-added-design tools (CAD) have also facilitated the emergence of user customisable system-on-chip (SoC) FPGAs that provide significant benefits for embedded system implementation.

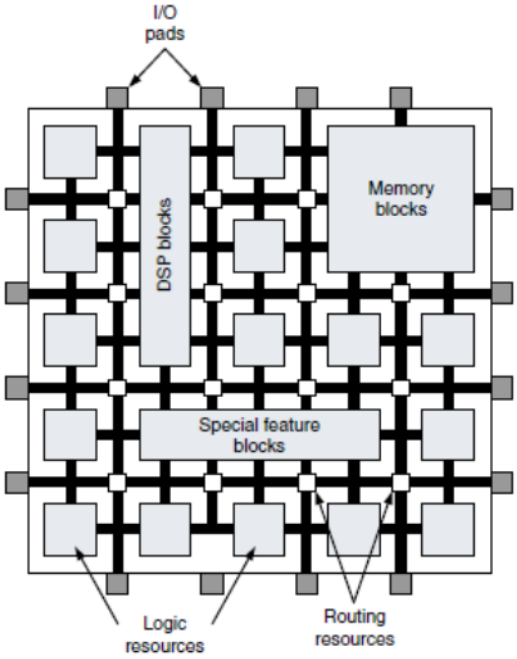

Figure 6: Modern FPGA fabric with Hard-block

2.2.4 Software and Hardware Programmable Devices:

Compared to general-purpose microcontrollers and microprocessors (μPs), FPGA-based circuit implementation is typically much faster. This is because in the FPGA, It is not necessary for the controller to move the data around between the data memory and working register in order to perform logic operations or in the context terms, the sequential fetch-decode-execute loop of soft-computation. The classic examples of software-programmable architectures are Von Neumann and Harvard processors. Instead, the underlying computation in FPGA is hardware-based. All of the possible combinations of output from a set of inputs is pre-calculated with Boolean algebra expression in a truth table and Karnaugh map and stored in the LUTs. The arrival of inputs will essentially become the address pointer to the specific

memory location of the LUT; therefore, complex and multiple iteration computations can be avoided and results can be obtained almost instantly. Similar techniques have also been used in microcontrollers to achieve the fast computation of complex calculations by using the "not-to-compute-all" technique or, in other words prefetching or pre-calculating and storing all possible results on LUTs[14]. This technique is very effective and commonly used in embedded system design to decrease computation time. In the FPGA, LUT techniques are exploited intensively across the whole architecture.

2.2.5 Difference between the FPGA and ASIC

The application-specific integrated circuit (ASIC) is a general term for fully customised designs. The main benefit of a device that is fully custom-designed is its smaller form factor from its manufacturing specifications and lower cost for high volume production. Whereas the FPGA is a hardware programmable device that its functionality can be configure by the end user after fabrication, which explains the term "field-programmable". The key advantages of the FPGA over ASIC are the low non-recurring engineering cost, which support rapid prototyping and fast-time-to-market. However, the disadvantage is that the FPGA may not be suitable for most electronic system design specifications because FPGAs are used for general purposes and therefore the logic density of the chip is multiple folds below that of the ASIC design. This translates into higher power consumption, higher cost and slower speed performance compared to equivalent systems implemented with ASIC. However, due to the

advancement of CMOS processes and the introduction of more "hardened" blocks such as multipliers and accumulators, the performance gap between FPGAs and ASICs is gradually becoming smaller [15, 16].

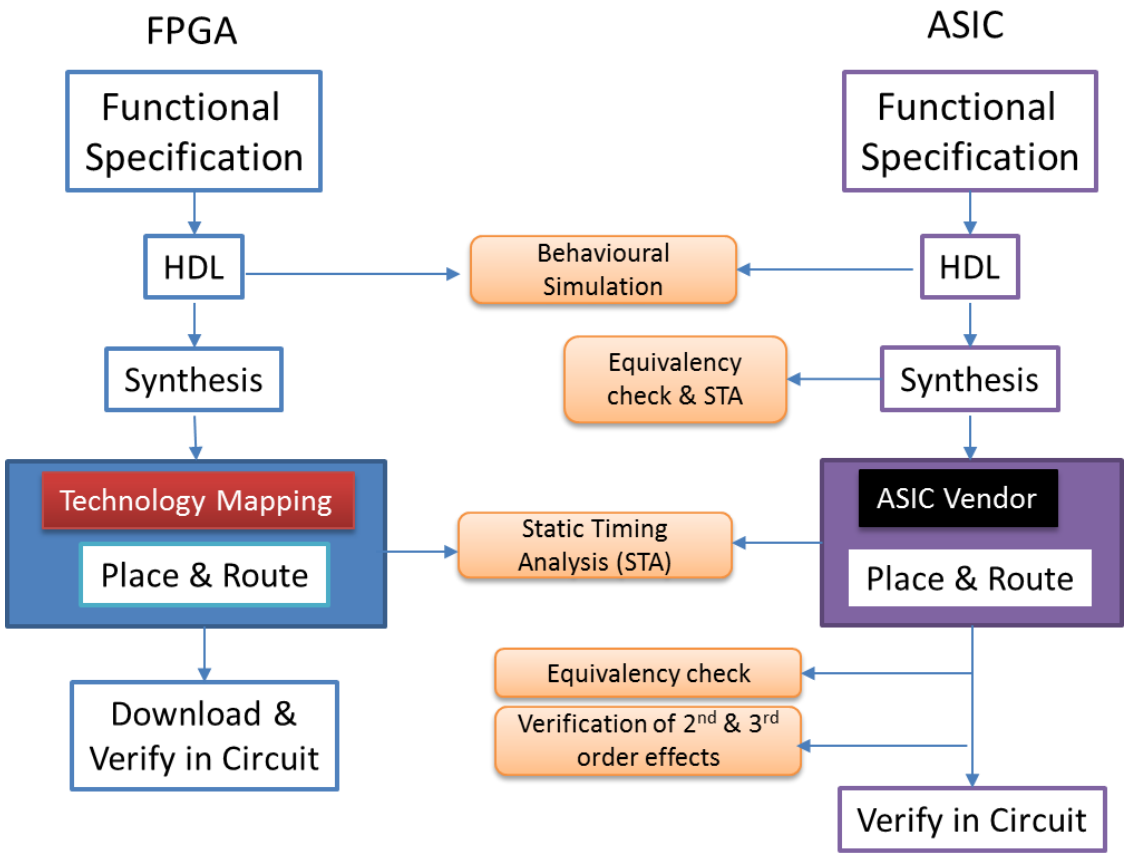

Figure 7: Basic FPGA and ASIC design flow[17].

The design of ASICs and FPGAs, however, shares a very similar tools flow. This is especially true for the upper part of the design flow, from functional specification normally in HDL (hardware description language) to logic synthesis and optimisation and later placement and routing. The difference in placing and routing at this point between the two flows is that the logic has to be packed and clustered into a fixed prefabricated structure on the FPGA and

the routing resources to join them together, whereas the placement and routing on the ASIC are free. These similarities between the two flows are shown in Figure 7. Thus, historically, a main application of the FPGA was primarily used for ASIC prototyping or function verification before committing costly manufacturing processes. Due to the levelling of performance, competitive cost and 'harden core' enhancement, FPGAs now move beyond their historical use and are becoming the core technology platform for applications such as high speed signal processing, industrial control, communication network data network switching and high frequency financial trading and computation accelerators.

2.2.6 Summary of Evolution

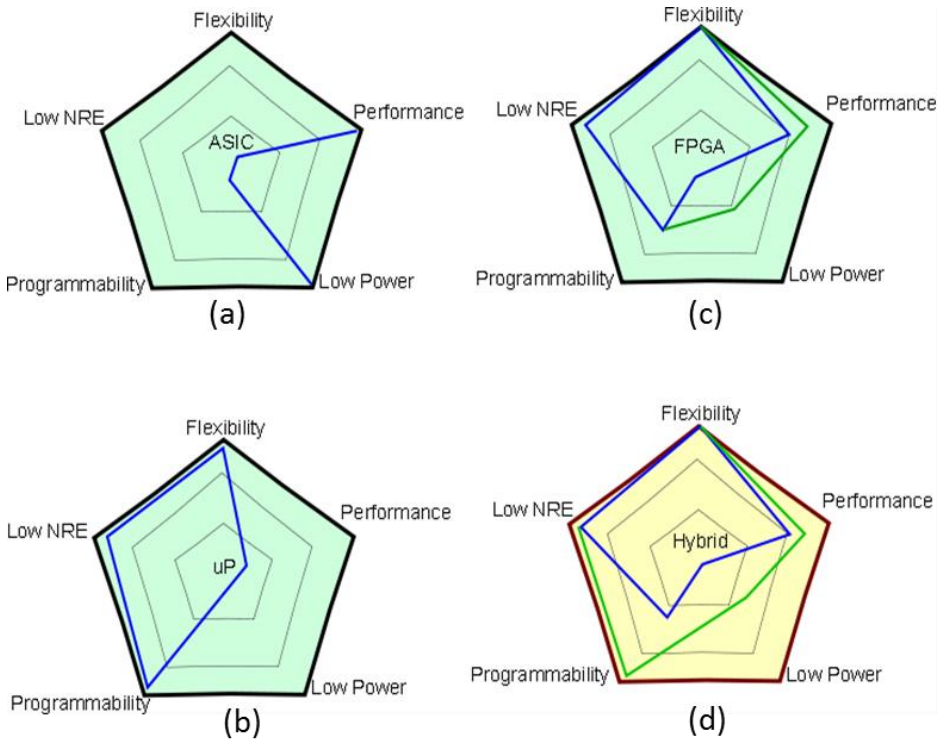

Figure 8: Key technology comparison vectors.

This section summaries the different between FPGA and two other key technologies for electronic system design, the microprocessor (μP) and ASIC. In Figure 8 (a), the main drives for the ASIC approach are mainly toward ultimate higher speed and lower power performance. However, the NRE costs for custom design, layout, fabrication and packaging are high. The mask for the silicon process is itself extremely expensive with a limited lifespan. However, in mass production runs this is still more cost-effective. From the reconfigurable software perspective, the standard processor architecture is more flexible in term of hardware configuration (such as I/O pin configuration), low non-recursive engineering costs and firmware programmability. However,

the downsides are that it is high in operating system overheads and compiler inefficiency, and there may also be a performance reduction due to the indirect relationship between the hardware and the software on the processor [18], as shown in Figure 8 (b).

Programmable devices or the FPGA architecture fit in between the other two design approaches and offer the greatest hardware configuration flexibility and higher performance compared to general processor approaches as well as lower NRE costs compared to the ASIC. In recent and past decade, advances in research and on the FPGA has been largely focused on improving the speed performance and optimising power consumption, as illustrated in the green line in Figure 8 (c). Given the benefit for both application-specificity and flexibility in a larger system, modern FPGAs are now also blending more and more application-specific hard-blocks with their traditional soft-fabric forming new hybrid architectures. The motivation for and benefit from the hybrid structures are also illustrated in the green line in the yellow pentagon at the bottom left of Figure 8 (d).

2.2.7 Fundamental Structure of the FPGA

This section explains the underlying building block of the FPGA soft-fabric architecture and the terms associates with it from the most basic primary elements to the hierarchy which is build up.

2.2.8 Logic Block

The basic building block in a FPGA comprises a lookup-table (LUT), a register (DFF) and a multiplexer (MUX), as shown in Figure 10(c). It is normally called a logic cell (LC) in Xilinx, while the equivalent from Altera is called the logic element (LE). For ease of explanation, Xilinx's terms will mainly be used in this thesis. Figure 9 demonstrates the primary concept of a simple logic implementation on a FPGA. This example demonstrates the implementation of basic logic circuit of a single bit adder in Figure 9 (a). The truth-table is first derived (Figure 9 (b)), this process is normally supported using a synthesis CAD tools. The synthesis processes basically computes each value of the logical expression of the circuit according to their functional arguments. In this example, the expression of sum = A + B+ C = 0x69 is stored in the k-input size lookup-table or K-LUT as shown in Figure 9 (c). The memory size of the LUT is defined as 2^k bits or 8 in this case for K = 3. Although the 4-LUT was once the more common structure, traditionally introduced because of area efficiency, it should be noted that modern FPGA structures are already built-in with 5 to 7 LUTs for better speed performance.

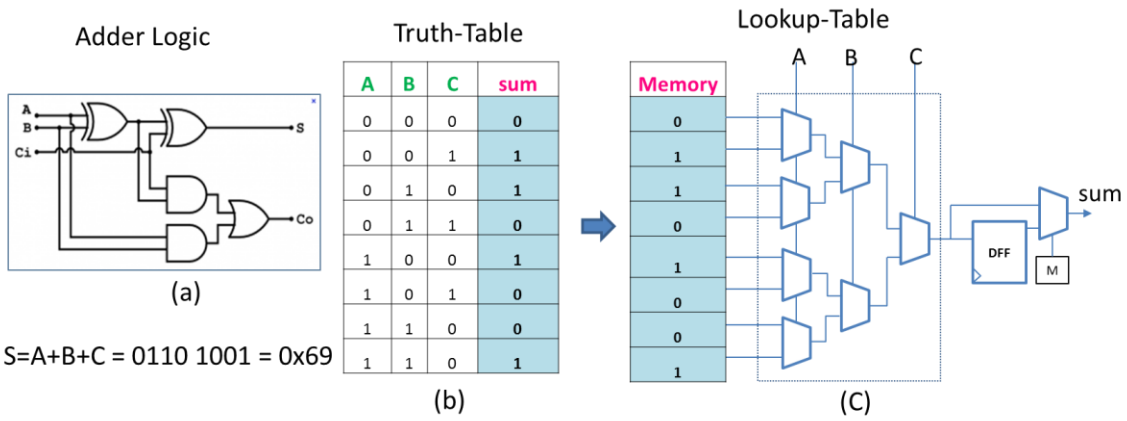

Figure 9: Basic logic implementation on the primary logic cell: (a) logic diagram of a 1-bit adder; (b) truth-table for SUM; (c) logic mapping on a lookup-table (LUT).

Figure 10 (a) shows a basic view of island-style FGA architecture. The cluster is the next level in the hierarchy of this architecture, consisting of a group of primary logic cells (LCs). In Altera, the terminology used is the logic array block (LAB); whereas deviating from Altera, Xilinx has another layer of hierarchy, a group of LCs called the SLICE and the two SLICEs constitute a Configurable Logic Block (CLB). The main idea for grouping LCs within a CLB is to avoid long global interconnects.

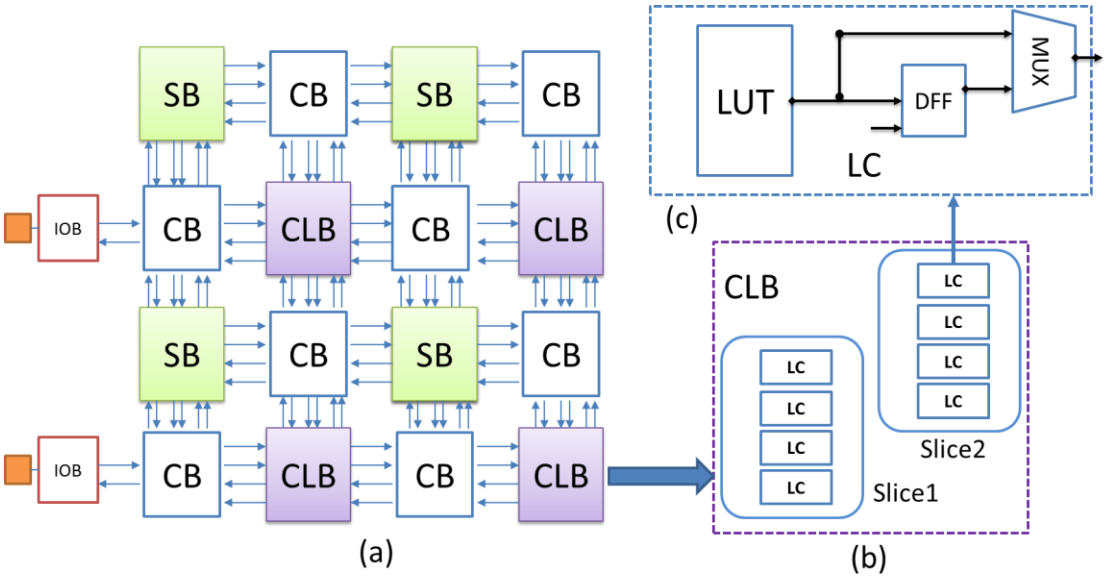

Figure 10: Hierarchy view of FPGA structure: (a) Island style structure, (b) Two slices in a CLB, (c) Basic LC structure.

2.2.9 Routing Structure

Surrounding the CLBs in the island style structure are the routing resources. The connection block (CB) links the inputs and outputs of CLBs with programmable switches. The interconnect grids are made of prefabricated wiring segments, and at each vertical and horizontal interaction of the wiring segments is a switching block (SB). The SB also consists of a set of switches that allows the possible routing of signals to the next intended CLB destination. For clarity of explanation, a simplified CB and SB block connected with only a few switches are shown in Figure 11.

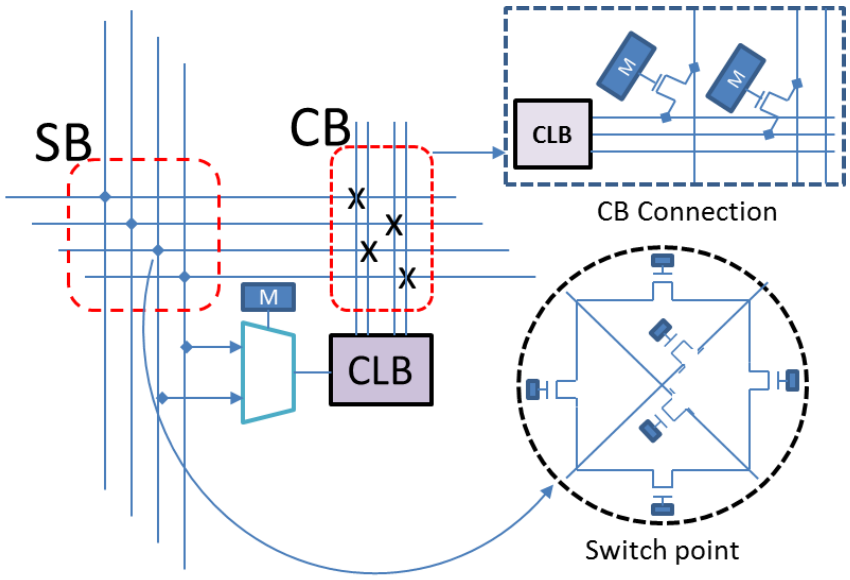

Figure 11: Routing resources structure.

2.3 Introduction to Variation

Variations have become more dominant with the continued scaling of the CMOS process. The complexity has increased, resulting in higher fabrication costs to achieve uniformity in die production. This limitation can result in random and spatially varying deviations from intended design parameters, and affecting speed, power and reliability. Conservative approaches to increase the operating timing margin across the whole chip to reduce the impact of parametric yield are imprudent and reduce performance, especially when the consideration is based on worst-case scenarios.

In addition to the physical parameter variation, dynamic environmental sources of variation such as temperature, or supply voltage changes during operation require engineers to employ more aggressive techniques. Similar to

all other CMOS devices, FPGAs are no exception. In fact, the impact of variation could be more severe compared to ASICs, because the circuit mapping and critical path routing processes may result in any combination of worst and best case variability path or regions. This section provides a general description of sources of variation and discusses its impact on FPGA technology. Finally published variation tolerance techniques are reviewed.

2.4 Classification of Variability

Sources of variation can be classified into two main categories. First, the imperfection during manufacturing and second operational environmental changes, degradation over time due to ageing and wear-out can all be broadly categorised as either spatial or temporal variations [19]. Figure 12 clarifies the classification of variation based mainly on timeline since the devices was manufactured. For spatial variation, the time assumption is constant (t=0s), and the changes of devices in the characteristics over time are therefore considered temporal (t = t').

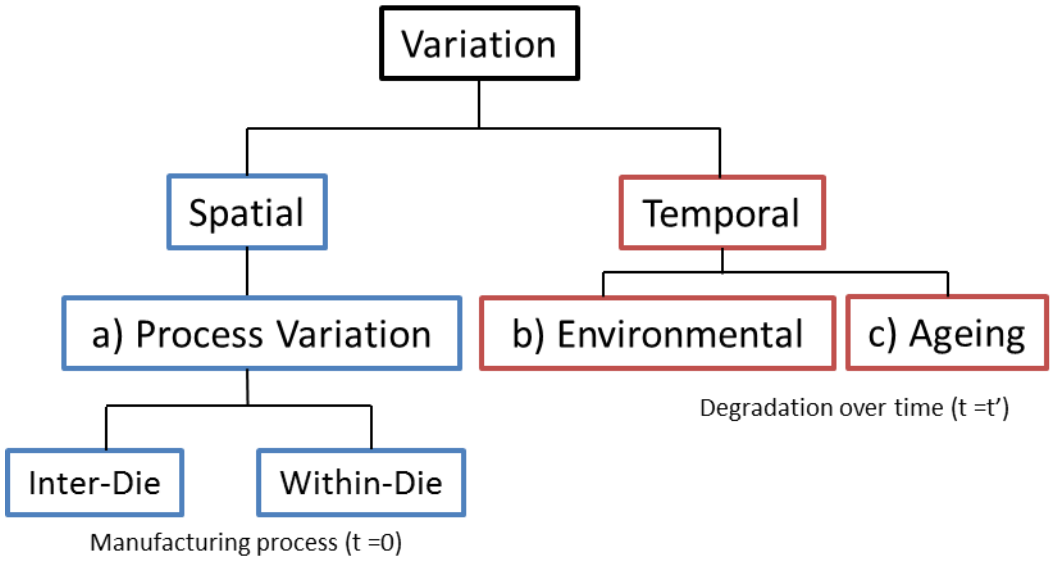

Figure 12: Spatial and temporal variation classification.

a) Process variation or the spatial variation mainly involves imperfection during the manufacturing process resulting in parametric deviation of transistor value between different die (inter-die) as well as variation within a same die (within-die/ Intra-die). Inter-die variation is a systematic type of variation which generally shows spatial correlation behaviour and normally results from varying MOS transistor dimensions in length or width (L/W), oxide thickness (TOX), and flat-band condition [20] whereas line-edge-roughness (LER) or random-dopant fluctuations (RDFs) cause within-die variation with stochastic characteristic [21].

b) Temporal variation, on another hand is due to changes in the characteristics of a device over its lifetime. Temporal variations can also be divided into two main branches, which are environmental and ageing,

where voltage and temperature variations can be classified as environmental.

c) Negative and positive bias-temperature instability (NBTI & PBTI), hot-carried-injection (HCI), time dependent dielectric breakdown (TDDB), and electromigration all fall into the Ageing category [22, 23].

2.5 Process Variation Sources

Figure 13 gives a summary of the key factors in process variations, which can be either systematic or statistical. Systematic variations are caused by imperfection in the mask and optical tooling mechanism and result in repetitive offset from chip-to-chip. Systematic variability is deterministic, and therefore can be estimated and improved using specific design techniques; however intrinsic variations are statistical and thus the impact cannot be reduced through improvements in the manufacturing process [24]. The following briefly explains and classifies them into two main categories of tooling-related and intrinsic variation.

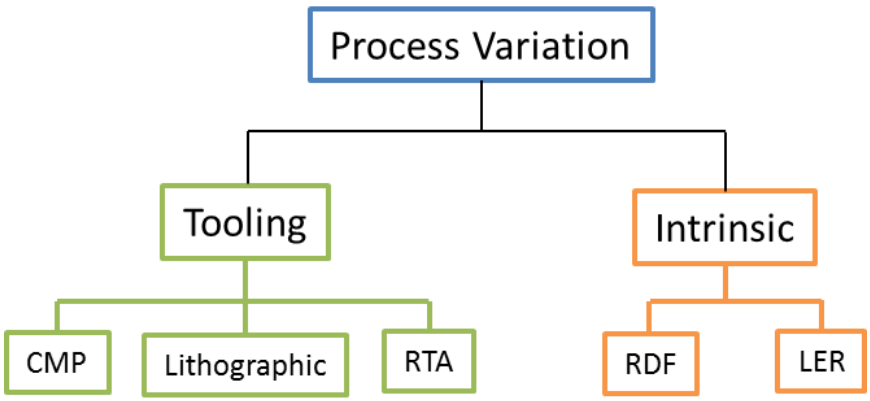

Figure 13: Subdivisions of process variation.

2.5.1 Tool-Related Variation

Optical lithography has been effectively used in fabrication for over thirty years. Due to technology scaling, optical lithographic are now in the subwavelength region where the feature sizes of the devices or transistors are now below the wavelength (λ) of light. For example, the value of λ has remained at 193nm from 130nm to more recent 65-nm transistors [25]. Therefore, it has become extremely difficult to print the wafer exactly as intended on the layout [22]. Chemical mechanical polishing (CMP) is used for planarizing the metal interconnect layer between adjacent metal layers due to copper damascene process. Variations in interconnect thickness at post-CMP affect resistance and capacitance and result in variations in the delay in interconnects that may cause non-deterministic circuit behaviour both chip-to-chip and within a chip. In addition to CMP, rapid thermal annealing (RTA) and the stress liner effect from the fabrication process also induce variations in length and width parameters on the device [26].

2.5.2 Intrinsic Variation

Beyond variations due to imperfect fabrication tools, some sources of variation are intrinsic to the technology involved. Two key sources of variation that are truly random in nature are random dopant fluctuation (RDF) and line-edge roughness (LER). RDF is variation resulting from variability in the concentration of the implanted impurity. RDF affects the transistor's channel region and alters its properties, particularly the device's voltage threshold. The impurity of atoms in modern process technology has a significant affect since the total number of dopants is decreasing drastically. Because of the limitations of lithography and etching tools, the resulting effect is line-edge roughness (LER). The impact of LER is less prominent for technology nodes above 90nm. However, in sub-50nm node, LER can critically affect the voltage threshold, since the ratio of roughness of the edges is becomes closer to the width of the transistor at the range of 5-10nm as illustrated in Figure 14.

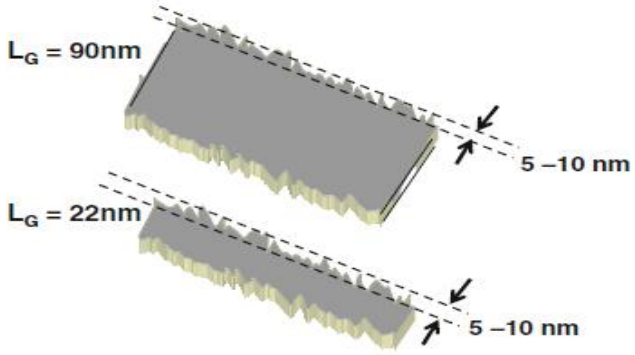

Figure 14: Line edge roughness at 90nm and 22nm technology [23].

2.6 Environmental Variation

Temperature and supply voltage variations are categorised as environmental. The performance of devices is strongly dictated by these conditions.

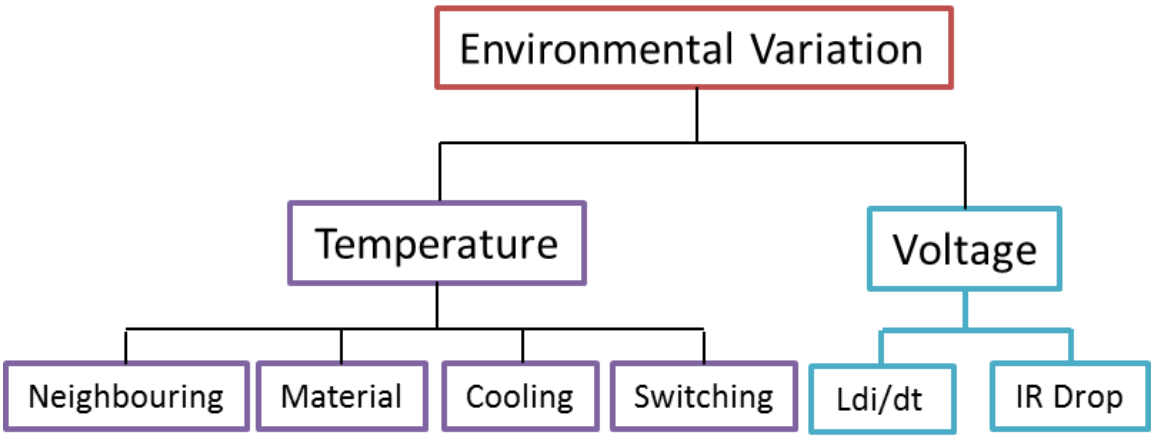

Figure 15: Classification of sources of environmental variation.

2.6.1 Temperature Variation

Several factors in addition to the ambient temperature affect the rise and dissipation of temperature within a chip. Regions of the chip with high activity and power consumption are normally associated with rises in temperature, or

so called hot spots. This increase of heat in a localised area creates temperature variation across a chip. Time constants for temperature variation are normally in the range of milliseconds to seconds. Circuit normally decrease in speed with a rise of temperature due to reduced carrier mobility and increased interconnect resistance. Therefore keeping the temperature within a chip well regulated is necessary to maintain the performance of the circuits. Delays normally increase with increases in temperature. Towards lower geometries below 65nm and beyond at lower threshold voltage, the temperature variation has shown contrarian effects on cell delay [27]. Figure 16 show the characteristic of a typical circuit at nominal voltage, Vdd = 1.2V where the circuit gradually slows down with increasing temperature. However, at a level of Vdd below the nominal value, from 0.9V and 0.8V, the circuit exhibits the reverse characteristic [28]. Therefore, extra-care has to be taken, especially in the extent of sub-threshold to reduce operation power and strategy for energy efficiency improvement with DVFS.

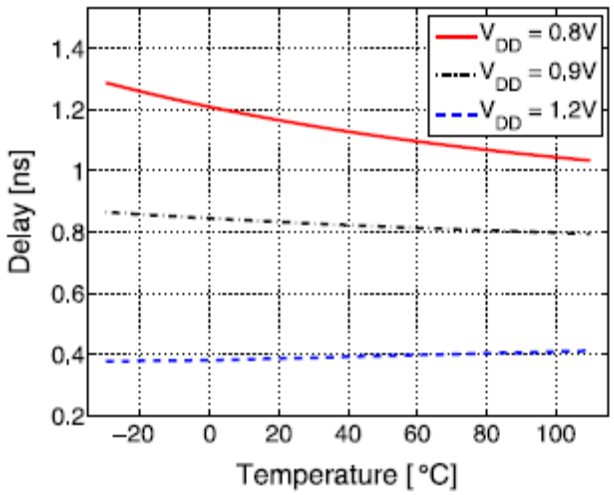

Figure 16: Inverse path delay characteristics at lower voltage level with increase in temperature [29].

Several factors that affect the temperature variation are listed as follow[23]:

- Neighbouring blocks power characteristic of the circuit switching activities and capacitive load around the location or within the same region will affect power consumption and heat generation.

- The thermal conductivity of material is closely related to power density. Heat generated in bulk CMOS device is dissipated through both the silicon substrate and the interconnecting wires. In SOIC (silicon-insulator) technology, however, heat dissipation occurs mainly along the wires and results in rapid heat increases in regions that consume a lot of energy. This disparity results in greater temperature gradients between hot and cold regions within a chip.

- Cooling efficiency of the packing or heat sink helps to improve the thermal profile. However, this issue exacerbated in the 3D (three-dimensional) stacking technology where circuits are sandwiched together. This means that it becomes more challenging to dissipate heat.

- Switching activity or the workload running on the system in a location or core can drastically increase the temperature in a specific region especially over a long period. In modern multi-core processor system or reconfigurable systems such as the FPGA, the workload may be distributed or inter-swap over time. This is however largely depending on the ability of the underlying support resources of the architecture for dynamic or partially dynamic reconfiguration. The strategy of periodically relocating the workload to different regions or cores will vary the thermal profile over time.

2.6.2 Supply Voltage Variation

Supply voltage variations mainly result from voltage drop across resistive interconnect (IR-drop) and inductive (or di/dt) noise. The power distribution grid within a chip come with its inheriting parasitic resistance, and when a steady state current flows through, this cause IR-drop which can be derived from the basic Ohm's Law as $\Delta V_{IR} = R_{grid} * i(t)$. Meanwhile, fluctuations of

voltage due to the parasitic inductance, commonly referred to as the di/dt noise, ($\Delta V_{\frac{di}{dt}} = L_{parasitic} * \frac{di}{dt}$**).** These rapidly changing power noise effects normally have time constants in the range from nanoseconds to microseconds [29]. In summary, the characteristics of the circuit depend significantly on the operating voltage level. A drop of supply voltage affects both the grain and gate bias and the impact is reduced in a flow of current. One profound impact of this on circuit operation is that it does not just increase the delay in the critical path, but may make those near-critical paths that have not been optimised become critical.

Energy harvesting system that tends to provide variable power levels can also be considered as environmental variation. With the expansion of wireless sensor networks and looking toward to the wider scope of the Internet-of-Things (IoT), it is becoming more important to prolong and support existing battery-powered system [7, 30]. In certain applications, energy harvesters have completely replaced traditional batteries. Examples of commercial applications are the battery-less (infrared remote control) and (wireless wall switch) [31]. Energy harvester devices tend to provide dynamic power, and voltage levels may vary at run-time. The strategy to allow circuit working in wider operating range is therefore intentional [32-34]. The rationale for this kind of circuit is that energy should be used while it is abundant, which means that circuit can run at their optimum speeds. This is because the process of energy conversion and storing incurs extra circuit complexity that reduces its efficiency. The

benefits of this kind of system able to operate under a wide range of operational voltage levels is maintaining circuit functional or at least part of the core features at a reduces rate while energy is scare and low [35-38].

2.7 Temporal Variation – Ageing Related

While environmental temporal variation such as changes in temperature and voltage add to the circuit marginalities, ageing-related temporal variation affects circuit performance gradually over a period. Key mechanisms contributing to such effects are TBBD, HCI and BTI [23], as shown in Figure 17.

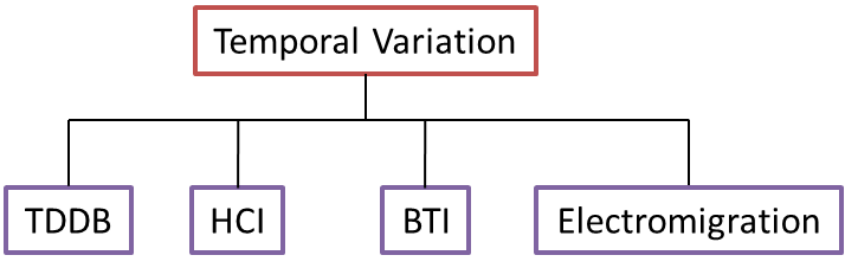

Figure 17: Ageing related temporal variation.

- Time-dependent dielectric breakdown (TDDB): The creation and joining of defects in the gate dielectric, causing gate dielectric breakdown.
- Hot carrier injection (HCI): Defects in the gate stack caused by highly energized carriers under large lateral (drain-to-source) electric fields cause shifts in the threshold voltage.

- Bias-temperature instability (BTI): The Capturing of holes (electrons) from the inverted channel in PFETs and NFETs by broken Si–H bonds, such as charge-trapping sites in high-K gate dielectrics (HfO2).

- Electromigration: is the transport of material caused by the gradual movement of the ions in a conductor due to the momentum transfer between conducting electrons and diffusing metal atoms.

2.8 Sensing and Characterisation

Sensing circuits play an important role in understanding and characterising the variability profiles of a particular batch or individual chip. The primary function of sensing circuits is twofold. First, to quantify between the deviated characteristic of a device and its ideal intended behaviour. Secondly, the on-chip sensing circuits can be used for continued health monitoring to help provide adaptive refitting for environmental changes and temporal degradation. Less conservative guard banding can be achieved with the availability of characterisation information, which can mean timing yield improvements. Furthermore, with accurate sensing and characterisation, a detailed variation map can be generated. Utilising such information a controller can supplement the power of weakening regions and critical paths can be diverted. Therefore potential run-time malfunctions can be avoided. This section looks at several frequently used sensing and characterisation techniques that can be applied to ASIC and FPGA design.

2.8.1 Off-chip Sensing

Off-line sensing is a non-intrusive approach of characterisation without built-in sensors; external measurements equipment is used instead. The most straightforward characterisation technique traditionally used is to incorporate extra test pads for direct access of test probes that are able to inject stimulus signals containing multiple electrical parameters to the sections of the circuits [39]. Accurate current and voltage characteristics of the device can be obtained with this measure. However, such an approach is expensive with the number of test pads required especially with large circuit, the area overhead makes this not viable. Although, area optimisation techniques such as multiplexing the circuit in the array matrix format is possible [40], yet precision and complex analogue voltage-current measurement setup may still be needed. For modern multi millions gates FPGAs, this characterisation technique is almost impossible.

Optical imaging is another attractive non-invasive approach for chip variability characterisation without the need of embedded hard sensors. This technique is based on measurements of the deflective of the electromagnetic wave from the emitting source such as infrared to provide visual representation of the study. In [41], the optical imaging technique was successfully demonstrated to map systematic and random variability effect of microprocessor chip in 65nm technology. Static imaging camera was utilised in this approach to capture the light emission from off-state leakage current

(LEOSLC). The authors suggest the recorded data that can be easily correlated to produce variation map and be successfully adapted for the evaluation and enhancement of the fabrication process as well as to develop countermeasure for the possible reliability issues.

Thermal and power characterisation using infrared imaging technique applied on FPGA is recently presented in [42]. In this work, run-time thermal characterisation is performed by capturing the emissions from the back of the chip. The result is the visualisation of operational thermal gradient and hot spot for the particular application mapped on FPGAs. Again, these off-chip techniques are attractive but require complex measurement equipment and procedures. In addition, due to the data being gathered externally, this makes the variation map correlation process less straightforward.

2.8.2 On-chip Sensing

An alternative to the off-chip sensing are built-in hard sensors. The state of the art of multicore processors is normally equipped with multiple thermal sensors. Accurate sensing requires fine granularity of build-in sensors that is scattered across the chip and the question for the research has always been at what cost or overhead.

Sensing and characterisation based on Ring oscillator (RO) was presented in the past and recent years due to its simplicity in implementation either on-line or off-line [3, 43-49] . In [43], authors utilised the method to measure random

variations in MOSFET threshold voltages. Die-to-die variability measurements with ROs that is sensitive to parameter was proposed in [44]. In [46], authors proposed to create Path-based RO to measure and monitor the targeted critical path under process variation. RO was also presented as a temperature sensor as an alternative to analog sensing circuits. RO circuits may be convenient to deploy, yet this approach may increase the overall area of the circuit. In addition, the circuit itself is reactive to temperature and voltage fluctuation. The RO method unfortunately has also been remarked as a bad instrumentation technique for FPGA variability as it does not accurately represent the circuit path in FPGA designs. At high frequency oscillation, RO circuit itself generates heat, this consequently adds extra complexity and variability to the situation [50].

Increasing technology scaling in nanometer regions results in local random transistor parameter variations. The effects of such phenomena as random dopant fluctuations (RDF) and line edge roughness (LER) can dominate mismatch in neighbouring devices. Particularly in SRAM cells with high circuit density, mismatch can deteriorate the circuit functionality greatly. Current latch sense-amplifier (CLSA) for example in [51] is proposed to measure mismatch between two transistors. Since only a pair of transistors can be measured at any one time, this limits its usefulness. Extension from the basic mismatch sensor, array based characterisation is also presented in [52, 53]. Yet, the limitation of this method has been the low sensitivity due to device

properties changing linearly with voltage threshold variation when the device-under-test (DUT) is biased in the saturation region.

2.8.3 Soft Sensing in FPGA

Reconfigurable architectures such as FPGA give a unique opportunity for sensing and mitigating the effects of the variability using the generic built-in flexible resources rather the dedicated embedded sensing circuits. This is called "soft sensing" in this thesis. Modern FPGA architecture such as Altera's Stratix family and Xilinx's Virtex series are all equipped with a thermal sensor. However, a single sensor cannot sufficiently provide the temperature gradient of the chip. Never mind the ability to identify the maximum value or hot spots of the chip.

Ring oscillator (RO) is a commonly used technique due to its simplicity in implementation either on-line or off-line. Off-line RO is normally used for characterisation purposes such as variability of delay with the changes of temperatures [54]. Authors of [47, 54] proposed one of the earliest thermal soft sensing approach on reconfigurable computing architecture. Flexible RO-based thermal sensing replaced conventionally used analog sensor and its complex control circuit. Example of works in [3, 55] also used RO, instead of thermal, authors perform characterisation of FPGA process variation effect by measuring its component delay.

On the other hand, to continuously monitor the health and provide adaptations to temporal effects [45, 46, 56], on-line soft sensing techniques can be beneficial. In [57], thermal soft sensing technique is proposed. This approach utilise an adder-accumulator multiplier to make the computation without the need of RO. Wong et al. [58-60] proposed novel characterisation techniques that enables accurate combinatorial delay measurement. This differs from the previous mentioned methods that used RO for latency measurement [3]. This work performs characterisation by stepping the system frequency gradually for error detection.

Leveraging the unique reconfigure structure of FPGA, extra-embedded analogue sensors can be avoided for PVT (process, voltage and temperature) characterisation. And this forms sound of the foundations for the work presented in this thesis. Furthermore, due the final application to be implemented on the FPGA is not known until it is fabricated, it is hard to predict where and how sensors should be distributed across the chip evenly. Therefore, soft sensing grants additional advantages for monitoring circuits, particularly in the use of on-chip hot spot tracking.

2.9 Conventional Variation Tolerance in FPGAs

2.9.1 STA and SSTA

In Static Timing Analysis (STA), timing analysis is carried out in input independent manner, and purpose to determine the worst-case delay or critical

path of the circuit over all possible input combinations. Therefore, STA approach often gives pessimistic timing estimation. Hence, this reduces the speed performance that could otherwise be much faster. Extensions of the STA are corner analysis, where worst-case and best-case scenarios for PVT variation can be presented. The best cases are defined as fastest processes at highest voltage level operating at the lowest temperature, and the worst case will be the opposite with a slow process at the lowest voltage and highest temperature. Examples of the effect of PVT on path delay are shown in Figure 18

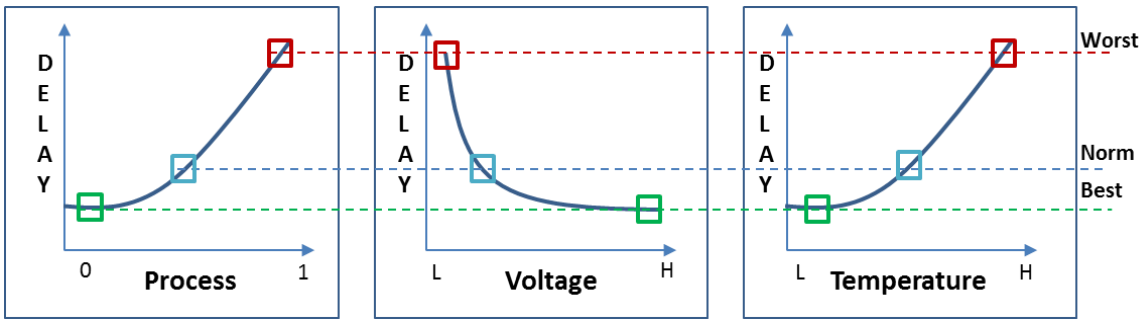

Figure 18: Corner analysis with STA tools

Despite the conservative timing estimation on the critical paths, STA is not able to accurately model intrinsic variability that is random and stochastic. Under random parametric fluctuations, the shorter paths or near-critical paths that have not been optimised have the tendency to become critical.

Statistical static timing analysis (SSTA) tools aim to identify these statistically critical paths and minimize the chances of these paths becoming critical. However, the drawbacks of SSTA tools include the uniform strategies used

across the whole chip and between different dies. Therefore, accurately modelling statistical variation from one die to another requires an accurate variation model value of mean (μ) and standard deviation (σ). Also it is becoming difficult to produce statistical models for the larger systems with high random variation that are expected in future node technology, making the characterisation cost un-scalable to deal with the complexity of a system with increasing numbers of statistically critical paths [61].

2.9.2 Optimisation of Structural Parameters

Structural parameter optimization is another proposed approach for mitigating FPGA variation, which focuses on traditional architectural parameters such as varying the value of N, the number of LUTs per CLB, and K, the number of inputs to a LUT [62]. However, study in [63] shows that varying the value of N and K value does not provide significant improvements over the variation concern [23].

2.9.3 Transistor Sizing

Transistor sizing can be used in ASICs to optimize path delay and power performance. However, the process of transistor sizing for its width and length (W/L) at layout level for FPGAs requires a huge effort and will consumes significant amount of engineering time. Research into automated transistor sizing on FPGAs for area and speed trade-off [64] is also promising in exploring the use transistor sizing to mitigate the effect of variability on FPGA

architecture. Yet, this technique is computational expansive and the variability-critical paths (VCPs) cannot easily predefined.

A recent project named the Programmable Analogue and Digital Array (PAnDA) architecture [24] represents a new approach to intrinsic variability, introducing reconfigurable transistor arrays at the analogue level. This approach allows low-level optimization during the post-fabrication stage and results in the recovery of the loss of performance yield introduced by stochastic variability. However, the extra configurability of the architecture also comes with a high area overhead.

2.9.4 Asynchronous Techniques

Asynchronous designs are highly adaptive to changes in voltage and delay, providing robustness depending on the delay assumptions that are made [65]. The most robust class is delay-insensitive (DI), where circuits will operate correctly without any assumption of delay in either gates or wires. Circuits with carefully identified delay assumptions on isochronic wire are called quasi-delay-insensitive (QDI) [66] or speed independent (SI) [67]. These circuits consider only the gate delay and neglect wire delay when ensuring circuit correctness.

There are many approaches or protocols for implementing asynchronous circuits. A taxonomy of potential protocol implementations is summarized in [65]. The choice of an asynchronous communication protocol affects the

characteristics of circuit in term of implementation power, area, throughput and robustness.

In the past decade, different asynchronous FPGA architectures have been presented motivated mainly by the pursuit of low power and/or high-speed performance. These architectures can be classified into two main styles. The first relies heavily on timing assumptions to guarantee the correctness of the logic, and the second alters the traditional architecture at fine-grained level with the intensive use of state-holding memory components (such as C-elements), which implies significant overheads in size and power [68, 69]. Details of asynchronous FPGA (AFPGA) designs are reviewed in Chapter 3.

2.10 Variation Aware and Late Binding Techniques

Process variation has become a hot issue with the continue technology scaling. The major challenges are to resolve reliability issues while maintaining yields. Unique functional configurability of FPGA provide extra-flexibility to mitigate problems such as variation aware techniques that leverage the knowledge of how each chip are affected by the variation. With the assumption of mature off-line and online sensing techniques, each chip can be characterised and treat differently using late binding techniques such as multiple-reconfiguration, region relocation, and path reconfiguration. Compare to conservative worst-case timing assumption approach the variation-aware approach are promising for better circuit performance.

2.10.1 Yield Improvement through Multiple-Configuration

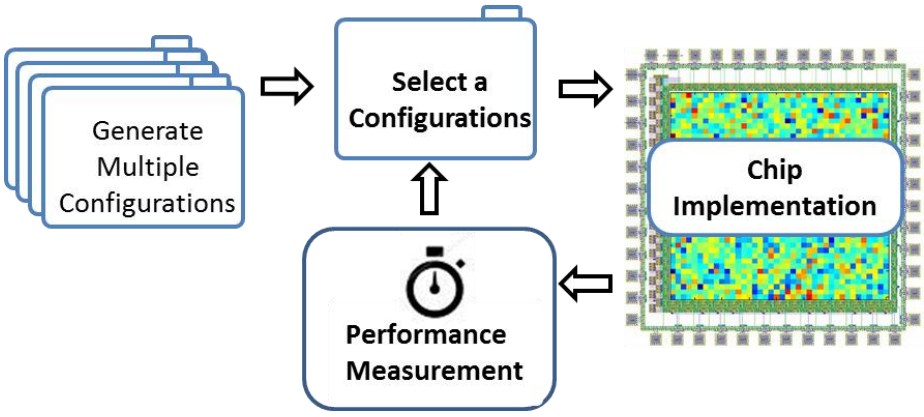

Figure 19: Multiple reconfiguration strategy flow.

Figure 19 shows technique for timing yield improvement through multiple reconfigurations. The placement and routing (P&R) of FPGA are flexible, therefore multiple configuration options for same functional results is possible. Supposed due to variability in delay, each bitstream generated from the P&R processes that have identical functional behaviour would have deviation in timing performance. Therefore, numbers of pre-generated bitstream can be exploited and test run at the configuration process for each chip until the best performance configured bitstream has been identified. Although this strategy may theoretically improve the speed and timing yield performance compare to the SSTA alone, yet it requires at-speed test for each configuration, which is a very timing consuming. Furthermore, the large number of configuration options means huge storage memory needed. This makes it not suitable for memory resources limited embedded platform. Detail descriptions of multiple reconfiguration strategy can be found in the work proposed by Sedcode et al. [70] and Matsumoto et al. [71].

2.10.2 Variation Aware Modelling

There have been several attempts at improving FPGA timing yield by providing statistical analysis and process variation modelling for variation aware placement and routing [70, 72-77] . Another example in [73] provides variation aware timing-driven algorithm to optimise timing statistically and maximize timing yield. Simulation result based on statistical enhance versatile place and route (VPR) tools [78] show 3.4x increase in yield with guard-banding and 25x with speed-binning using the variation aware placement techniques. However, the guard-banding and speed-binning techniques may not be sufficient with the presence of within-die variation. This is because the chip performance will be greatly degraded with the wide banding, removing the part of the incentive for technology scaling in the first place.

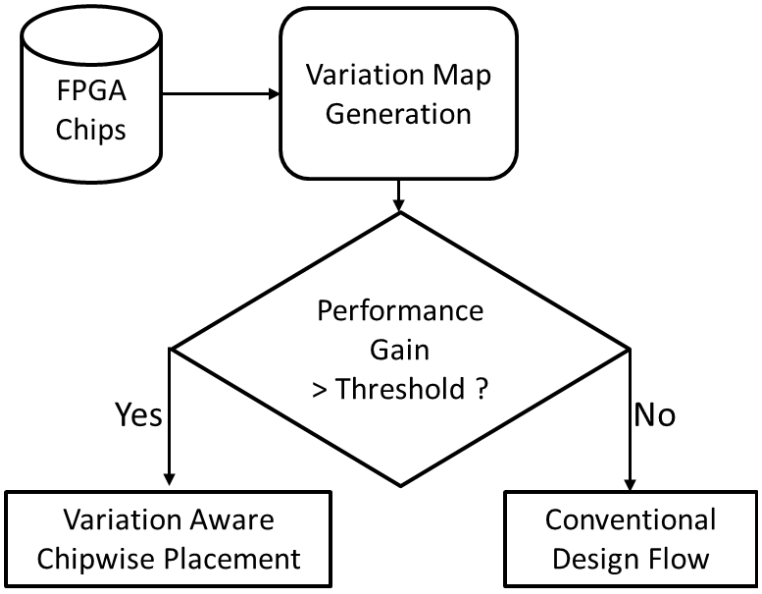

Figure 20: Variation aware chipwise placement design flow [72].

One of the earliest variation aware placement for FPGA is proposed by authors in [72], the design flow is shows as in Figure 20. The authors suggest with the help of the software model that have been developed within the VPR framework [78]. Worthwhileness of variation ware placement is first evaluated for performance gain can be expected. Simulation result shows up to 19.3% performance improvement can be achieved with chipwise placement. Part of this thesis is also based on the assumption that a variation map is obtainable.

In nanometer process technology, variation in FPGA has shown both correlated and random effects. Authors in [75] proposed an improvement model that consider both inter-die and intra-die variability including the delay variability in routing resources. The purposed model also enhanced with statistical timing analysis, supported by variability aware P&R based on VPR framework.

2.10.3 Relocation, Remapping and Rerouting

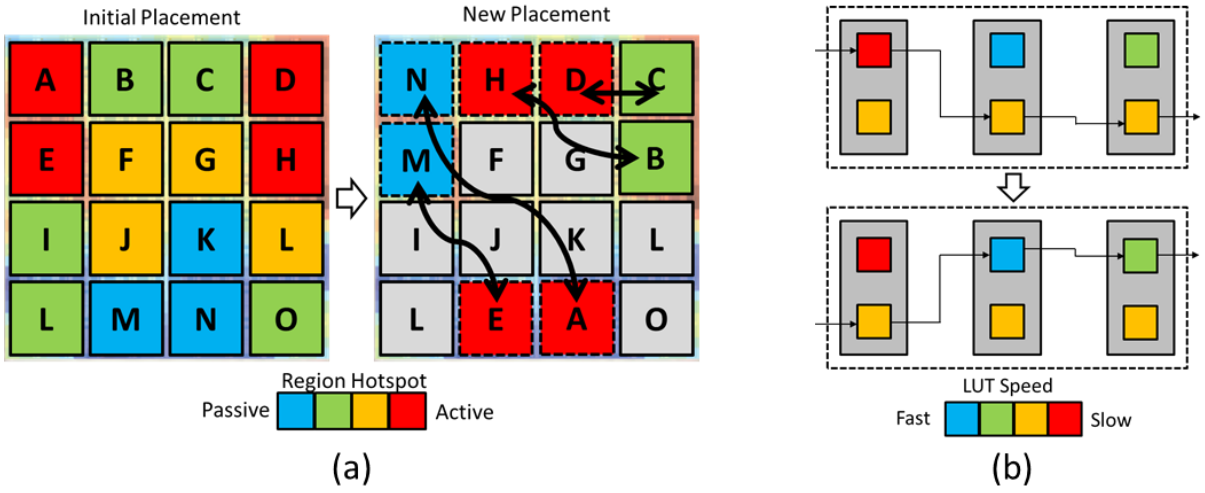

Figure 21: (a) Region relocation, (b) Path reconfiguration.

The idea of region relocation is similar to the strategy used in wear levelling for managing and prolonging the lifespan of traditional flash memory that have limited write cycles due to wear out. The wear levelling technique uses algorithms that track the frequency each location has been written and works to distribute data evenly across each memory block of the entire flash drive. This process decreases the total wear on the drive, thereby increasing the lifespan of the drive. A similar concept applies to the region relocation where the FPGA are partitioned into regions and circuit can be configured into the allocated regions. As a region with configuration ages, the circuits can be swapped to a region that has not been assigned before. This wear-levelling technique is particularly useful for the extending lifetime of the FPGA as well as improving its reliability [79].

Srinivasan et al. [80] suggest the relocation of circuit over time with the unused region of the FPGA to reduce the effect of HCI. Figure 21 (a) illustrates the regions swapping strategy between high switching activities and the less active region to minimised the age acceleration effect of HCI. Also with the assumption of enough modular level of the available regions, partial dynamic-reconfiguration can also be supported. Contrast with the multiple reconfiguration techniques, there is no need for generation of multiple bitstream/netlist, therefore huge storage space requirement can be avoided [70]. Yet, the challenges with this approach are strategically circuit partitioning into sub modules and then the support for reassembling them.

Figure 21 (b) shows the path reconfiguration strategy to improve timing yield in FPGAs compensating for variability by re-mapping and re-placement [81].This work exploit the flexibility of LUTs mapping and presented a software tool that can systematically compute all the possible way for a given logic network. The experiment results show mean and variance of a critical path delay can be reduced similar to using the statistical Monte Carlo simulation techniques.

2.11 Summary

Variability issues in sub-nanometer CMOS technology have appeared as a critical challenge to the ability to deliver a design that meet all the timing, power and reliability specification. With the continuous scaling of the

technologies and increasing power density, the pressure to deliver the design within the time frame while dealing with the variability issues is going to get worse. The two main variability challenges are, first the static variability due to process scaling and limitation of lithography and etching tools. The imperfection during of manufacturing process results in parametric or spatial variability for inter-die and intra-die. Secondly the environmental changes and temporal ageing variability is dynamic changes after deployment. Tackling the dynamic variability such voltage changes due to increasing workload and temperature during operation is relatively more challenging. Traditional techniques that apply excessive operating margin across the whole chip based on worst-case scenario reduced system efficiency. This thesis aims to explore the practical variation tolerance strategies without scarifying the system efficient that relies on worst-case guard-banding.

In advanced technology nodes, a design with multiple billion atomic-scale transistors; the assumption that not all of the transistor will work or some will fail at the later life of the device may not be unfair. FPGA architecture has been the centre of this work because its inherit reconfigurability nature that provides unique opportunities to cope with these static and dynamic variability challenges. For example, rerouting and remapping to achieved thermal and wear-out balance.

The cornerstone for adaptively to changes is the ability to measure and quantified the variability profile of a specific chip as well as to track the

changes during operation. The characterization can be performed either with off-chip or on-chip sensing. The result is chip variability profiles or variation maps.

Off-chip sensing offers a non-intrusive characterization – for example, optical and infrared imaging techniques. However, the downside being costly and complex equipment needed. Also, it's less intuitive to correlate data collected externally with the operation activities. On the other hand, the on-chip sensor allows continue monitoring the health of the chip. Yet, the major challenges for on-chip sensing are the distribution of the sensors and reduced chip density due to the area occupied by the sensors. The alternative to the on-chip and off-chip sensor is soft-sensing. This technique is unique only to FPGA. Soft-sensing in this thesis context exploits the generic built-in resources of the FPGA replacing the conventional analogue sensor. For example, the ring oscillator can be temporally configured across the FPGA fabric evenly and characterise its thermal profile for "pre" and "post" system implementation. The "pre" implementation thermal profile gives the static variability map of the chip while the "post" for dynamic thermal gradient results after a fixed period of operation. In addition, the soft-sensing technique also provides extra gratification to implement and track variability on targeted area rather, to widely distribute them across the whole chip. This reduces area overhead.

Various variation tolerant techniques have been proposed, some are unique only for FPGA and some are common between the FPGA and ASIC. The summary of the techniques is shown Table 2.

Table 2: Summary of Existing Variation Tolerance Techniques in FPGA

Techniques	Remarks
STA	Pessimistic timing variation analysis based on worst-case. Reduce performance.
SSTA	Less conservative than STA for intra-die variation but still a "One-size-fits-all" approach.
Transistor sizing	Time-consuming engineering efforts for over million transistor circuit.
Structural Parameters Optimisation:	Do not provide significant improvement for variation concern.
Multiple-configuration	Expansive computation at speed test and required huge memory for all possible configurations storage.
Variation-aware Modelling	Improve yield over STA and SSTA, however accurate variation map generation is required for inter-die and intra-die variability.
Relocation, Remapping and Rerouting	Improve large storage problem compare to multiple configuration techniques, however, the challenges are system partitioning and regions allocation.
Asynchronous Techniques	Highly adaptive to changes in voltage and timing variability. However, asynchronous circuits are more complex to design and normally incur high handshaking's circuit overhead. Also, traditional FPGA architecture only has limited resources to support Asynchronous implementation.

STA guaranteed correct operation based on worst-case estimation and, therefore, reduced in possible performance. Whereas, SSTA is less conservative compared to STA for intra-die variation and the accuracy of the model relies heavily on the statistical mean and standard deviation values. The drawback of these approaches is uniform parameter applied across a whole batch of dies. Yet, this has been a preference strategy for industry thus far

because it is the only practical approach for mass production solution. In reality, most of the chip in the market can perform much better than the manufacturer's conservative specification. The late-binding and variation-aware techniques for example proven to achieve higher efficiency above conservative timing specification recommend by the manufacturer.

Above all, the asynchronous technique that is known to be robust to timing variation and possibility provide an attractive solution. Despite the potential benefits, asynchronous FPGAs presented in past have not centred on improving the reliability aspects – rather mainly focus on low power and throughput performance. Also, to implement asynchronous logic in synchronous FPGA is proven to be difficult because it's required manually manipulate the existing FPGA resources that are designed for the synchronous system. Introducing asynchronous friendly logic block to traditional FPGA architecture, therefore, has been the motivations for this work.

Chapter 3. Existing Asynchronous Techniques in FPGA

3.1 Introduction

This chapter discusses the context of incorporating asynchronous logic into the programmable logic to tolerate and reduce the negative impact of variability. The focus of this chapter is divided in two main parts as follow:

Firstly, the principle of asynchronous logic and its potential trade-off is introduced. Popular delay-insensitive encoding strategies such as 4-phase dual-rail (4P-DR) and 2-phase dual-rail (2P-DR) are reviewed. Circuit robustness based on timing assumption made is also classified including speed-independent (SI) and delay-insensitive (DI) circuits. This section serves as a basis for further understanding and ease of explanation is the following chapters.

Second part of the chapter reviews different styles of asynchronous FPGA architectures presented from the past decade motivated mainly by the pursuit of either low power and/or high speed performance. These architectures are classified into four main types for ease of explanation in overview as follow. Type-1, the architecture that is heavily relies on the timing assumption using bundle data. Type-2, the architectures that target on high throughput performance by adopting fine-grain pipelined structures. Type-3, handshaking based optimisation architecture to improve the coding efficiency in dual-rail

communication for dynamic power reduction in the communication, and Type-4, the architecture that combine the benefit of both synchronous and asynchronous circuit that fit the global asynchronous and locally synchronous (GALS) paradigm. Other type of asynchronous implementation motivated different benefits such security advantage also reviews, however this is not the main focus of this work.

The final section summarise the trade-off of each type of these asynchronous reconfigurable architectures in the context of its benefits and trade-offs to be used on a FPGA to mitigate the negative effect of the variability.

3.2 Principles of Asynchronous Design

Digital electronic system designs are predominantly synchronous and sequential. A sequential circuit is specified by a time sequence of inputs, outputs and internal states. In synchronous sequential circuits, a change of internal state occurs in response to synchronous clock pulses [3]. Figure 22 shows a high-level representation of a typical synchronous circuit where the communication of data is governed by the global clock.

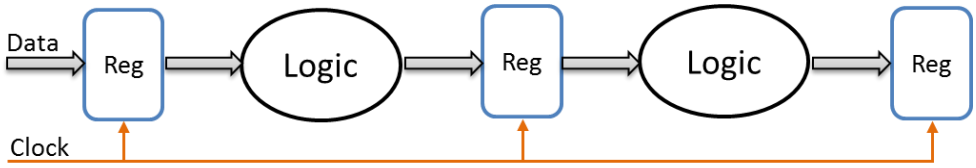

Figure 22: Synchronous clocking system.

In asynchronous designs, no global timing clock is used and communication is achieved through some sort of handshaking protocols. Typical communication involves a data request (req) and acknowledgement (ack) to initiate communication and indicating the response to the request. Often the req/ack signals are referred to as the control signal or the control path (CTL) and the data line as the data path (Data). Figure 23 illustrates an abstract view of an asynchronous circuit with handshaking control. Although the pipeline structure is shown, this is just for ease of explanation and in reality both synchronous and asynchronous designs can have different topologies.

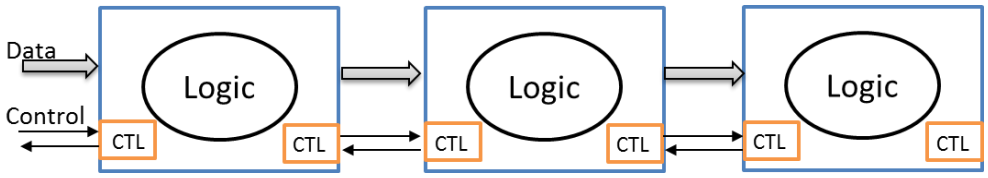

Figure 23: Abstract view of Asynchronous Circuit.

3.3 Bundle Data Design

The solution space can be expressed as the cross-product of a number of options, including:

(2-Phase, 4-Phase) x (Bundle-data, Dual-rail, 1-of-n,…) x (push, pull)

The choice of protocol affects the characteristics of the circuit implementation, such as power, area, speed and robustness. This section explains the terminology commonly uses in asynchronous circuit design. The most popular handshaking protocols are discussed, including 2-phase and 4-phase communication together with dual-rail or bundle-data.

3.3.1 Single-Rail Bundle-Data (SR-BD)

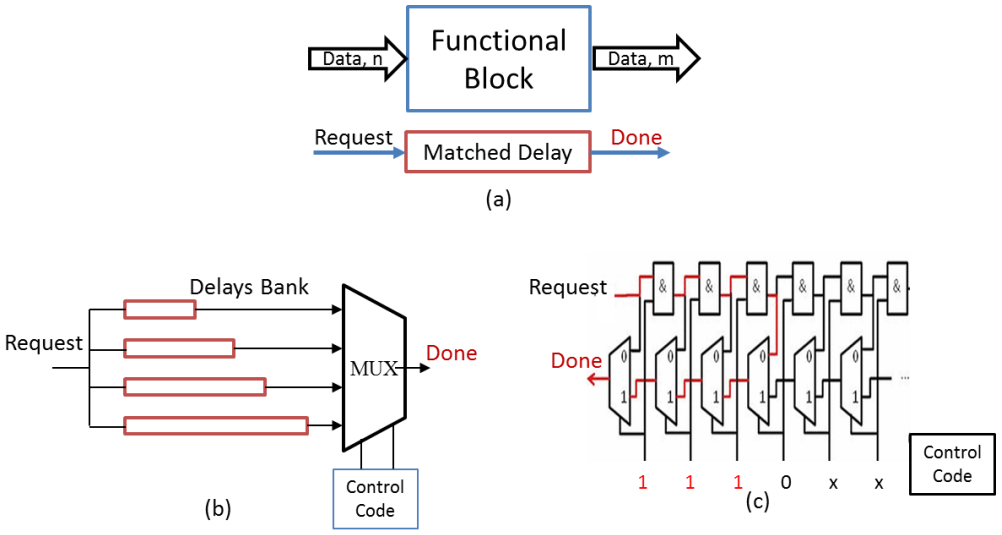

Figure 24: (a) Abstract view of delay matching bundle-data approach; (b) example of programmable delays bank. (c) AND gate and muxes fine tune programmable delay [82].

The simplest and most widely used asynchronous protocol is single-rail bundle-data (SR-BD**).** The advantages of the SR-BD are its simplicity in design, small size and ease of validation. An abstract view of the SR-BD approach is shown in Figure 24 (a). The functional block in this scheme is maintains similar to the synchronous design and replace the clock line with matched-timing delay line to indicate the completion of computation or valid data have been received

using the "done" signal. Hence in many ways the design can easily be migrated between the synchronous and asynchronous domains by interchanging the clock line with match delays. Match delay lines are normally fixed and realised by an inverter chain. However, to deal with the variability, tuneable delay line has also been proposed. Figure 24 (b) shows an example of a programmable delay (PD) with a control code for the selectable delay bank. The matching delay can be either fixed or tuneable. Usually, this type of design cannot be fine-tuned. The headroom in the non-fine-tuned matching delay means that the circuit may not operate at its optimum speed. Another example of PD implementation shown in Figure 24 (c) allows more accurate tuning. The trade-off for the accurate or fine-tuneable PD is increased complexity in control and need for more configuration logic.

3.3.2 4-Phase and 2-Phase Bundle-Data Handshaking

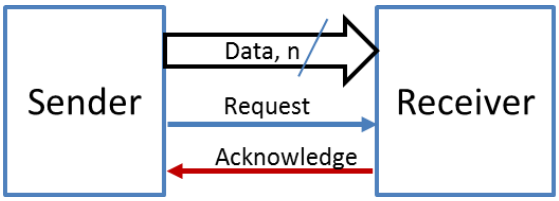

Figure 25: Send and receive handshaking.

In the bundle-data handshaking scheme, data lines are bundled together with the request and acknowledge line operating independently. The most common handshake protocols are 4-phase and 2-phase bundle data. This communication scheme is easier to elaborate with the concept of data exchange between sender and receiver units or two subsystems as shown in Figure 25.

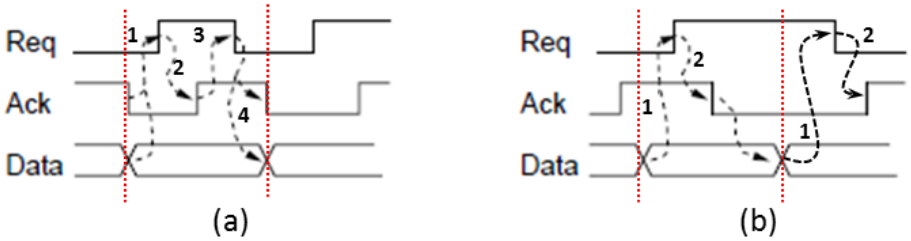

Figure 26: (a) 4-phase bundled-data protocol; (b) 2-phase bundled-data protocol [83].

The 4-phase bundle-data (4P-BD) communication cycle involves four signal transitions and this illustrated in Figure 26 (a). The sequence of actions is as follows:

(1) The sender prepares the data and set the request signal to high,

(2) The receiver accepts the data and responds by setting the "Ack" signal to high,

(3) The sender then notifies the completion of the transmission by resetting the "Req" signal back to low,

(4) Finally, the receiver reverts itself to the "ready to receive" state by setting the "Ack" signal to low to complete the handshaking cycle. Hence a new cycle is ready to start with both "Req" and "Ack" returned to the low state.

The advantage of the 4P-BD method is that it is relatively simple in term of circuit implementation. However, the logic has to always be returned to the zero state to be ready for the next communication cycle (also known as return-

to-zero (RTZ)). Thus 4-phase communication loses its attractiveness for design specifications concerned with power and speed performance.

2-phase bundle-data (2P-BD), on the other hand, is a non-return-to-zero (NRZ) protocol. As illustrated in Figure 26 (b), only two signal transitions are needed to complete a data transfer operation in reverting to the "ready-for-next-transition" cycle. The 2-phase protocol is based on signal encoding built into the "Req" and "Ack" signals, where the transitions between 0 -> 1 and 1->0 both represent a valid "signal event". As for example illustrated in Figure 26 (b), at (1) when data is ready (at the odd-phase where the "Ack" signal is at the high level) in first transition cycle, the transition from 0->1 is indicated "Req" and transition from 1 -> 0 to indicated "Ack" event. In the second cycle (data ready at even-phase with the "Ack" signal remaining low), the opposite signal transitions are valid compared to the odd-phase.

Based on the above signal transition graphs, 2-phase communication might be expected to provide higher communication efficiency and faster throughput compared to a system using 4-phase communication. However the 2-phase system requires extra logics for phase differentiation (odd or even), and this will introduces extra complexity in to the circuit's design and hence result in increased silicon area on the controlling circuits. Because of this, there is no clear criterion to decide which protocol is better. Rather, the best strategy is to carefully choose the appropriate schemes tailored to the optimisation objectives for the overall circuit.

Push and Pull protocol, The Previous example was based on the assumption that the sender is in the initiating position to start the communication. Therefore the data was "pushed" from the sender side, or the so-call push channel. Conversely, the receiver can also request data to be transferred. This case is classified as the pull channel and the "Req" and "Ack" signals will operates in reverse.

3.4 Delay-Insensitive Encoding

Bundle-data protocols rely heavily on matching the delay with the data paths. However, this may incur hefty safety margins in the presence of variation. Hence the alternative is to use more sophisticated and robust techniques that are less susceptible to variation in delay. The following section introduces more robust protocols that can tolerate disparities in delay resulting from for example, PVT variation. These techniques have data validity built-in within the coding, and this kind of circuit is classified as delay-insensitive (DI).

3.4.1 4-Phase Dual-Rail Handshaking

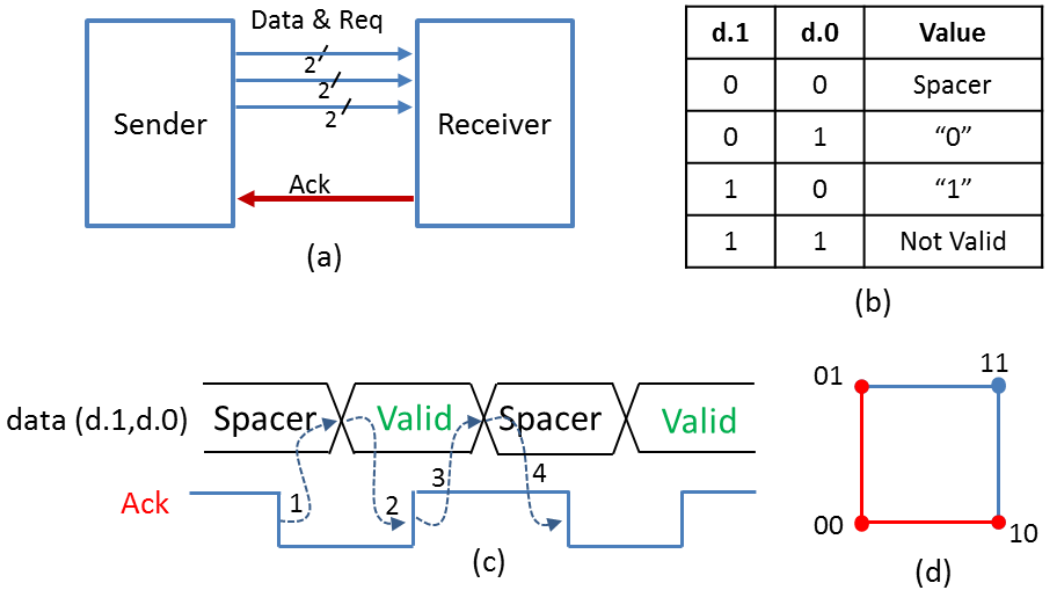

Figure 27: (a) Request sign embedded in dual-rail coding; (b) the codewords; (c) signal transition waveform; (d) code with Hamming distance = 1.

4-phase dual-rail (4P-DR) is one of the most popular forms of DI encoding. In this encoding, the request signal is embedded directly into the data-path. Figure 27 (a) shows a similar "sender and receiver" scheme as in bundle-data but with a dual-rail data line and without a dedicated "Req" signal. Instead the request signal is encoded within the data lines with 2-bits of binary coding. Combined with the 4-phase protocol, the validity of data can be discriminated with a "spacer" or "NULL".

The 4P-DR codeword is shown in Figure 27 (b). (d.1,d.0) are the dual-rail wire pair, with the combination showing a valid value only when they are either "0,1" or "1,0" (as shown in the table, logic 0 and logic 1 respectively for the

codes). The codeword "0, 0" is equivalent to of reset position with Humming distance equal to 1 from both valid data, as shown in Figure 27 (d), and therefore this serves as a spacer to indicate that data has been cleared and the next cycle of transition can take place.

The sequence of 4P-DR handshaking shows in Figure 27 (a) & (c) at the abstract level as follow:

(1) The receiver indicates that data is ready to be accepted, with "Ack" at the low state.

(2) The sender then issues the data. At the receiver side, when valid is data detected, "Ack" is set to high.

(3) The return of "Ack" to the the low state tells the sender that the data has been completely absorbed and thereby the data can be cleared.

(4) Consequence from the retreat of valid data, "Ack" returns to its initial low state and a new cycle is ready to start.

It should be noted that the commonly used dual-rail (DR) term is also the case of m-of-n coding ('m' is the number of ones out of the total 'n' number of wires) [84]. For example the dual-rail code in the m-of-n term is 1-of-2. Another example of commonly use encoding is 1-of-4, which also fit in the n-of-m paradigm. This encoding is more balanced in power consumption because computations are always performed at a balanced Hamming weight. Therefore

it is less vulnerable to side-channel attack. This technique has been exploited and proposed for implementation on programmable logic for security applications [85].

3.4.2 Completion Detection (CD) Circuit

The derivation of valid data in the absence of a timing clock is using circuitry that can determine the completion of transient within a logic block. As demonstrated in the bundle data scheme, this can be done with the matched delay. For dual-rail signalling, request signals are embedded together with the data. The common completion detection circuit for dual-rail communication is shown in Figure 28 (a) which consists of OR gates and a multiple inputs C-element. The OR gates are used to detect valid data or mutual-exclusive dual-rail inputs bits and the result is merged with a Müller "C-element". The C-element truth table is shown in Figure 28 (b), where "Done" will output the logic '0' only if all of the inputs are '0', and likewise for logic '1'. If not, the output value maintains its value.

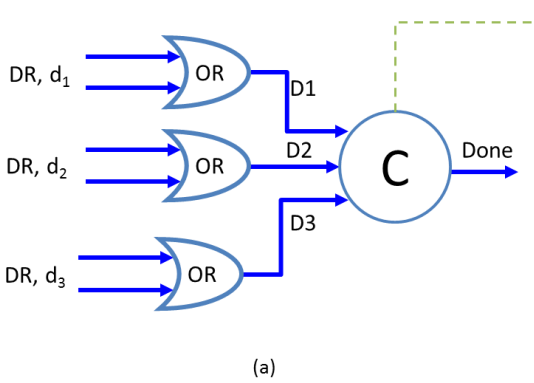

Inputs			Output
D3	D2	D1	Done
0	0	0	'0'
0	0	1	Maintain
0	1	0	Maintain
0	1	1	Maintain
1	0	0	Maintain
1	0	1	Maintain
1	1	0	Maintain
1	1	1	"1"

(b)

Figure 28: (a) Example of dual-rail completion detection circuit; (b) truth table for the C-element.

3.4.3 2-Phase Dual-Rail Protocol

The 2-phase dual-rail (2P-DR) or level-encoded dual-rail (LEDR) protocol also uses two wires to encode one bit of data, but information is encoded differently with level/phase detection. The 2-phase handshake neither requires an empty "spacer" value nor uses an elegant non-return-to-zero (NRZ) scheme. Figure 8 (a) shows the signal waveform of LEDR signalling where the parity-rail alternates the phase at each data item and the data-rail carries the valid value at each phase. Therefore there is only one signal transition per each new data item. LEDR uses level encoding where the data-rail will hold actual data value and the parity-rail holds a parity value. The encoding of parity alternates between odd and even phases. Figure 8 (b) shows the truth table for LEDR encoding.

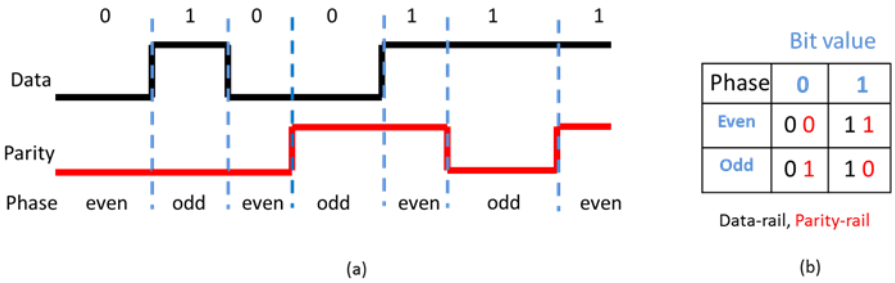

Figure 8: (a) LEDR Signalling; (b) LEDR encoding.

In summary, the 2-phase dual-rail (2P-DR) protocol should have better power dissipation performance than 4-phase dual-rail (4P-DR) because of its efficient coding with fewer transitions per data bit and no spacer required. However, its complexity in circuit implementation makes it an impractical choice, especially at the fine-grain level. Therefore none of the above protocols are ideal for replacing the traditional timing clock scheme. Yet, to tackle the global variability concern the DI circuits can still be valuable when applied strategically by mixing SR and DR in a architecture. For example, circuits at the coarse granularity level, such as the GALS paradigm can be used, or the protocols may be combined. Such system has been proposed in [7, 8] in which the 4P-DR was applied in the local functional blocks and LEDR for global communication.

3.5 Asynchronous Circuit Classification:

Asynchronous circuits are classified based on the delay assumption made. At the circuit level, asynchronous circuits can be classified as being either self-time, speed-independent (SI) [67] or delay-insensitive (DI) [66]. This section

provides an overview of the theoretical understanding of these circuit classifications. Jens and Furber [86-89] summarised the principles and techniques for asynchronous design in [83]. The concepts of delay models are easier to illustrate with a classical case study example with three logic gates (A, B and C) connected together with wires as shown in Figure 29.

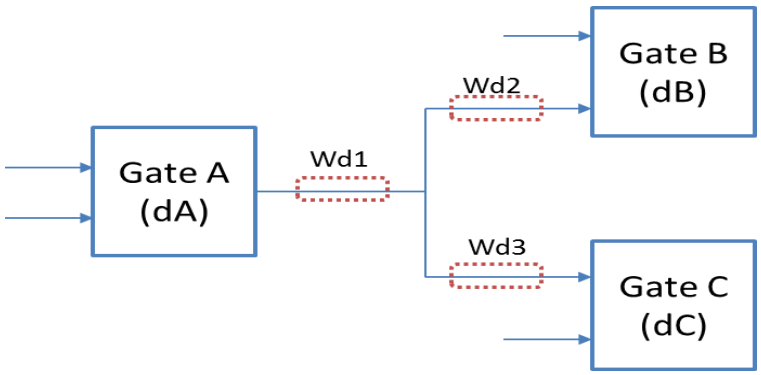

Figure 29: Case study of delay model circuit classification.

3.5.1 Speed-Independent (SI)

The speed–independent circuit consider only gates delay and assume wires are ideal without delay. This assumption may be valid on board-level small circuits where the wire delay is significantly low or negligible. However, in modern silicon technology, at very large scale and with long interconnects, this assumption can no longer be valid. Referring to Figure 29, in the SI classification the wire delays wd1, wd2 and wd3 are all equal to 0. Note that, from another theoretical point of view, if wd2 and wd3 are equal the wire delays can actually be lumped together with the delays of their associated gates. In this case considering the wires delays the circuit can be still SI.

3.5.2 Delay-Insensitive (DI)

In delay-insensitive circuits no delay assumptions are made for either wires or gates. Referring to Figure 29, the wire delays wd1, wd2 and wd3 cannot be ignored and must be considered alongside gate delay. Therefore this model is the most robust of all asynchronous classes. However, due to its strict restrictions only a very limited number of circuits can be classified as DI. One view [87] concluded that almost no useful DI circuits can be built due to these heavy restrictions. In order to build a practical circuit, relaxation of the DI requirement is needed.

Instead, the concept of isochronic forks was introduced by Martin [87] where an isochronic fork allow signals to reach two destinations with negligible different in delay or with the assumption that the delay in forks wires wd2 and wd3 as in Figure 29 can be equal. I this example, if transition observed in Gate B then transition can also assumed to have happened on Gate C.

3.5.3 Quasi-Delay-Insensitive (QDI)

Quasi-delay-insensitive (QDI) circuits are those using the isochronic fork assumption. In some senses, this is the best compromise towards a fully DI circuit. Technically, the QDI circuits are the same class of circuit as SI with the difference that QDI circuits involve acknowledgements of each transition,

whereas in SI no such assumption is made between circuit nodes with and without isochronic forks.

3.6 Reconfigurable Asynchronous Architectures

Different styles of asynchronous FPGA architectures have been presented since 1992 [5, 18-24] motivated mainly by the pursuit of either low power and/or high speed performance. From the point of view of implementation techniques, these architectures can be classified into four main types. Type-1 includes the bundle data and timing assumption architectures, whereas type-2 architectures focus mainly on high performance using highly pipelined and fine-grain structures. Type-3 uses 2-phase instead of 4-Phase or so-called non-return-zero (NRZ) protocols to improve the coding efficiency in order to give potential power savings in communication, and type-4 includes hierarchical coarse-grain structures that can fit the GALS paradigm. A summary of reconfigurable asynchronous logic architectures is shown in Table 3.

Table 3: Summary of asynchronous FPGAs

Year	Architectures	Unique Style	Handshaking	References
1994	Montage	TRIPTYCH	Timing assumption	[90]
1995	PGA-STC	Delay Matching bundle data	4-Phase Bundle-data	[91]
1996	STACC	Delay matching bundle data	4-Phase Bundle-data	[92]
2001	Phase Logic	Phase logic, fine grain	2-Phase Micropipeline	[93]
2003	PAPA	Highly pipeline, Fine grain	4-Phase Dual-rail	[6, 94-98]
2003	GALS	Homogeneous GALS	4-Phase Bundle-data	[99]

2003	CalTech	Cluster, e1of2	e1of2	[100]
2005	GAPLA	Heterogeneous GALS	2-Phase Bundle-data	[101, 102]
2007	NCL	NULL Convention Logic	NCL /QDI	[103]
2007	TARTAN	NoC (Hierarchical RF architecture)	4-Phase Bundle-bundle	[104, 105]
2007	Achronix	Pipeline, Fine grain	4-Phase Dual-rail	[106]
2008	e-FPGA	1-of-n QDI (security)	1-of-n QDI	[85]
2010	Distributed AFPGA	David Cell control	Hybrid 4P-DR and Bundle-data	[68]

3.6.1 Type-1: Bundle Data and Timing Assumption Architectures

Asynchronous FPGA solutions have been presented in the literature since 1992 [3-14]. Payne [92] provided a summary of the MONTAGE [90], PGA-STC [91], and STACC [107] .

MONTAGE from the University of Washington proposed in 1994, was the first asynchronous FPGA, though it includes a clock signal for implementing synchronous circuits as well. It was extended from their own synchronous FPGA architecture by adding special arbitration cells and modifying the function unit. The MONTAGE architecture relies heavily on the regular routing structure and fast feedback path to achieve state holding on the functional unit (LUT), as shown in Figure 30. Under variation, the wire delay of large and long interconnects cannot be guaranteed, and therefore the chance of glitches occurring is high.

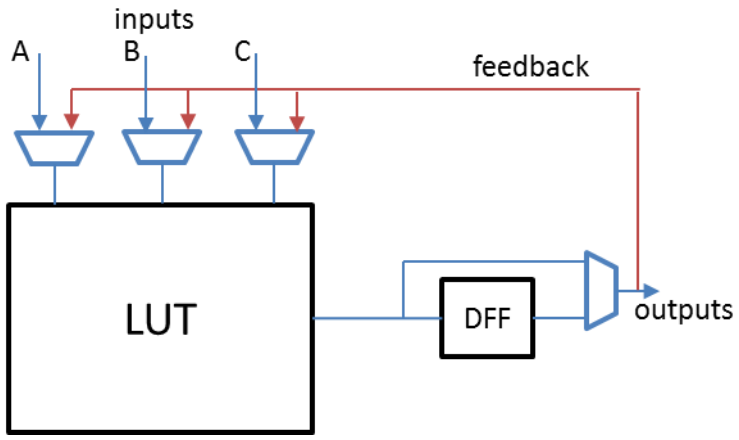

Figure 30: MONTAGE functional unit (configured as C-Muller gate).

The PGA-STC was developed at U.C. Davis in 1995. The author basically proposed that the Xilinx XC4000 series structure should be modified [91] by replacing the clock with programmable delay elements, as shown in Figure 31. The idea of the delay-matching bundle-data structure is very similar to clock design but distributed across the whole fabric by matching the timing of each individual functional-unit computation time. This bundle data technique could be highly-efficient in terms of minimizing the area and power overhead. Yet under variation and at below nominal voltage level, the delay element might suffer more than the function unit itself. The walk-around strategy could be used to increase the matching delay line with an extra-long margin for variability, but this will then defeat the objective of self-time implementation since a similar result in dealing with variation can be achieved in an asynchronous architecture by lowering the clock speed or by providing an extra timing margin or guard-band.

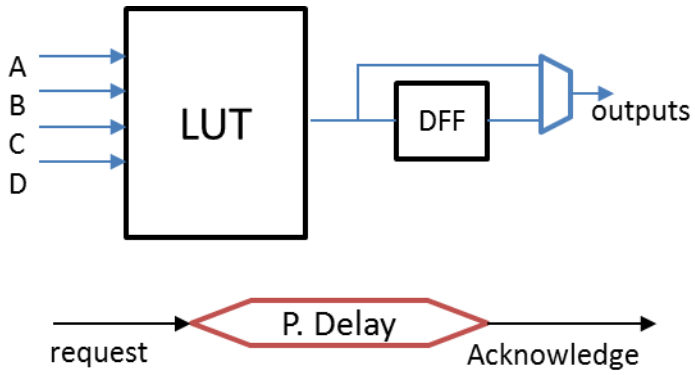

Figure 31: PGA-STC functional block with programmable delay element.

The STACC is an architecture developed at the University of Edinburgh by Payne [92]. It is a dedicated architecture for the implementation of four-phase bundled-data systems. Its architecture is based on that of fine-grain FPGA architectures where the global clock is replaced by an array of timing-cells that generate local register control signals. All of the above asynchronous FPGAs amend the function units to avoid hazards in signals, and use timing assumptions to guarantee the correctness of the asynchronous circuits. This structure has been proposed to replace the clock resources with a structure similar to a micropipeline [108] together with programmable delay (PD) elements . This could be a promising strategy to deal with variation. However, the original paper presented a very conceptual design without a detailed description of implementation and only simulation data.

3.6.2 Type-2: High Performance Architecture

Teifel and Manohar presented a fine-grain and highly pipelined asynchronous structure as a basis for their high performance asynchronous FPGA architecture [96]. The proposed programmable-asynchronous-pipeline-array, or so-called PAPA [94, 98] architecture comprises a completely new logic element compared to the traditional FPGAs in which there are special design functional units and merge, split, source, sink, copy, token units are used to support dataflow control, as shown in Figure 32. The handshake protocol used is 4-phase dual-rail (4P-DR) where each functional unit can be closely pipelined from one to another with the supported routing structure.

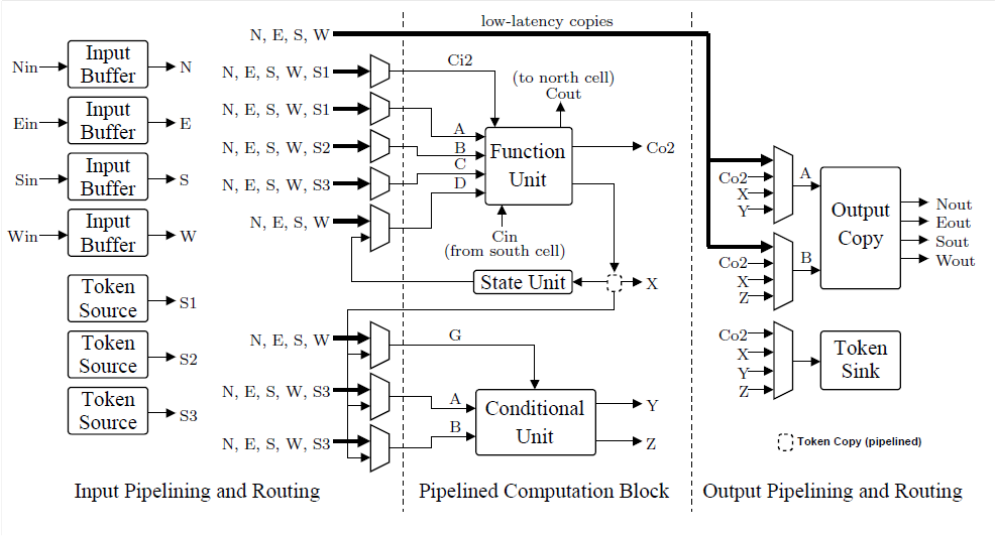

Figure 32: PAPA architecture logic block [98].

The LUT of the PAPA architecture LUT uses pre-charge half-buffer (PCHB) circuit, which is similar to the architecture presented by Wong, et al. [100], so that the PCHB circuit performs computations using a network of pull-down n-

type transistors. Both architectures use the similar general PCHB template as the building block, but architecture presented by Wong, et al. [100] is fundamentally different in that the granularity is coarser with a cluster or CLB-equivalent structure. Both of these architectures are not only great for high throughput performance thanks to their inherent pipeline structure, but also robust to PVT variation as in a QDI circuit. Measurement results [6] demonstrated that these asynchronous architectures can work at wide ranges of voltage and temperature. This further proved that this class of asynchronous circuit designs might be a promising avenue addressing the concerns about variability.

Several patents have also been successfully filed resulting from collaborative work on PAPA's architecture as follows:

- Reconfigurable logic fabrics for integrated circuits and systems and methods for configuring reconfigurable logic fabrics, US 8575959 B2 [109].
- Programmable crossbar structures in asynchronous systems, US 8300635 B2 [110].
- Synchronous to asynchronous logic conversion, US 8291358 B2 [111].
- Programmable asynchronous pipeline arrays, US 7157934 B2 [98].

The **Achronix Semiconductor Corporation** [106] used the PAPA architecture as the basis for the launch of the first commercially available asynchronous FPGA. Their product family targeted high performance markets such as the military, networking and telecommunications sectors. Fabricated at TSMC 65nm technology with a density of 164K LUTs with all the additional memory, multipliers, SerDes, PLLs and memory controller hard blocks, the company's products were claimed to be the fastest FPGAs in the market in 2008 with a maximum frequency of 1.5GHZ [112].

3.6.3 Type-3: Communication Efficiency (2-Phase Dual-Rail or LEDR)

Phase logic (PL) [93] and level-encoded dual-rail (LEDR) [113] both use 2-phase dual-rail (2P-DR) delay insensitive (DI) data encoding schemes. In this communication scheme, two wires/rails are used. Similar to the 4-phase dual-rail (4P-DR), both data and control information are encoded in the dual-rail package. In 4P-DR, the (0,0) codeword is used as a spacer and (1,1) is unused or invalid, as shown in Figure 33 (a). In this type of communication, the codeword always has to return to (0,0) as the "spacer" between valid data. Whereas, in 2-phase communication the efficient is higher, this is because all the codewords are set to indicate a valid data. As such, the upper wire/rail of the code holds the standard single rail data value and the lower one is the parity bit indicating the phase; see Figure 33(b). Since no return-to-zero phase is required, the 2-phase or LEDR is also classified as a non-return-to-zero (NRZ) protocol.

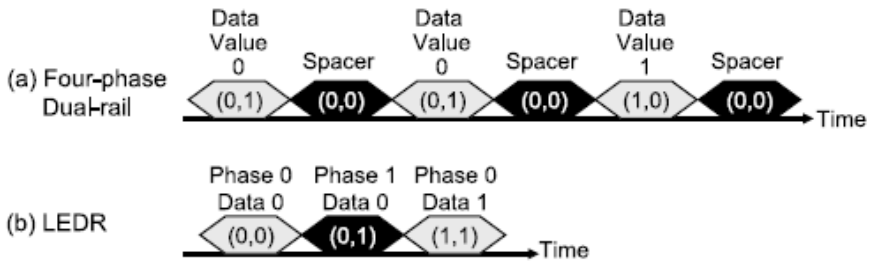

Figure 33: 4P-DR and LEDR communication.

The uniqueness of this encoding technique lies in the fact that the phase always alternates with every new data arrived, between phase 0 and phase 1 (or "even" and "odd" phases). For example, in the even phase the code word for 0 = (0,0) and for 1 = (1,1). In the odd phase 0 = (0,1) and 1 = (1,0).

Investigation of the programmable phase logic (PL) with this protocol started in 2001 by Traver et al. [114-116]. The authors proposed the design of the LUT4-based phase logic cell to form their basic FPGA logic elements (LEs) as shown in Figure 34. This was achieved by wrapping the phase control logic around the 4-input lookup table (LUT4). The idea of keeping the original LUT structure intact has the potential benefit of minimising the need to completely redesign or reuse the existing FPGA design tool flow. This bears some similarity to the work presented in chapter 4, but at a different level of granularity. The problem with the fine-grain PL structure is that it massively increases the area overhead with the consequence of higher power leakage compared to its synchronous counterpart because of the complex coding. Furthermore, similar to the earlier asynchronous FPGA structures presented above, the interconnection and communication block that occupied the lion's

share of the soft fabric has not been realised and therefore it is difficult to evaluate their potential power and throughput performance.

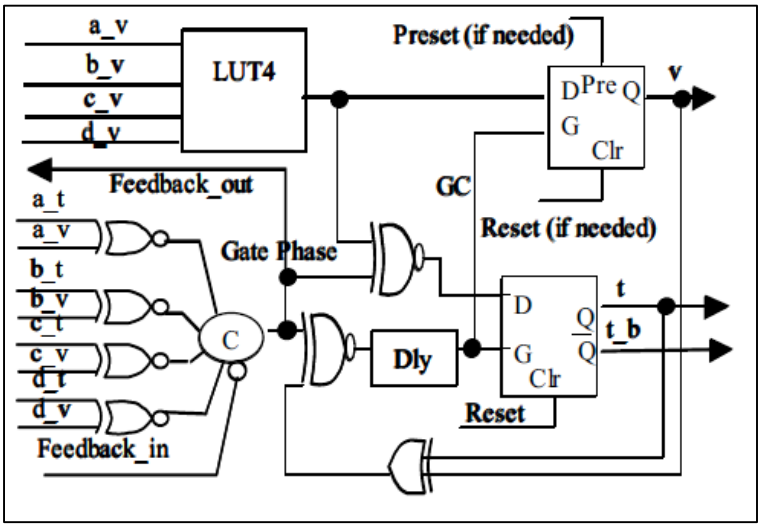

Figure 34: LUT4-based phased logic gate [115].

In summary, theoretically, due to the NRZ scheme, the LEDR protocol has potential advantages compared to the 4-Phase return-to-zero (RZ) protocol in terms of power and throughput. The potential power improvement is based on the efficiency of the coding that reduces the number of transitions on the global interconnect. Also, because the NRZ protocol means that no 'spacer' is required, hence a higher throughput yield may be expected. However, in the hardware implementation and due to the complex phase detection logic, data encoding and decoding required, the circuit's size and power increases significantly compared to synchronous circuits, for example in the LEDR protocol converter shown in Figure 35. This overhead makes it impractical to be implemented, especially at the fine-grain level.

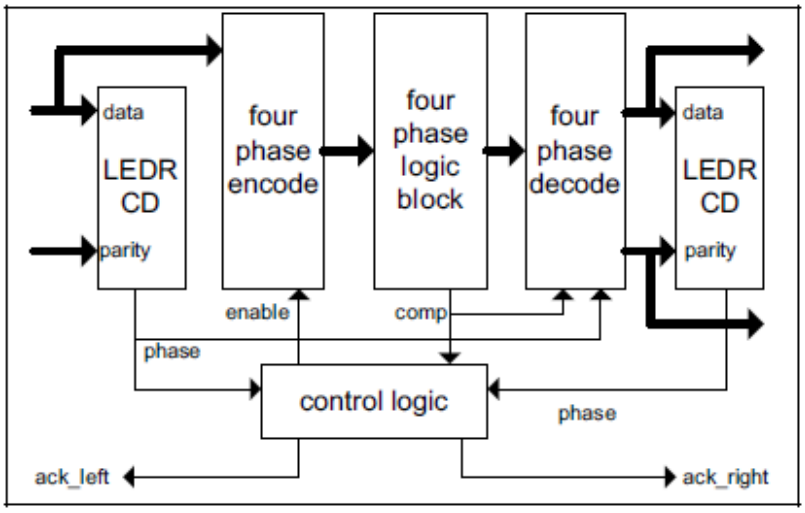

Figure 35: More complex LEDR protocol converter [117].

Nevertheless, as the subsequent work demonstrated [117-120], the LEDR protocol can still be beneficial when exploited appropriately. The results suggest that the strategy should be to employ the LEDR protocol for global data transfer, leaving the local functional and computational units with the RZ protocol. Examples of this kind of coarser grain structures are the GALS, MPSoC and NoC.

3.6.4 Type-4: Hierarchical and Coarse Grain Reconfigurable Architecture

The previous sections have demonstrated that the fine granularity asynchronous FPGA may have high flexibility and throughput performance, yet it comes with a silicon size penalty. The robust QDI circuit normally requires dual-rail interconnects and this may massively increase interconnect and routing resources composed of switches and configuration bits that constitute a large proportion of the PPGA soft fabric. The idea of increasing

granularity by packing together several LUTs to reduce global interconnects is not new, and may be called the CLB or cluster. However, for certain applications, increasing the granularity to a higher level such as by grouping multiple CLBs or functional-units (FUs) together into the same timing domain may result in better area and power performance. Each group of FUs can work at their individual local clock domain and the interface between island FUs will use the asynchronous principle. With the combined benefits of both synchronous and asynchronous elements, this has given rise to new approach as such as globally asynchronous and locally synchronous (GALS) and network-on-chip (NoC) designs.

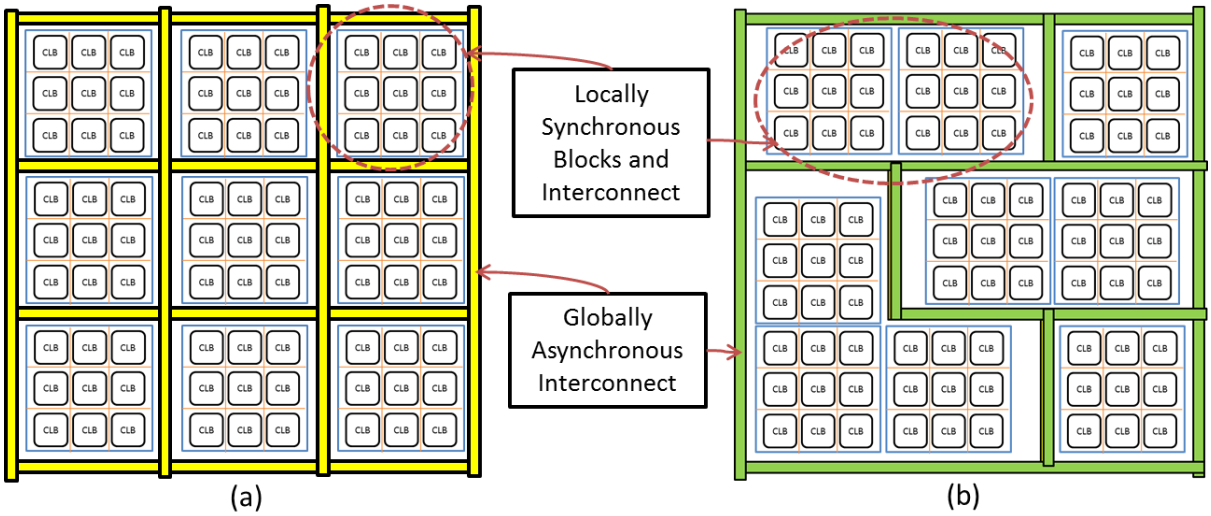

Figure 36: GALS in FPGA: (a) Homogeneous; (b) Heterogeneous.

Homogeneous GALS

The GALS scheme was introduced in ASICs level as early as 1984 [121], and Royal and Cheung [99] then proposed to apply the technique to FPGAs. The

proposed structure uses a 4-phase bundle-data handshake protocol to ease the synchronization problem for systems with multiple modules working at different clock domains. The architecture also features micropipelines in the routing. The unique aspect of the implementation of this architecture concerned their proposal to convert the conventional synchronous FPGA into GALS by introducing an asynchronous interface around the regular packed synchronous block, known as the asynchronous wrapper. This GALS paradigm introducing an asynchronous circuit at a coarse regular size synchronous block could reduce the overhead that otherwise may be incur by the fine grain AFPGA; however the tradeoff would be reduced flexibility. Also, because of the shapes and sizes of the wrappers for computation blocks across the whole fabric are the same, as shown in Figure 36 (a), this may reduce the logic utilization within each island. The authors also recommended using accurately tunable delay lines, which would have the potential benefit of reducing the effect of PVT variation [122]. However, this proposed idea required further development from it conceptual state.

Heterogeneous GALS

Jia and Vemuri [101] proposed a globally asynchronous-locally synchronous programmable logic array (GALSPLA) architecture together with a CAD tools design flow [102]. Compared to in [99], their proposed architecture is distinct in two respects. Firstly, the size and shape of their synchronous logic blocks are not fixed or can be in heterogeneous shape, which therefore may help in

improving the logic utilization. Secondly, their asynchronous wrapper uses a 2-phase instead of 4-phase bundle-data communication. Similar to the LEDR, the tradeoff of this handshaking protocol is better energy and throughput performance, but the phase conversion circuit may be more complex. The estimated size overhead for GAPLA architecture adaptation is small (at about 7%), and experimental results showed a performance improvement of 55% can be expected.

The results show that the concept of using heterogeneous GALS could be promising. However, from the point of view of variation tolerance, this proposed architecture may have some limitations due to the fact that bundle-data handshaking protocols rely heavily on timing assumptions. Furthermore, at a technology scale beyond 90nm, extrinsic and intrinsic variations become more prominent. Research has shown that circuits demonstrating the characteristics of both correlated as well as stochastic variability can be observed already in commercial off-the-shelf FPGAs [3]. This means that within the large locally synchronous block, the variability issue still remains.

Networks-on-Chip (NoC)

Networks-on-chip (NoC) represent the next higher level of coarse-grain architecture that fit well into the GALS paradigm. Instead of the traditional direct wire-to-wire bus connection, the NoC uses a networking strategy where data are grouped and transferred in packets. Similar to the pack switching

network system, routers are needed at each node to communicate data across the chip. Several asynchronous NoC have been proposed in the literatures that are composed of asynchronous routers. These include the ASPIN [123] architecture that uses bundle-data within the router and QDI circuits for long interlinks, MANGO and QNOC[124] which use standard 4-phase bundle-data and later use 2-phase mousetrap protocols [125], and the TARTAN [104, 105] architecture that uses a 4-phase pipelined protocol interfaced with complex memory support.

3.6.5 Other Asynchronous Style FPGAs

NCL Logic FPGA:

The NULL Convention Logic™ (NCL) [103] was patented and trademarked by Theseus Logic, Inc. [126] in 1994. It was derived from a mathematical expression of process completeness and provided inherently convenient in expressing asynchronous digital circuits.

The NCL is built in a design of 27 fundamental gates with a hysteresis state-holding capability to retain the output state until all of the input has been de-asserted again. Each NCL gate is custom-designed at transistor level to exhibit state holding behaviours similar to those of the C-element.

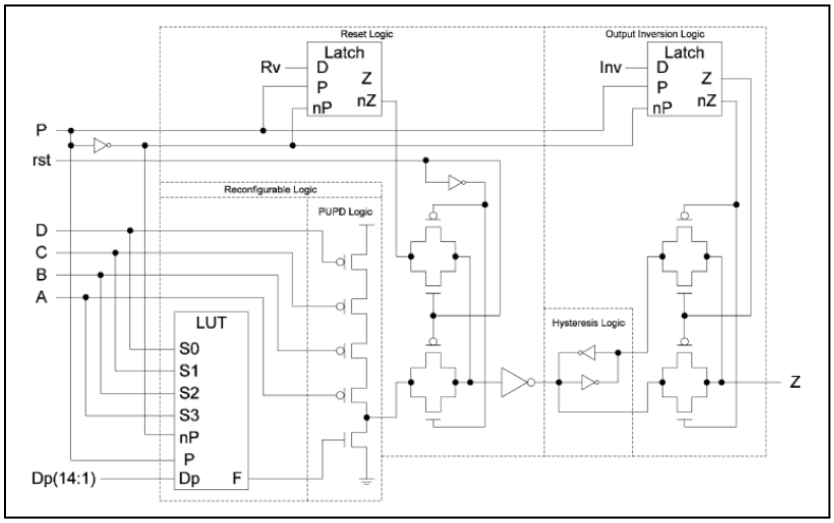

(a)

NCL Gate	Function
TH12	A + B
TH22	AB
TH13	A + B + C
TH23	AB + AC + BC
TH33	ABC
TH23w2	A + BC
TH33w2	AB + AC
TH14	A + B + C + D
TH24	AB + AC + AD + BC + BD + CD
TH34	ABC + ABD + ACD + BCD
TH44	ABCD
TH24w2	A + BC + BD + CD
TH34w2	AB + AC + AD + BCD
TH44w2	ABC + ABD + ACD
TH34w3	A + BCD
TH44w3	AB + AC + AD
TH24w22	A + B + CD
TH34w22	AB + AC + AD + BC + BD
TH44w22	AB + ACD + BCD
TH54w22	ABC + ABD
TH34w32	A + BC + BD
TH54w32	AB + ACD
TH44w322	AB + AC + AD + BC
TH54w322	AB + AC + BCD
THxor0	AB + CD
THand0	AB + BC + AD
TH24comp	AC + BC + AD + BD

(b)

Figure 37: (a) Basic reconfigurable NCL LE; (b) 27 fundamental NCL gates [127].

Smith [127] has proposed two versions of an FPGA logic element (LE) designs that can realize all the 27 NLC fundamental gates, as shown in Figure 37. The design wraps the modified LUT with threshold logic at the fine-grain level. The NCL gates could also be delay insensitive, but the author only cited comparative simulation results for only the area efficiency, without any attention given to speed performance and strategy toward PVT variation. Even with the significant saving of logic gates presented in the optimized version of the LE, its fine granularity structure means that massive area overheads might be expected on area compared to the synchronous counterpart. Also the structure presented was incomplete, lacking interconnect strategy and potential flow control between the proposed LEs. Even though the proposal

was later elaborated [128] with grouped LEs or CLB for hierarchical approach, the work is still very immature in terms of what be required to form a basic FPGA architecture.

Multi-Style and SAFE – eFPGA

The TIMA Lab in France has presented a unique fully-customized asynchronous FPGA that has been prototyped in 65nm CMOS technology [85, 129, 130]. The architecture supports multiple style asynchronous logic, including 2-phase, 4-phase communication protocols and 1-of-n encoding. The main motivation for using asynchronous logic in this work was to present an electrically balanced circuit that is robust against side channel attacks (SCAs) dedicated for security applications.

The lack of a global clock in asynchronous logic mean that the system is more immune to simple-power-attack (SPA) and differential-power-analysis (DPA) attacks, and the QDI circuits or the general 1-of-n coding lead to data computation and communication at a stable Hamming weight. This reduces the power consumption dependency that can be exploited by SPA, DPA and electromagnetic-analysis (EMA) attacks.

The research in the above work focuses on two aspects. The first is a platform to support flexible styles of asynchronous implementation, and the second is to increase security levels against SCAs. The inherently asynchronous structure may also be robust to environmental variation, yet no relevant data was

presented by the authors. The security benefits of asynchronous logic might be an interesting direction for investigation in research but is not the main focus of the present study. It should also be noted that flexibility in style also implies that extra configurability resources are needed and will this consequently increase silicon area and power overheads.

3.7 Summary

This chapter has presented an overview of commonly used asynchronous design styles including the bundle-data and dual-rail communication schemes.

The asynchronous techniques applied on FPGA in the past decade have been reviewed. Motivated by either lower power, high throughput performance and in the context of variation tolerance, these architectures summarised as follows:

Type-1, the early development of the AFPGA relied on significant elements of timing assumptions to guarantee the correctness of the asynchronous logic. This method combines the delays for both FPGA intra-block and inter-block connections and replaces the local timing assumption with global timing assumption. In general, these types of asynchronous circuits are easier to implement and may be with less overhead. However, it is hard to match delays for FPGA inter-block connections since the connection path cannot be determined at design time. In the larger technology node wire delay can be negligible compare to the logic delay, but at modern sub-nano meter technology,

delay matching based on delay assumption is hard to achieve especially considering process and environmental variations.

Type-2, this advanced development of the AFPGA focuses on high performance. On the one hand, they are somewhat tolerant to operational variations (process, voltage, temperature) through SI/DI with none or minimal reliance on timing assumptions. On the other hand, they modify the entire FPGA fabric and replace the fundamental basic logic block of current FPGA technology. This makes the system design process less accessible by significantly reducing the usefulness of existing design tools. Furthermore, some of these architectures utilised very fine-grained pipelined architectures consisting of excessive numbers of C-elements, implying high area and power overheads.

Type-3, 2-Phase Dual-rail (2P-DR) and LEDR architecture aim to improve power and throughput with the optimised NRZ scheme rather the 4-Phase return-to-zero communication. Theoretically, higher throughput and less energy would be expected because of reduced transitions on the global interconnect. However, due to complex hardware implementation of the phase detection circuit, the benefit maybe offset with the increase of circuit size. This overhead will increase significantly if implemented at fine-grain levels.

Type-4: As for the NoC and GALS, the trade-off arguments are the same, where the higher or coarser grain architecture will improve power efficiency but the challenges in technology scaling and increase in logic density result in

inevitable variability issues that affect the chip at both the global and local levels.

With the technology scaling continues and transistor sizes shrink to the nanoscale, timing variability have becomes a growing concern. Maintaining global clock in multimillion logic cells FPGA is becoming difficult; therefore asynchronous design styles are receiving growing attention, since asynchronous circuits operation do not rely on tight timing margins. Although various style asynchronous FPGAs exist as presented in this chapter, but they have not achieved it widespread use compare to its synchronous counterpart due two main reasons. Firstly, its lack of supportive automated design tool and unfamiliarity of the non-clock design concept to the community. Most of asynchronous architectures presented in the study modified the traditional structure greatly and make it hard to incorporate or to reuse with existing design flows. Secondly, asynchronous handshaking logic normally incurs large area overhead especially implemented in fine granularity level.

The works in this research focus on improving the reliability of the FPGA architecture with the support of asynchronous techniques while keeping most the fundamental structure of traditional FPGA intact and therefore allows the reuse of existing commercial design flows. The proposed architecture will compromise between types (1), (2) and (4). The objective is tries to strike a sensible balance between maintaining the fundamental FPGA's structures whilst achieving full asynchrony in places where it matters most as follow:

1. Maintaining the existing FPGA block structure and maintain the possible reuse of existing commercial design flow.

2. Making critical interconnects paths DI for latency variation tolerance.

3. Improve or at least maintain throughput performance.

4. Keep the area and power overhead of the asynchronous handshaking logic at minimum by clustering the logic block similar to type-4 but balance at the right granularity level.

Chapter 4 present the implementation and analysis of the asynchronous FPGA architecture base on the above specification.

Chapter 4. Distributed Control Asynchronous FPGA Architecture

4.1 Introduction

As mention in the previous chapter, the purpose of this work is to investigate a practical approach from the architecture point of view to deal with the variability challenges faced in the current and future FPGA technology. Asynchronous logic is known to be highly resilient to variability; therefore the potential for this approach is attractive. However, various trades-offs with asynchronous logic implementation need to be studied in detail in the context of field programmable gate arrays (FPGA). This chapter proposes an asynchronous FPGA architecture that maintains the basic logic element of the conventional FPGAs, allowing maximum reusability of existing automatic design flows. Interconnects of this architecture are delay-insensitive (DI) and the handshaking is achieved through a distributed controller on every cluster. This architecture is mainly aimed to tolerate latency variability resulting from the process and environmental variations in modern CMOS process technology. In addition, this newly proposed asynchronous architecture also facilitates the investigation of systems powered by nondeterministic Vdd sources such as energy harvesting systems. Variation tolerance of the architecture is achieved by retaining the local computational logic element in single-rail and replacing the global clock resources with DI handshaking interconnects. The remainder

of the chapter describes the implementation of the medium-grain wrapper based asynchronous FPGA structure and its essential components in detail followed by a proposed design flow. Variability simulation results are also presented with case study implementations.

4.2 Asynchronous Wrapper

The Fully-Asynchronous FPGA architectures that are fine-grain or completely modified the conventional FPGA structure, for example the highly-pipelined PAPA architecture [94, 96] may be highly resistant to variation. However, these architectures come with high area and power overheads. Moreover, the design process for fine-grain FPGAs is not straightforward and usually presents a steep learning curve to the designer.

The proposition of wrapping the synchronous-block or Intellectual-property (IP) units with handshaking logic that communicated asynchronously is not new. Such GALS scheme has been introduced since early 80's [121] and was later proposed to apply the technique to FPGAs in [99]. However GALS scheme is normally coarse-grain architecture. The granularity of the GALS scheme affects the logic usability and tolerability and not able tolerate random variation within the synchronous island block. Also, such systems generally require a significant alteration of existing FPGA tool design flow. Therefore one strategy to increase acceptability is to retain the existing design flow as much as possible. This can be done by keeping the underlying FPGA's logic

structure untouched and introducing a wrapper circuit around it to replace the clock tree. This would allow the reuse of the flow in logic synthesis, with the optimisation and packing processes largely the same for the data path.

In addition, asynchronous circuits tend to be based on relatively complex coding methods, such as 4-phase dual-rail (4P-DR) or, in general, m-of-n [83]. This implies large area overheads. Asynchronous circuits supposedly involve low power since they can be made to work only when necessary and do not require clock trees. However, in general, complex coding may result in an increase of interconnects and switching activities in the FPGAs unless in low power coding such as 1-of-4, leading to more dynamic power consumption, potentially negating the savings from removing clock signals. The larger circuit size may also lead to greater power leakage. Thus the proposed wrapper structure is medium-grain, with one wrapper per cluster. This structure sits between the fine-grain structure, with one wrapper per logic cell, which is high in area overhead and dynamic power, and the fixed coarse-grain structure with one wrapper per multiple clusters may reduce the number of global interconnects but potentially also reduces its logic utilisation such as in the GALS or NoC approaches. The top-down descriptions of the distributed control asynchronous wrapper in the FPGA architecture are given as follows.

4.3 Top Level Overview of the Architecture

The proposed wrapper architecture maintains the commonly used island-style structure as in most commercial FPGAs, as shown in Figure 38 . The routing channels consist of wire segments, switch boxes (SBs) and connection boxes (CBs) surrounding the logic cluster (LC). Apart from the clock circuits, the conventional FPGA structure has two types of circuits: 1) small logic islands (logic clusters); and, 2) large interconnects. In each logic cluster, there are several programmable logic elements (PLEs), which are the same as the logic clusters in standard existing FPGAs, and a David Cell (DC) element [131]. Because the global clock signals have been removed, the DC is used to implement distributed control in their place.

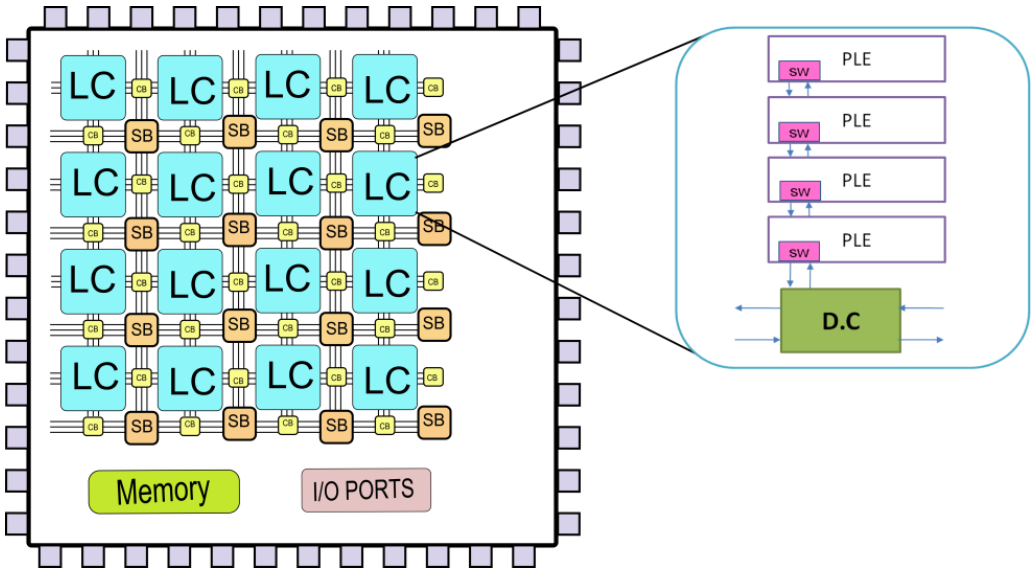

Figure 38: Island style architecture.

Latency variation within the local areas of limited size tends to be easier to manage, however, tolerance for unpredictable latency variations in extreme

cases is more crucial for long interconnects. Therefore the approach taken is retaining the basic conventional FPGA cluster-based structure relatively unchanged, this makes each of the cluster behave functionally as a block self-timed to its environment and replace the synchronous clocking resources with distributed DC-based control and DI interconnects. The design of the LC and the principles of DC control are demonstrated in the following sections.

Table 4: Choice of architecture structure.

Architecture Overview		
Parameter	***value***	***Reference***
Architecture	Island style	[132]
LUT Size (K)	4 * Inputs	[133]
Logic Cluster Size (N)	4 * PLE	[133]
Cluster input Channels (i)	16	[133]
Channel Type	Dual- rail/Channel	[83]
Switch Box (SB)	Universal	[134]
Connection Box (CB)	Normal	[134]
Process Technology	UMC-90nm CMOS	-
Handshake Protocol	4-Phase Dual-Rail	[83]
David Cell (DC)		[135]

The granularity or structure choice of FPGA affects the logic utilization, speed and power performance. This is usually based on three vital logic cluster

parameters which are the size (*K*) of the lookup table (LUT), the cluster size (*N*) or the number of LUTs in a cluster, and the number of inputs per cluster (*I*). In general, increasing the sizes of *K* and *N* will improve functionality and performance, but at the same time escalate the area exponentially. Cluster input size, *I*, should be kept as small as possible; however, if *I* is too small, numerous logic elements in the cluster may be unavailing [9, 136]. The classic FPGA architecture uses four LUTs per cluster and four inputs for each LUT. In this setup, the default values are chosen. Table 4 shows the structural choices made for the proposed asynchronous FPGA architecture.

4.4 Asynchronous Wrapper Structure

The fundamental block of a conventional FPGA comprises a lookup table (LUT), a register (DFF) and a multiplexer (MUX). The terminology in Altera is called a logic element (LE) or logic cell in Xilinx. In this design, asynchronous logics are introduced wrapping around the fundamental logic blocks or LEs. The newly designed structure that combines the wrapper and logic blocks constitutes the new programmable logic element (PLE). This is shown in Figure 39.

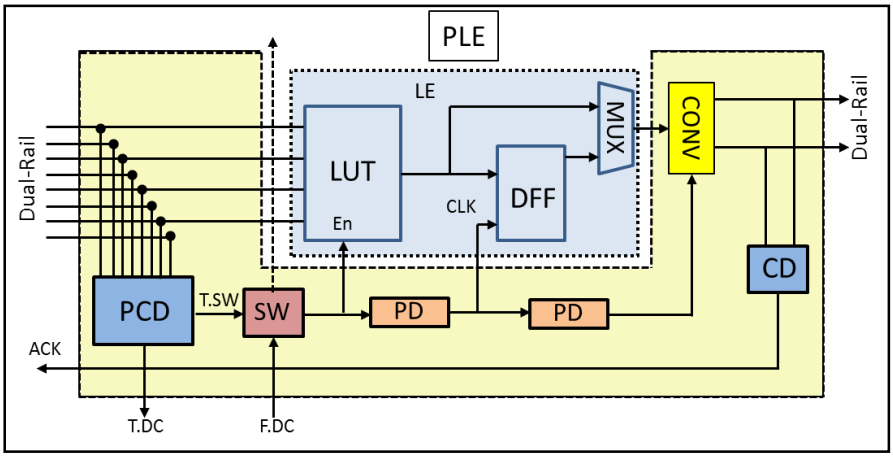

Figure 39: Wrapper based programmable logic element (PLE).

The wrapper consists of the following circuits:

- Programmable completion detection (PCD)
- Trigger selection switch (SW)
- Programmable delay (PD)
- Single- to dual-rail converter (CONV)
- Completion detection (CD)

The PCD is used to compute the complete arrival of all valid data. When all data arrived, two "ready" signals will be generated from the PCD. This is for the two possible used for this input data. Firstly, if the data could be used for an operation involving only the local PLE the "ready" signal goes directly to the (T.SW – "to SW") to enable the local LUT to start data processing. Secondly, the data may be used for a concurrent operation with other PLEs which may or may not be in the same cluster. In this case, the ready signal goes to the David Cell (DC)-based distributed control to synchronize with the input data for other PLEs (via T.DC – "to DC") and when the synchronization is complete, the SW will be enabled by the F.DC ("from DC") signal from the DC circuit.

The SW is basically a dual-input multiplexer which can select ready signal either directly from the PCD or from the distributed DC control when synchronization is required. In order to minimize the intermediate transitional activities of the circuit and guarantee that the LUT is activated only when the data is ready for the entire operation, the enable logic is implemented on the LUT.

The PD is used to set up delays to match with certain operations. Here the first PD is used to match the latency of the LUT and the second PD the latency of the latch data and to indicate the "ready" state of the single-rail data from the MUX.

CONV is purposed to transform the original single-rail data into a dual-rail encoded data for DI communication. CD is completion detection indicating validity of dual-rail data has been generated. The CD is optional depending on where the control signal came from (either "T.SW" for independent acknowledgement or "F.DC" for consolidate acknowledgement).

The wrapper commission in the following manner, when all input valid data are detected, PCD generates a trigger signal. The trigger signal will then act as a start indication for LUT to commence computation. PDs match the computation time and used to control the effective latching timing. The computed result can be then converted from single-rail data to dual-rail before propagating to the next stage. The output of the CD is an "ACK" or "Done"

signal, generated to the previous stages when the input data has been consumed.

4.4.1 Programmable Completion Detection (PCD)

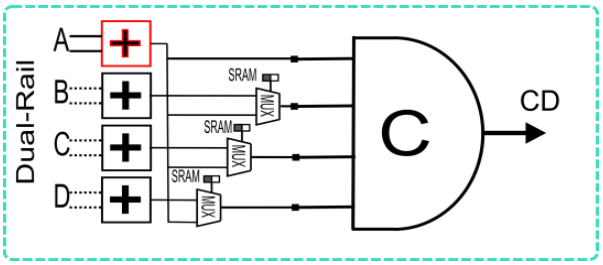

Figure 40: Programmable completion detection.

The PCD is the programmable completion detection circuit constituted with C-element and OR-gates as shown in Figure 40. The OR-gates allows the straightforward detection of valid signals from spacers or empty code-words in dual-rail encoding. The typical dual-rail code show in Table 5

Table 5: Dual-rail code-words.

Code-words	Code
0,0	Spacer
0,1	0
1,0	1
1,1	Not valid

Because the code-word (1, 1) is illegal and cannot occur, an OR gate is sufficient to safely indicate that a single data channel is “valid” or “empty”.

The completion detection valid-signals can be achieved with C-element that is a commonly used component in asynchronous circuits [83]. The C-element

provides the hysteresis in the empty-to-valid and valid-to-empty transitions required for transparent handshaking. It waits till all inputs to be valid before setting the output to high, and waits for all its inputs to become empty to set the output to low. For other input combinations, the output does not change. C-elements are thus ideal for collecting the states of multiple channels.

The proposed PLE, the input size of the C-element is four, however, in the actual implementation, not all input will be usable. In order to allow the 4-inputs C-element to function correctly, flexibility configuration are required in such case. This is resolved by utilising extra three multiplexers to link the idle channel (B, C or D) to Channel A, which is assumed to be always in operative if the PLE participates in the computation. The process of enabling or disabling the relevant MUX for the relative channel is assumed to be handled by automated tools during the synthesis and mapping flow.

4.4.2 Switch Box (SW) Circuit

The SW trigger switch box in Figure 41 is a simple programmable multiplexer. The purpose of this SW is to facilitate the selection of the trigger or valid signal between the PCD block and the DC-control. For concurrent operation, the "F.DC" signal is used to synchronise operation for multiple PLEs. The example, the subsequent case study section clarifies the function of the SW.

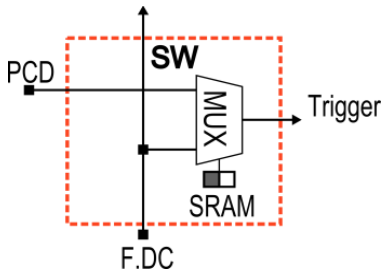

Figure 41: SW box circuit.

4.4.3 Programmable Delay (PD) Unit

The bundle-data is one of the most efficient approach asynchronous handshaking. Delay-element is used here for matching for the latency of the data path element being bundled; this local control signal has the equivalent functions of clocks of conventional LE. Various delay elements was introduces in chapter 3. However, the most common implementation is the chain-inverters circuit. Considering the process and environmental variation, the presented PD is made to be tuneable. The circuit with four selectable ranges PD is shown in Figure 42.

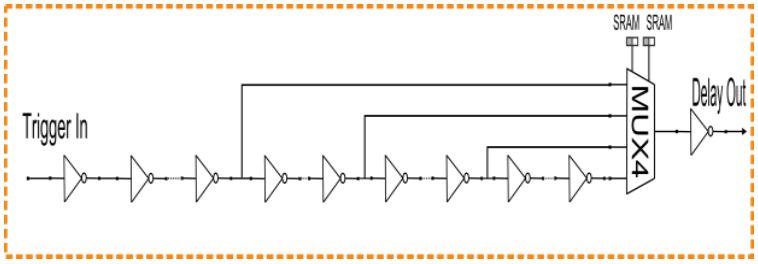

Figure 42: Programmable delay circuit.

Provided that the variability information concerning the environmental and power supply is availble from characterisation process, the PD range can be

set at configure time. The PD also can be beneficial in facilitating variation mitigation techniques such as chip-wise configuration or late binding [3].

In order to retain average rather the worst-case performance under a wide range of variability, finer tune of programmable delay element may be required. However, the implication is higher area overheads in PDs.

4.4.4 Single-Rail to Dual-Rail Conversion Circuit (CONV)

Converting the single-rail data output from LE to dual-rail format for the DI interconnects is the responsibility of CONV in Figure 39. This is shown in Figure 43.

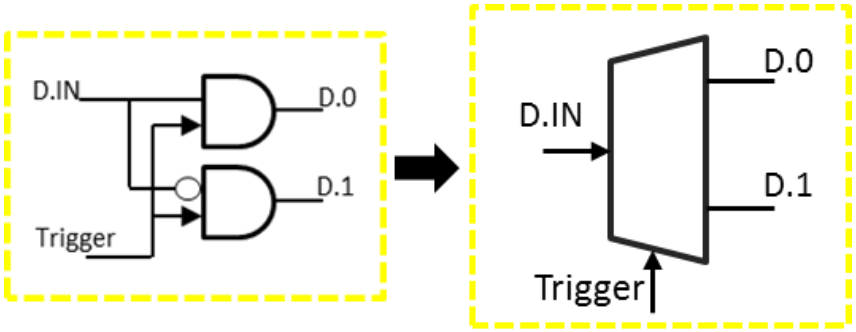

Figure 43: Dual-rail conversion or DEMUX circuit

At the input of the LE, one of the data wires gives the single-rail binary value of valid code-words directly. Once it has been ensured that spacers do not propagate to LE, this wire can be used directly for the data input.

4.5 Area, Power and Speed Performance

4.5.1 Area Overhead Calculation

Asynchronous circuits tend to be larger than synchronous ones. In the case of full SI/DI there are overheads in both the control circuits replacing clock systems and data path circuits due to the complex coding, such as 4P-DR. Even with bundled-data scheme, the clock replacement delay-elements may still be more sizable than the synchronous clock scheme.

Table 6: PLE size in terms of number of transistors.

BOX	BLOCK	Parts Included	Total
Logic Element	LUT	SRAM * 16	96
		Mux Tree (K = 4) $\sum_{i=1}^{k} 2^i$	30
		Buffer * 30	60
	DFF		24
	2:1 MUX		4
Total:			214
Wrapper	PCD	SRAM * 3	18
		2:1MUX * 3	12
		Gates	60
	SW	2:1MUX * 1	4
		SRAM * 1	6

	(PD)*2	(Buffer * 10) * 2	40
		(4:1MUX) * 2	20
		(SRAM * 2)*2	24
	CONV	2:1MUX * 2	8
		Buffer	2
	CD	OR2	6
Total:			200

With this added resource, many advantages can be gained. This includes improved variation resilience, avoiding the inevitable issues synchronous clock systems face with technology scaling, and lower power utilisation in low duty-cycle process.

Table 6 shows the complexity of the proposed PLE. Notably, the wrapper circuit introduced consist of almost equal number of circuit elements to the LE itself. This implies that the PLE is almost twice as big in terms of size. Despite, the circuit size overhead, the following power analysis shows that power does not increase much.

4.5.2 Power Comparison

The proposed PLE is roughly double in size the conventional LE. Typically, bigger the circuit higher the dynamic power consumption, but this PLE uses asynchronous techniques, which is even driven and without the complex global

clock tree should save the power used. Yet, the combined effect of these changes is uncertain. Although power optimisation is not the main focus for this section, it needs to be studied to see if there any radical changes are likely.

The most fundamental block or the PLE is used as an example. As variations are introduced, it is unreasonable to predict that all of the data will arrive at the same time. Here the worst case has been assumed where all four data bits arrive at different moments in time. This has no effect on the synchronous FPGA, since correct operations are guaranteed by the global clock. Only during the clock rising edge, stable data is required. But this is achieved by spending power on clocks. In the proposed AFPGA, data computation starts only when all of the data has arrived.

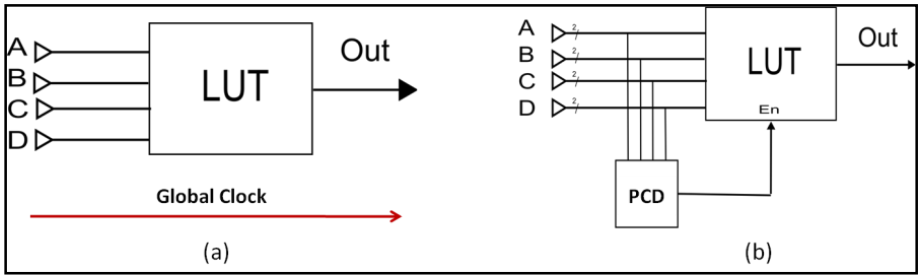

Figure 44: (a) Synchronous LUT; and (b) PCD asynchronous LUT.

The power consumption of conventional SRAM-based LUTs and CD-based LUTs are investigated in a comparative study using the following set-up shown in (Figure 44):

- Four signals, namely A, B, C and D, arrive at the input of LUT at different times.

- Signal A is assumed to arrive last and other signals were changing before it becomes stable, with 16 transitions between “0000” to “1111”, changing 1 bit at a time.
- When every signal, including ‘A’, eventually settles, output ‘1’ will be produced.

The simulation results are shown in Figure 45. When there is a transition in an input signal, the power line will spike. In the synchronous circuit, every change of data between valid clock signals changes the state of the LUT address and consumes energy. In the asynchronous design, data will not be read from the SRAM until it has received the enable signal (En) from the PCD, as shown in Figure 45 (b). The PCD circuit consumes relatively little power, and they are corresponds to the tiny power spikes between each pair of high power signature spikes in Figure 45 (a) and (b).

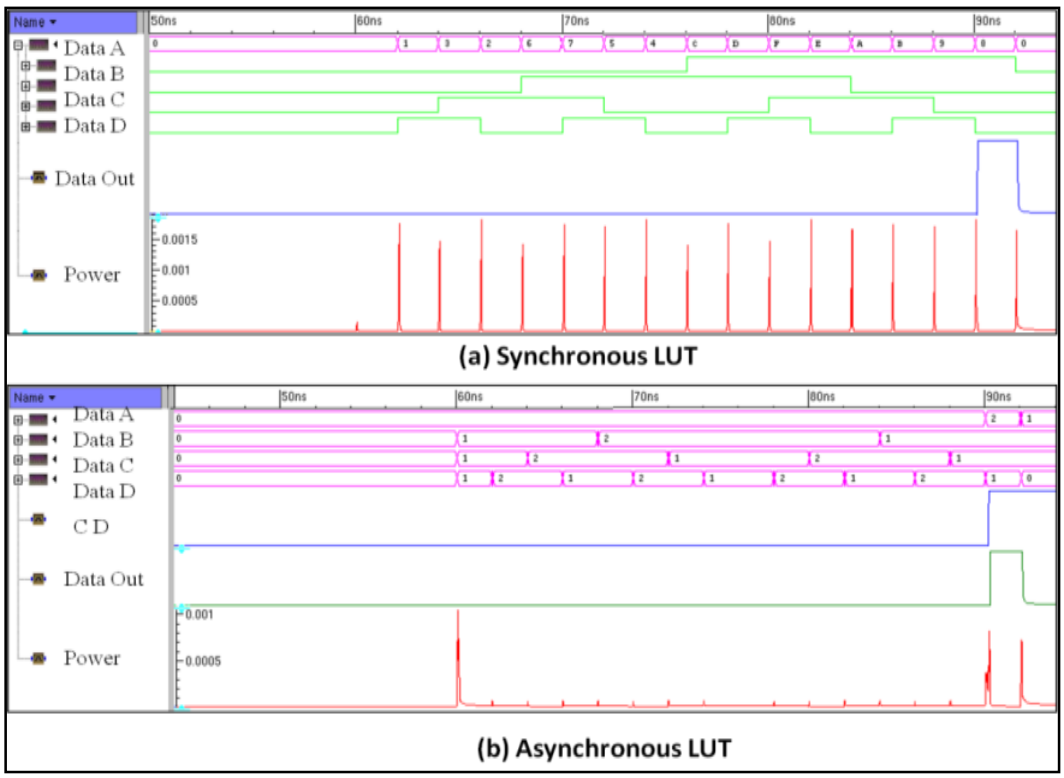

Figure 45: Operation power: (a) synchronous LUT with timing clock; (b) asynchronous LUT with PCD.

This simulation shows that, although the size of the PLE circuit has increased, it consumes roughly the same power and energy as the equivalent clock based-LUT in this setup. Taking into account the power used by the clock tree circuit and dynamic clock transition, the asynchronous LUT with CD may produce better power consumption characteristics in overall. The power data can be found in Table 7. The simulation is relevant to a relatively low duty-cycle situation, but because clock distribution is not included for the synchronous case, it was not put at an unfair disadvantage.

Table 7: Power and energy comparison.

Circuit	Operation Energy	Average Single Operation Power	Operating Voltage
LE (sync)	1.037pJ	32.41uW	1.0V
PLE (async)	0.544pJ	17.00uW	1.0V

Both the power and area comparisons may show significant advantages for the asynchronous architecture if the clock tree network resources are taken into account. In the synchronous FPGA, the clock itself brings challenges ranging from skew, tree distribution and global buffers. Special resources, such as DLLs (dynamic link libraries), PLLs (phase-locked loops) and clock multipliers, are also needed. Taking all of this into account, the clock resources in the synchronous FPGA will require significant amounts of area, power and management effort. In general, a 10% overhead on the maximum clock rate is recommended to guarantee operation in the presence of temperature variation. Due to the scaling of CMOS feature size, FPGA density increases, replacing the complex global clock with the asynchronous handshaking circuit provides a promising solution to alleviate the above-mentioned problems [137].

4.5.3 Throughput Performance

In synchronous system design, maximum operating frequency is set based on the critical path, and normally the maximum clock frequency is set according to it. In asynchronous system design, there is no global clock. Data is transferred through stages of logic controlled by handshake protocols which are inherently pipelined. The faster the data can be transferred from input to output, the higher the throughput can be achieved. To evaluate the maximum operating rate, the configuration bits or SRAM of the PLE is first configured with predetermine logic (within Cadence Virtuoso environment) and the input signals are stimulated. The time between the complete valid input data having arrived and valid output generated was recorded. The inverse of the delay from input to output is the frequency. The peak frequency of the proposed architecture was compared with those of various reported asynchronous FPGAs and also a commercial synchronous FPGA (Xilinx-Spartan3). Table 8 shows the throughput performance of various architectures based the literature at their nominal voltage level. Throughput performance of this work based on a single proposed PLE also included as a reference.

Table 8: Throughput comparisons of various architectures.

Architecture	Technology	Peak Throughput	Nominal Voltage
[100]	0.18um	235MHz	1.8V
[94]	0.25um	395MHz	2.5V

[6]	0.18um	674MHZ	1.8V
AFPGA (this work)	90nm	1.5GHz	1.0V
[138]	90nm	326MHz system clock	1.2V

Variations may result in changes in signal arriving times. A signal arriving too early or too late may lead to hold and set-up violations in synchronous system design. This can be dealt with by slowing down the clock by an appropriate degree to allow extra margins for safety reasons. However the problem of deriving the appropriate degree of slow-down in any case is significantly non-trivial [75]. In general, a 10% slowing down on the maximum clock rate has been recommended for temperature variation [137]. However, the results of another study [139] indicate that chip frequency variation can be up to 30%. Table 8 shows that, at a constant Vdd, all asynchronous FPGAs are faster than the synchronous Xilinx Spartan3. Moreover, the experiment described in the next section demonstrates that the asynchronous structure also exhibits the elastic operation of the PLE at a continuously changing Vdd without the necessity for specific retiming and slowing down.

4.6 Variability Evaluation

4.6.1 PLE Characterisation with Variable Vdd

The simulation of the PLE circuit was on Cadance tools on UMC 90nm CMOS technology. In the analog design flows, the PLE circuit works correctly as

designed without logic errors with Vdd sweep between 0.45V~1.00V. The result for delay and energy-per-operation over Vdd performance is shown in Figure 46.

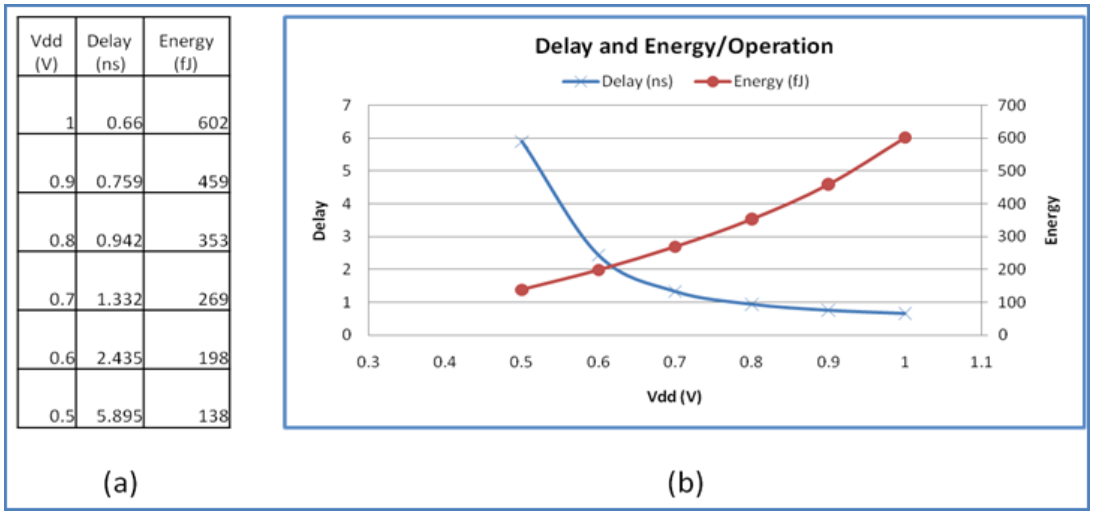

Vdd (V)	Delay (ns)	Energy (fJ)
1	0.66	602
0.9	0.759	459
0.8	0.942	353
0.7	1.332	269
0.6	2.435	198
0.5	5.895	138

Figure 46: Delay and operational energy at below nominal Vdd level: (a) results table; (b) delay and energy plot over Vdd.

During the simulation, the circuit shows error operation when Vdd is dropped below 0.40V. The observation on the timing graph indicated that this is due to the mismatch in bundling data in PD. Similar phenomenon, has previously been noticed [140], where inverter-chains based delay-element not maintain the correct temporal bundling for memory circuits (such as the SRAM cells here in the LUT) when Vdd is lowered towards the sub-threshold region. This is due to the rates of slowing down on data path are not in parallel with the delay-element when Vdd is reduced.

The PLE works well under different but constant Vdds as long as the bundling delay are matched. In terms of energy usage performance, the result is as

expected where operation energy are reduced with the drop of Vdd. Another observation from the graph indicated that there is a significant increase in latency when lowering the Vdd below 0.6V where the two lines crossed as in Figure 46 (b), this is the optimum operation energy point where significant energy savings can be achieved without much scarified on speed performance.

Simulation result in Figure 47 shows that the circuit work correctly within 0.45-1.0V constant Vdd range. Further simulation is carried out to investigate how the PLE behaves under a continuous varying Vdd over the range Vdd rage. In this experiment, a relatively slow sinusoid signal was applied to the power supply instead. The LE was configured as a parity checker for the value of A, B, and C and D. The experiment setup was in self-looping test environment with the feedback on the completion triggering the next operation. Figure 47 shows that the parity-checker was producing correct “even parity” bits on the output line continuously under varying Vdd. The output speed (out) and power rate (Pwr) are relative to the level of the Vdd.

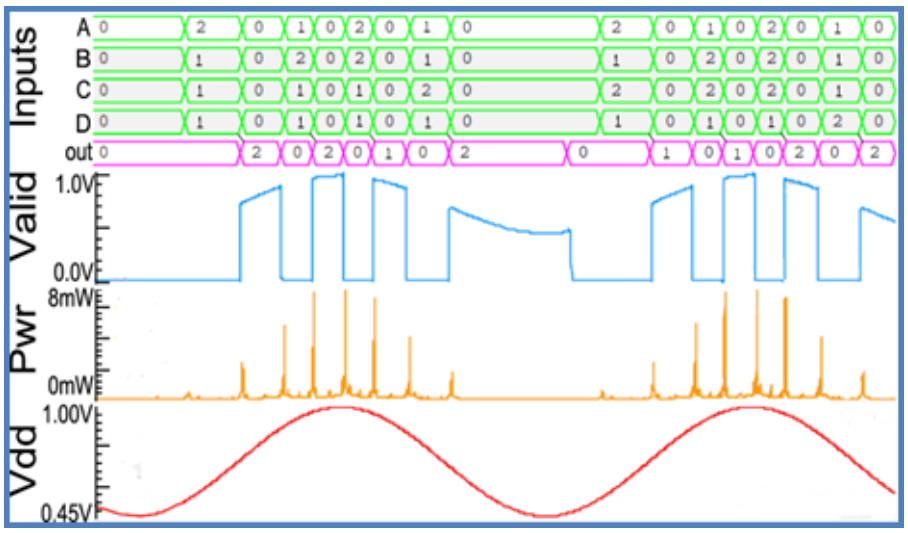

Figure 47: PLE working under variable Vdd.

4.6.2 Corner Analysis for PVT Variation

Taking into account manufacturing tolerances for devices as well as environmental variations in voltage and temperature, circuit behaviour can be obtained through simulations with ranges of PVT (process, voltage, and temperature) variation. Process corners for the MOS transistors are ss, tt, ff, sf, and fs, where t stands for typical, s for slow and f for fast. The first letter in a pair usually pertains to NMOS and the second to PMOS. Fast NMOS slow PMOS is referred to as 'fs' or 'fnsp'.

The worst-case (longest) latency is mainly associated with a high PMOS/NMOS threshold voltage (ss), high temperature and low supply voltage (Vdd) and the best-case is the converse. The programmable delay (PD) and data path (or LUT) delays in all process corners have been obtained to provide an

overview of the best- and worst-case scenarios for the circuit with respect to slow and fast environments:

Slow environment corners (V =0.5v & T=400K):

- LUT (ss: tt: ff: snfp: fnsp) = (1.56ns: 0.79ns: 0.43ns: 0.82ns: 0.75ns)
- PD (ss: tt: ff: snfp: fnsp) = (1.82ns: 0.91ns: 0.53ns: 1.01ns: 0.84ns)

Fast environnement corners (V=1.2V & T=273K) :

- LUT (ss: tt: ff: snfp: fnsp) = (0.20ns: 0.15ns: 0.12ns: 0.18ns: 0.14ns)
- PD (ss: tt: ff: snfp: fnsp) = (0.22ns: 0.16ns: 0.13ns: 0.19ns: 0.15ns)

Figure 48 (a) and (b) show that this PD successfully bundled the LUT delay across a wide voltage range when both are in the ss & ff corners. Further analysis was carried out to study cases where the PD and the LUT are in different corners. The results show that miss matches can occur in both slow and typical corners as shown in Figure 49(a) and (b). This demonstrates the need for the use of programmable delays (PD) as mentioned in section 4.4.3 above.

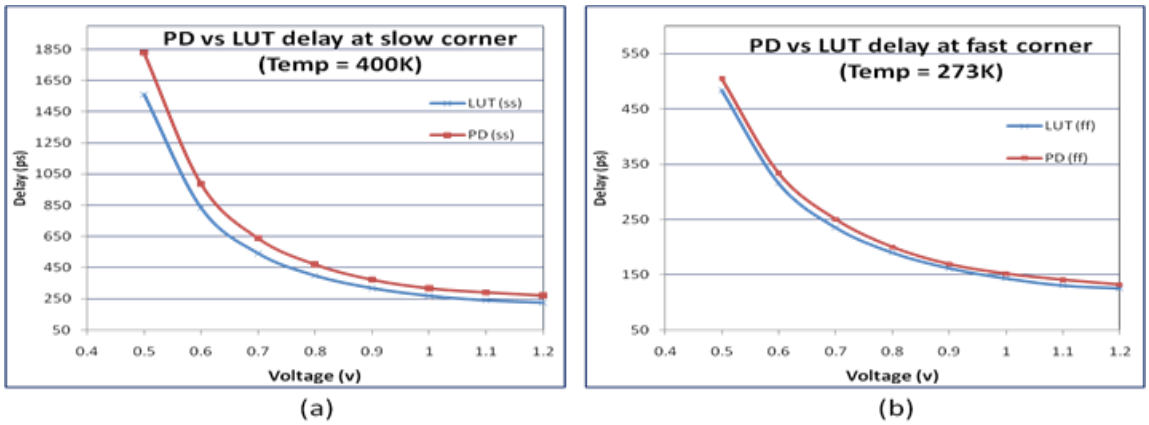

Figure 48: PD and LUT delay successfully bundling: (a) Slow corner (temperature=400K). (b) Fast corner (temperature=273K).

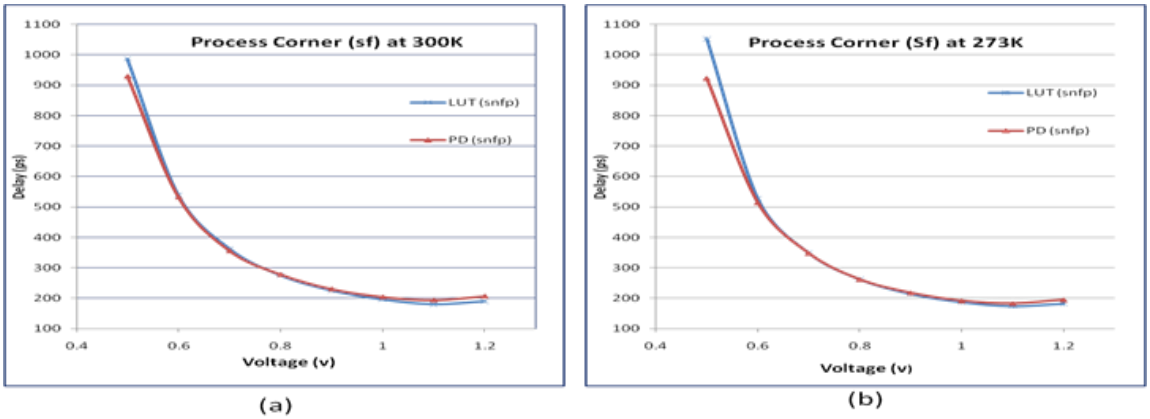

Figure 49: Cross over at (sf): corner (a) Temperature=300K. (b) Temperature=273K.

4.7 Logic Cluster Design

The logic cluster (LC), consisting of a group of PLEs, is the next level in the hierarchy. The unit in the same hierarchical layer in conventional FPGAs is known as the configurable logic block (CLB) in Xilinx terminology and the logic array block (LAB) in that of Altera.

Similar to most commercial FPGAs, the cluster in the proposed architecture (Figure 50) consists of four PLEs with the addition of one David cell (DC), which forms part of distributed intra-cluster and inter-cluster control. The general cluster structure is shown in Figure 50.

The DC-based distributed control in the cluster takes charge of the control path. When input data is ready, the PCDs in the PLEs in the cluster will generate trigger signals which may be collected by the DC control for group triggering. Some PLEs may need to execute concurrently and others sequentially. The SW allows either the selection of self-triggering directly from its corresponding PCD for sequential operation or group-triggering from the DC for concurrent operation. After computation is completed, the DC withdraws the data and propagates the control signal to the next stage. This structure also allows data feedback channels from the output of each PLE to the input PCDs of other PLEs. The principle of DC control is demonstrated in an example in the following section.

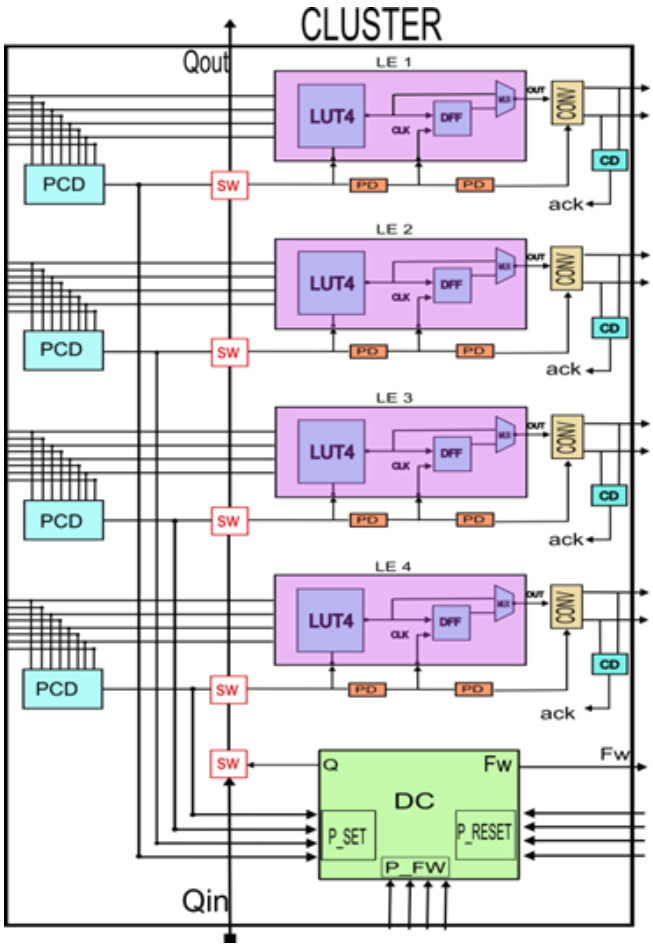

Figure 50: Logic cluster with DC.

4.7.1 Distributed Control with David Cell

In this proposed architecture, David Cells (DCs) are used to implement the distributed control, since this kind of control works based on handshake protocols. Distributed control using DCs was first proposed by David [131]. Extensions with the direct mapping of asynchronous control circuits from Petri Nets to DCs have also been reported [135, 141-143].

Basic structures of DCs are shown in Figure 51 (a), consisting of two inputs ("set" & "reset"), two outputs ("back" & "Fw"), and an SR latch for state keeping

(Q and Qb). Both of the inputs are active-low in the implementation. When the input "set" is active, Q will be set to high and the inversely active "reset" input will set Q back to low. The "back" output signal basically works as an acknowledgement of the previous stage of the pipeline for the signal having been received, and the "Fw" output signal tells the next stage that the new signal is ready to be consumed.

Figure 51 (b) shows how the basic structure of DC can be modified as distributed control for PLEs for computation in the cluster. The signal coming into a logic cluster can be from multiple sources, and therefore there will be a group of "set" signals (s1 – sn) to trigger signal "Q". When the control signal "Q" is activated, computation will start. An acknowledgement signal "ack" will then be generated after the valid signal of the valid output has been produce by the CD circuit. The "ack" signal replaces the "back" signal of the basic DC structure. Likewise for the output, there may be multiple reset signals (r1 - rn) to reset the control signal "Q" of the DC.

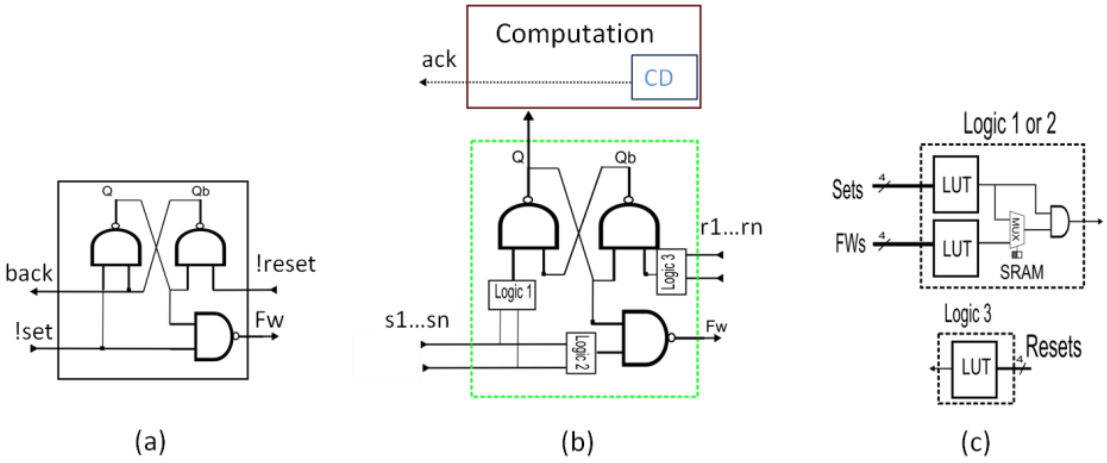

Figure 51: (a) Basic David cell Structure; (b) DC for distributed control; (c) set and reset logic boxes for DC implementations.

The control flow between LCs can occur in different topologies. Programmable logic blocks, namely "Logic 1", "Logic 2" and "Logic 3" are used to provide this required flexibility. "Logic 1" and "Logic 2" are the set function of signal (s1 – sn) that will trigger signal "Q" and the forward signal ("Fw"). The reset function "Logic 3" based on signals (r1 – r n) will reset the DC back to its default state.

The programmable logic blocks can be implemented with LUTs to cover all possible combinational relations of their inputs. Each logic block has four inputs with a cluster structure of n=4. This is shown in Figure 51 (c) in more detail.

A basic timing assumption in these programmable logic blocks can help to restrict them to a practical scale. Although this makes them not strictly SI, the delays within such small local areas can be more easily and reliably managed.

Based on this argument, it was decided to choose small-scale timing assumptions in this tradeoff.

4.7.2 David Cell Control Transition Flow

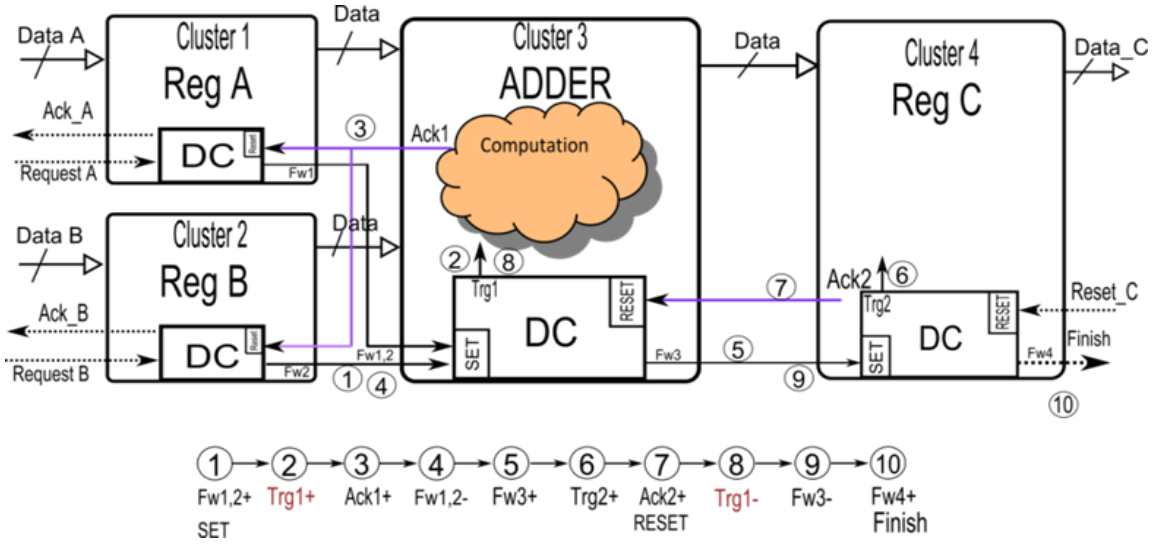

Figure 52: Data flow transition example with DCs.

DC control may be used to manage a control path across multiple clusters, dealing with both intra- and inter-cluster management. Figure 52 shows an implementation of a sub-unit of an ALU, where input data 'A' and 'B' will be stored in registers before being passed to Cluster 3 for computation. The output of the computation will then be stored in Register C (Cluster 4) to complete the sub process (in logic terms: Reg C = Reg A + Reg B). The numbers 1 - 10 are used to show the sequence of the transitions.

(1) Assuming data A and B were stored in Clusters 1 and 2, the forward signals Fw1 and Fw2 will be collected as the SET signal to trigger the DC in Cluster 3.

(2) The trigger (Trg1) rises, and computation will start.

(3) The completion of computation in Cluster 3 will generate an Ack signal that will then reset both of the previous stage's clusters to allow the RESET or clearing of data. Note that the result of data computation is ready at this stage.

(4) The Fw1 and Fw2 signals will go "low" after being reset in stage 3, indicating that the data is cleared.

(5) The Fw3 signal will be activated following the transitions in stage 4 allowing the data generated in stage 3 to be passed along and consumed by Cluster 4.

(6) Then the same transition as stage 2 happens again in Cluster 4 to start storing data in Reg C.

(7) Upon the completion of storing data in Reg C, the Ack2 signal is generated to clear its previous stage. The DC in Cluster 3 will then be reset.

(8) The Trg1 signal goes to "low" after being reset.

(9) Then the Fw3 signal will also go to "low" following the reset of stage 7.

(10) The process is completed and the DC in Cluster 4 can send a new request to its output (next) stage and a new sequence of transitions can start.

4.7.3 Implementation Case Study

This section describes an example of a sub system design which demonstrates the possible ways of configuring such systems on the architecture described in the preceding sections, as well as indicating the flexibility and features of this architecture.

A four-bit ripple-carry full adder demonstrates the flexibility of intra-cluster operational organization and the independent DC control of the PLEs. Figure 53 shows the implementation of the four-bit ripple-carry adder using two logic clusters. This can demonstrate the typical behaviour of the ripple-carry adder, where each stage waits until the previous stage has completed computation and propagated its carry output signal.

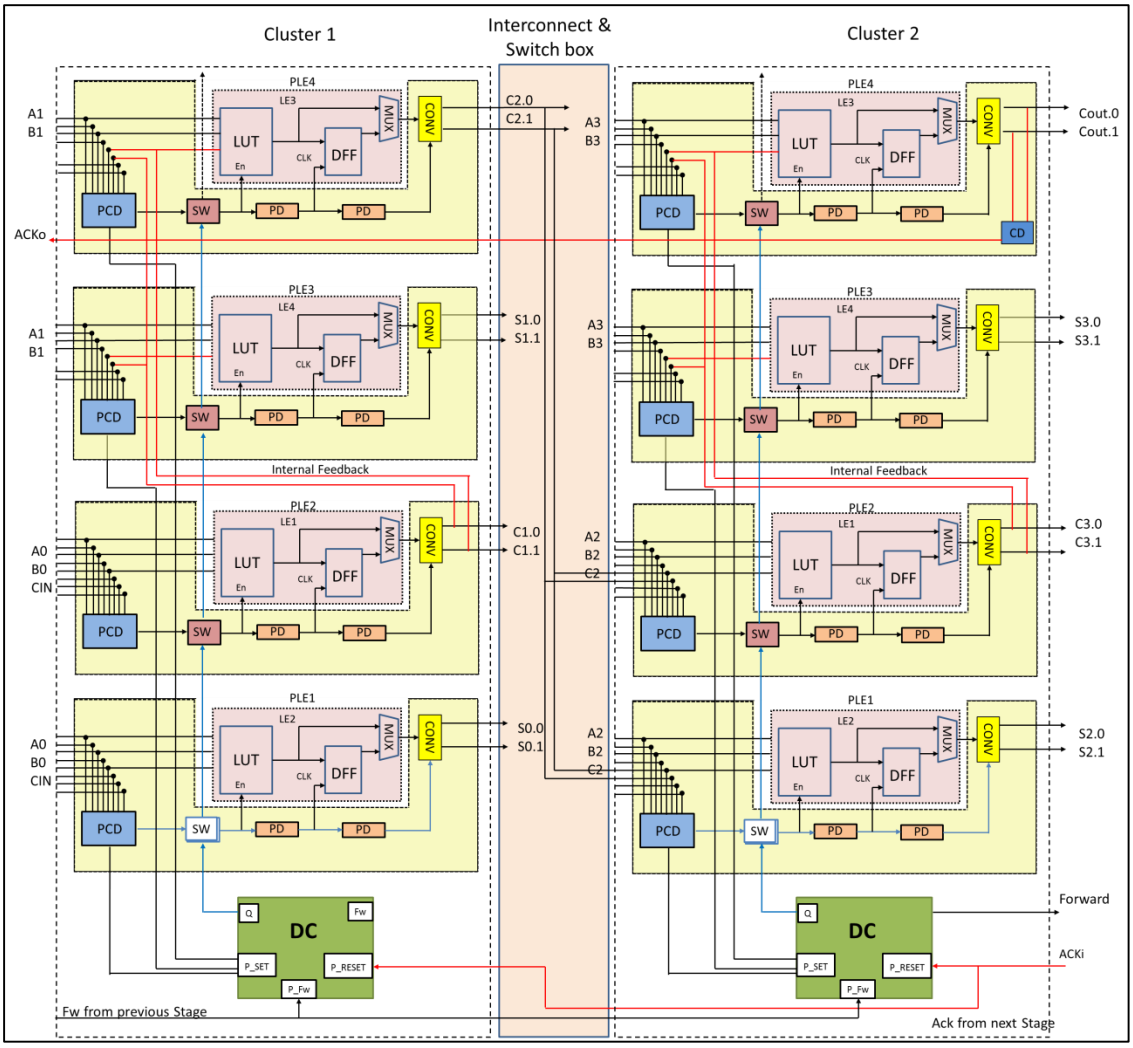

Figure 53: Four bit full Adder example.

Signals A0-A3, B0-B3 and CIN are assumed to be from the previous stage. The arrival of the signals can be in any order due to irregular interconnect lengths and computation latencies, based on the assumption of overall DI inter-cluster communication. When some of the inputs, A0-1, B0-1, CIN, from the previous stage have arrived in Cluster 1, some of the PLEs in this cluster can start computation. For example, LE2 may start its computation to generate its carry out signal C1. The trigger signal for LE2 was initiated from its corresponding

PCD once valid A0, B0 and CIN signals have been detected without any mediation from the DC control.

The C1 signal generated by LE2 is fed via an internal feedback channel (such channels were mentioned above although they are not shown in Figure 11) to satisfy the PCD conditions of LE3 and LE4. Their PCDs produce two trigger signals to the DC, which is waiting to collect these along with the PCD signal from PLE1. Once all three of these signals have been collected by the DC, it generates a merged trigger signal for the parallel triggering of LE4, LE3 and LE1. This merged trigger signal is in fact passed through all four PLEs through a chain consisting of all four SWs. The SW in PLE2 will not generate a second trigger locally for LE2 because it is programmed to respond to its local PCD instead of the DC control. The resulting concurrent action among PLEs 4, 3 and 1 generates three latched outputs S0, S1 and C2.

After both clusters have completed their computations, the acknowledgement signal ACK will be generated by the output CD together with the output data to allow the previous stage to clear its data. There may not be a need to collect the CDs from all PLEs for this acknowledgement, since the designer may view the cluster as a small enough block so that internal timing assumptions can be made. In this case, a subset of CDs is used instead. An acknowledgement is generated for the previous stage (only 1 “ack” for all input signals).

The forward signal (Fw) will then be generated once the previous stage releases its data and passes the control to the next stage to start a new round of operation. The same operation happens at the next stage interface, and once the data has been used, the ACK coming from the right will reset the DCs in both clusters 1 and 2. In this work, these "Fw" & "ack" control signals will be routed using the share flexible interconnect resources discuss earlier in section 2.2.9.

The circuit in this example demonstrates that not all PLEs must have all of the components included in Figure 39 in use. For instance, only when an acknowledgement signal is needed from a PLE will be use its right hand side CD block. The example also demonstrates the flexibility and programmability of the DC set and reset blocks. In this case, the DC setting is not directly related to the PCD of PLE2.

4.7.4 Design Flow

By retaining the LE structure of conventional FPGAs and having a similar organization at the cluster level, the proposed asynchronous FPGA architecture to a large degree allows the synthesis of PLEs or clusters through the existing FPGA design flow. Because of the replacement of clocks with the DC based distributed control, not all parts of the existing LE and LAB design flow can be directly applied. However, the basic mapping method should be

directly applicable in principle, although modifications are needed to accommodate the new control structure.

As for the DC-based distributed control, direct mapping for asynchronous circuits provides a suitable solution. Petri net specifications of the control path can be directly mapped onto a DC-based control structure. The proposed design flow for systems using this asynchronous FPGA architecture is shown in Figure 54.

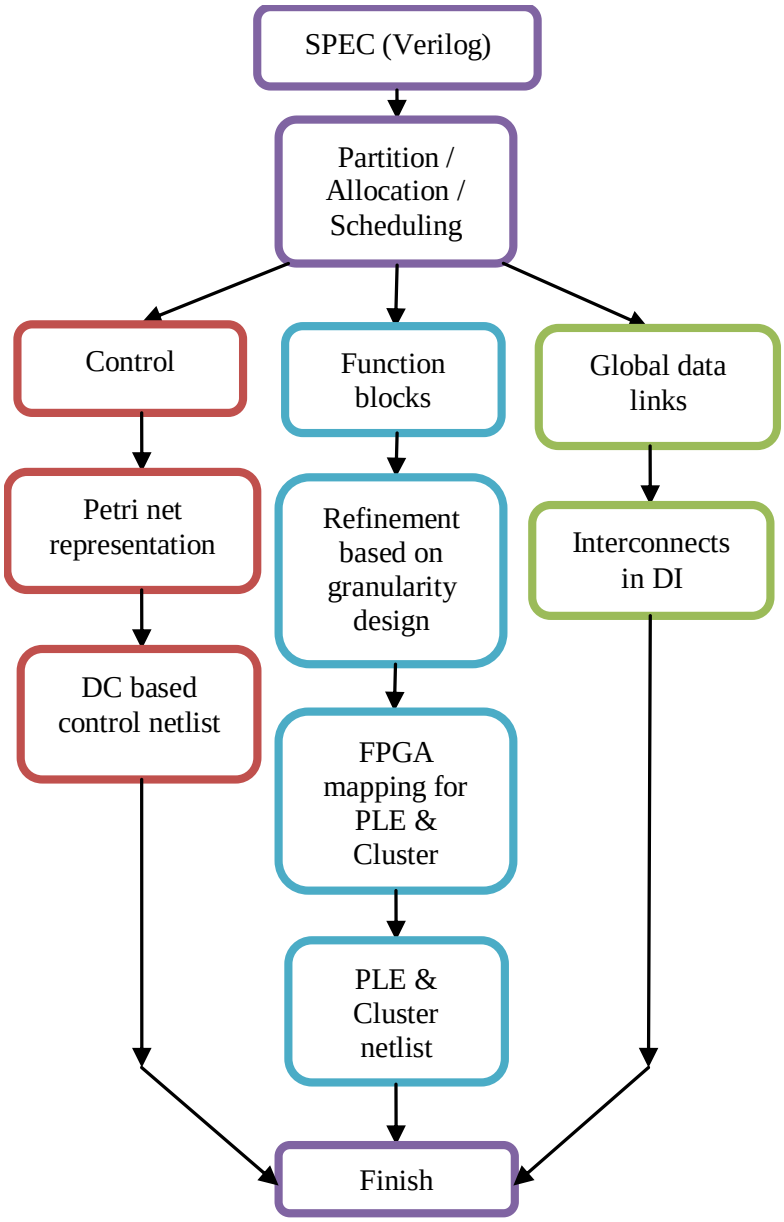

Figure 54: System design flow.

The system specification is assumed to be in a design language such as Verilog. Certain existing asynchronous FPGA design flows, based on de-synchronization techniques, apply the existing synchronous EDA toolkits directly. In this work, the Verilog specification, before applying the existing synchronous toolkits, is passed to the next step where, after partition,

allocation, and/or scheduling, the design is divided into control, data path function blocks, and global data links. This step is similar to the automatic division of control and data paths in the process described by Shang [135] and their techniques there can be re-used with minimal modifications. Here, only after partitioning are the functionalities synthesized using the existing synchronous toolkits.

Control is represented in Petri net models, which can describe all of the types of control flow found in a Verilog system specification. For instance, common control elements such as fork, join, and arbitration can be represented by the Petri net models in Figure 16 which is taken from [135].

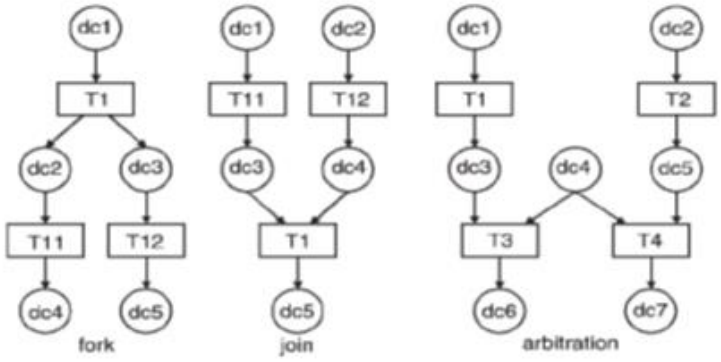

Figure 55: Petri net models of control elements.

Such a Petri net control model can then be used to generate the DC based distributed control with the direct mapping techniques described by [135]. For example, as shown in Figure 16, the positions in this Petri net model directly indicate the DCs. In other words, for each position in the control Petri net model, a DC is specified in the final implementation. The transitions and

connection topology among the DC positions are implemented through the SET and RESET logic of the DCs and the interconnections between them.

The data path function blocks can be similarly derived through a step of colour Petri net modelling [143]. Once the general function blocks have been synthesized, they need to be refined based on the FPGA's granularity for partitioning, depending on the PLE and cluster sizes. This is not available directly [143]. However, this is a standard step in converting a general VLSI design to FPGA implementation, and so the same methods can be applied. By keeping the PLE and cluster sizes of the conventional FPGA, this step is made straightforward. This is then followed by obtaining the PLE and cluster circuits using existing FPGA mapping techniques.

The global data interconnect fabric mainly consists of the channels for data communication. In this design flow it is implemented directly in dual-rail DI circuits. Their generation is also a straightforward process.

4.8 Summary

This chapter describes the detailed circuit realization of an asynchronous FPGA architecture. This is different from existing asynchronous FPGA architectures, and strikes a sensible balance between homogeneity to modern synchronous FPGA architecture and full asynchrony in places where it matters most, namely long interconnect links. This approach allows more flexibility in adjusting levels of DI according to application needs.

This approach retains the single-rail data representation of conventional FPGAs “in the small” or local cluster. This maximises the reusability of exiting FPGA logic mapping tools. On the other hand, by introducing delay-insensitivity “in the large” into the inter-block long data links, the variation tolerance and latency robustness inherent to asynchrony is provided.

This hybrid structure also provides advantages of both single-rail computation and dual-rail communication. This is due to the efficient computation with single-rail and the correct operation across a wide Vdd range from dual-rail asynchrony.

A number of structural choices were made; for instance, the granularity and block structures follow current commercial FPGA practice.

The basic building block of the architecture, the programmable logic element (PLE), has been designed in detail. It includes a number of finer grain components, including a logic element (LE) inherited directly from current commercial FPGAs, completion detection circuits and delay matching / data bundling circuits.

Programmable completion detection and bundling delays in the PLE cater for functional configurability and variation tolerance. This type of PLE has been shown to work under widely variable Vdd with reasonable latency and energy behaviours.

On the next level above, the PLEs are the clusters. The standard cluster has a David cell (DC) distributed control unit managing the operations of the PLEs in a cluster. This asynchronous control fully replaces the intra-cluster clock system in current commercial FPGAs, providing the complete equivalent functional set which includes both in parallel and sequential operations of the PLEs in any possible arrangement.

A design flow for systems in this architecture has been proposed which makes maximal use of existing asynchronous and FPGA synthesis methods. Case studies demonstrate the functional capabilities of the architecture. A four-bit ripple carry full adder showcases the flexibility of intra-cluster DC control. A further example additionally demonstrates inter-cluster control from a single DC.

Summary of the performance analysis shows that, although power and performance can be achieved with the asynchronous wrapper based technique, the area overhead is still substantial. In particular, the computation logic is compact compared with existing fine-grain asynchronous FPGA methods, but the fully dual-rail structure for interconnects required by DI may not be necessary. In the next chapter, the interconnect structure will be optimised based on information made possible from recent advancements in variation instrumentation and variability maps.

Chapter 5. Asynchronously Assisted Logic (AAL) Scheme

5.1 Introduction

Asynchronous logic has been shown to be more robust to variations but may have higher circuit size and power overhead compared to synchronous systems. However the degree of asynchrony employed in system designs is the result of a trade-off between resources and functionality, and the complete "DI in the large" method for interconnects the previous chapter may turn out to be too expensive. This chapter describes the implementation of Asynchronously Assisted Logic (AAL) hard circuit blocks into the Xilinx FPGA's CLB. This optimised scheme is intended to increase wide range latency variation tolerances caused by parametric, voltage supply and temperature (PVT) fluctuations, where there is a need, to improve on the global DI interconnect structure from the previous chapter. The proposed method suggests deploying configurable AAL blocks to reinforce only the variation critical paths with the help of variation maps, rather than to re-map and re-route. The layout level result shows this method's worst case increase of CLB overall size to be 6.3% only. If taking account of the interconnect area size into the area calculation, the area overhead will be significantly lower. This optimised variation aware strategy retains the structure of the global interconnect resources that occupy a large proportion of the modern FPGA's soft fabric, and yet still permits the

dual-rail completion-detection (DR-CD) protocol without the need of globally doubling the interconnect resources. Simulation results with the injection of voltage variability on both interconnect and computation blocks demonstrate the robustness of the method. The propose structure also allow implementations of several popular asynchronous styles to support different asynchrony at different variability levels. This chapter therefore provides the best scenario of practical implementation of variation tolerance support logic in FPGA for tolerating variability.

5.2 Architecture Overview

Asynchronously assisted logic methods is proposed here in order to provide the appropriate level of variation tolerance and yet still preserving as much of the modern FPGA overall structure as possible. This approach applies the asynchrony only when necessary provide the key for significant overhead minimization.

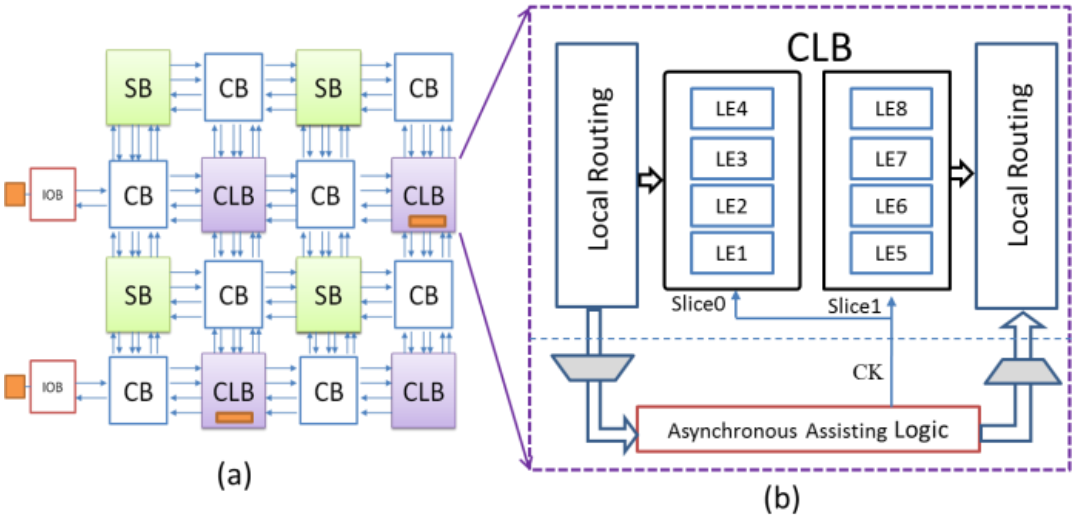

Figure 56: Architecture overview: (a) Island style architecture, (b) AAL within a CLB.

Figure 56 (a) Shows overview of an island style FPGA with AAL architecture. The structure preserves most of the common blocks of a typical FPGA such as the Connection Block (CB) and the Switch Block (SB). Four logic elements (LE) normally assemble a slice and cluster or CLB consist of two slices and some local routing resources. As in Figure 56(b), the method introduces an AAL block within a CLB with minimum expansion of MUXes bridging the existing local routing with the AAL when deployed without affecting the global interconnects. The impact on latency from variations could affect the data communications between CLBs. Therefore maximally one configurable AAL block can be introduced to each CLB to provide the appropriate degree of timing elasticity. Depending on how dispersed and the severity of the variations, the granularity of AAL placement can be reduced. As an example, in Figure 56(a) AAL was introduced on every other CLB. The area overhead evaluation and detailed

description of an AAL interface within a CLB will be discussed in the following sections.

5.3 AAL Architecture Implementation

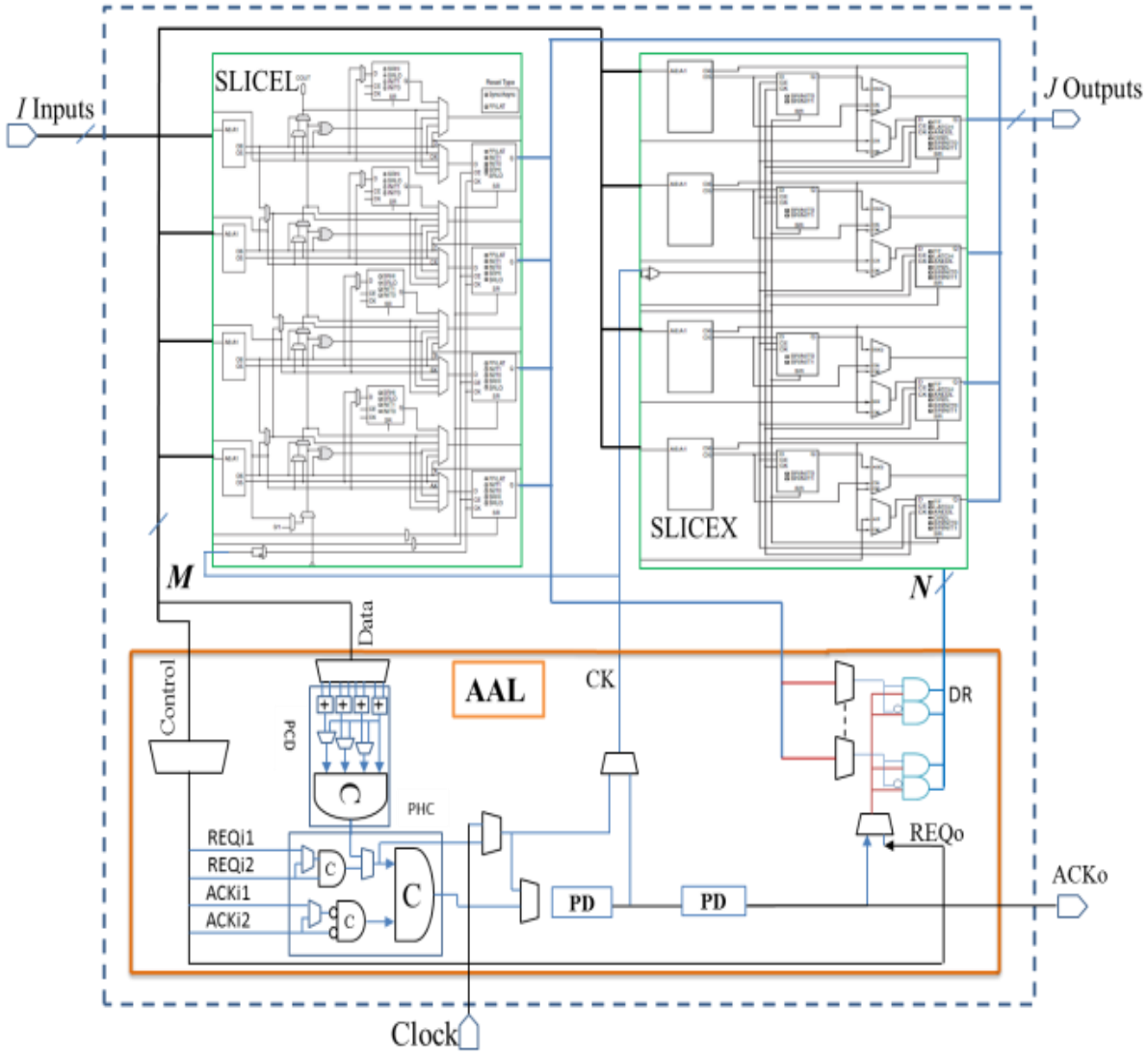

Figure 57: AAL plugin to Xilinx's CLB with SLICEL & SCLICEX.

Figure 57 shows a more comprehensive AAL block schematic view and its interface with the Xilinx's CLB containing a SLICEL and a SLICEX [144]. To

allow interchangeable communication between the synchronous clock and asynchronous handshaking signal controls, the trigger line (CK) has been made configurable in a CLB containing an AAL. There are M number data signal lines for implementation of dual-rail or 1-of-2 protocol. When configured as dual-rail, the utilization of slices in a CLB will be decreased. However this design tradeoff was aim to avoid the need of doubling the global interconnect resources. The output is also interchangeable between single-rail and dual-rail. There are N lines connecting the AAL dual-rail line to the spare MUXes inputs in SLICEX. Therefore, the J outputs and I inputs of the original CLB remain the same. The "ACKo" is the only extra line added in this case.

5.4 Area Overhead Calculation

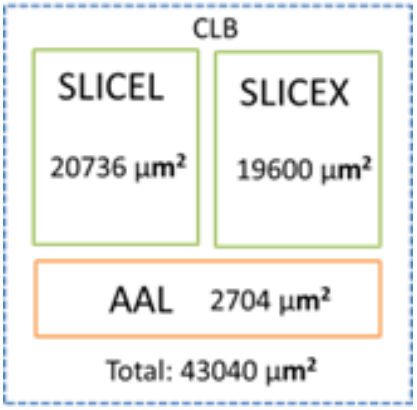

Figure 58 Area calculation of CLB with AAL.

The implementation of this design is in UMC-90nm CMOS technology and evaluated the area overhead of the AAL with a CLB containing a Xilinx's SLICEL and SLICEX. Both slices containing 6-inputs lookup table (LUTs) but

the more complex structure, SLICEL (20736μm^2) takes more layout area compared to SLICEX (19600 μm^2). The AAL occupies a layout area of 2704 μm^2 out of the total CLB size of 43040 μm^2. The area overhead of the AAL in this case is only 6.3%. If the more complex SLICEM [144] was chosen, the ratio will reduce further.

Table 9: Overhead of various asynchronous schemes.

Architecture	Wrapper Type	LUTs/ Wrapper	I/O Overhead
Fine-Grain AFPGA[6, 95]	Fine	1	>4x
Distributed Control AFPGA[69]	Medium	4	2x
AAL (this work)	Coarse	8	Same + 1

Table 9 shows the overhead comparison between different asynchronous FPGAs architectures. The fine-grained architecture provides every logic element with a wrapper increasing the size of the global interconnect resources over 4 times higher. The main advantage of this type of architecture is potential fine-grain pipelining for high throughput and high reliability. Yet, the overall overhead in size is too large, reduces the chip functional density and to some extent negates the technology scaling objective. Distributed control AFPGA proposed in [69] reduced the overhead to the factor of two with clustered architecture wrapped four LUTs with a wrapper. The wrapper consists of dual-rail handshaking logic plus a distributed David Cell (DC)

controller. However, this medium grain scheme still doubles the global interconnect for dual-rail communication. The DC based controller was also made to be programmable to accommodate multiple combinations of control logic. Due to the extra-configurable resources, the wrapper occupied about 50% of the CLB area. This newly proposed scheme use spare resources in the existing slice structure and are trading the utilization of CLB with interconnects overhead. The reduced utilization of CLB when AAL are deployed is acceptable in this context because only the Variation-critical path (VCP) will be used. This can be achieved with the help of tools that allow the identification VCPs. The overhead reduction is very significant and makes more sense as indicated from simulation results in the following sections.

5.5 Multi-Style Handshaking Support

An FPGA's functional implementation is defined after fabrication. Although this may make it suffer more from the variability at nanometer scale regime compared to ASIC design, FPGA provides a unique opportunity to reconfigure unused resources to mitigate the problem, for example to remap the degraded computation block to a region that is not used [77, 81]. The re-routing and re-mapping techniques are interesting and may work well. However, the place and route process normally takes a lot of time and effort. Even worse, it may be too late for the system to sense its level of degradation before system starts

malfunctioning. We therefore propose to enhance the VCP path with AAL that is highly tolerant to variation and does not require exhaustive P&R efforts.

The AAL block provides the flexibility to implement various styles of asynchrony, including single-rail bundled data (SR-BD), dual-rail completion-detection (DR-CD), and hybrid completion-detection (HB-CD) as needed. The structure consists of Programmable Completion Detection (PCD) block, Programmable Handshake Circuit (PCH) and Programmable Delay element (PD) [69] as shown in Figure 57 and Figure 59.

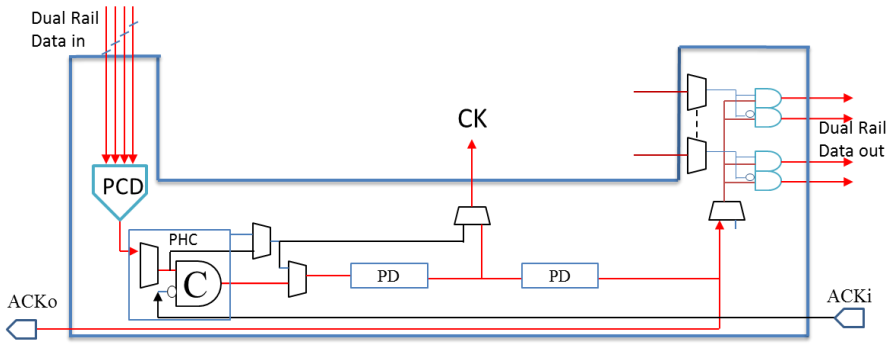

Figure 59: Dual-Rail Completion-Detection (DR-CD) resources.

Figure 59 shows the resources used when the AAL is configured to the DR-CD mode. Complete arrival and retrieval of all dual-rail valid input data are detected by the PCD and PHC for handshaking between AAL blocks. In this scheme, encoding within the data itself provide the trigger signal "CK" substituting the global clock. The PDs in between the "CK" are closely matched with its corresponding slices. Internally delay matching is acceptable as the variation within a small region is more manageable. Output data from this

scheme can be then converted into dual-rail before propagated to the next stage. Figure 60 show an example implementation of a four stage pipelined 4-phase DR-CD using AAL.

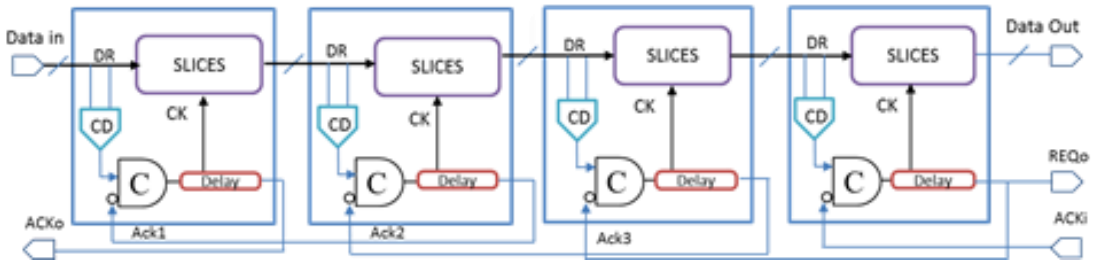

Figure 60: Four Stages implementation of DR-CD circuit.

In the SR-BD scheme, the handshaking relies closely on the local matched delay line. Data are remained in single-rail and not used as part of the control; hence the PCD is not used (Figure 61). This scheme basically replaces the global CLK trigger line with the locally handshaking CK trigger. The main benefit of this structure is simplicity in control handshaking and circuit size that will result in higher operational energy efficiency. Investigation of throughput vs energy performance of the architecture will be discussed in the next section. Figure 62 shows an example implementation of this bundled-data delay matching circuit in four stages.

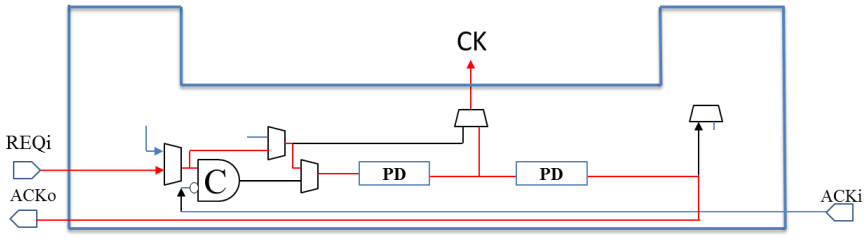

Figure 61: Single-Rail Bundle-Data (SR-BD) resources.

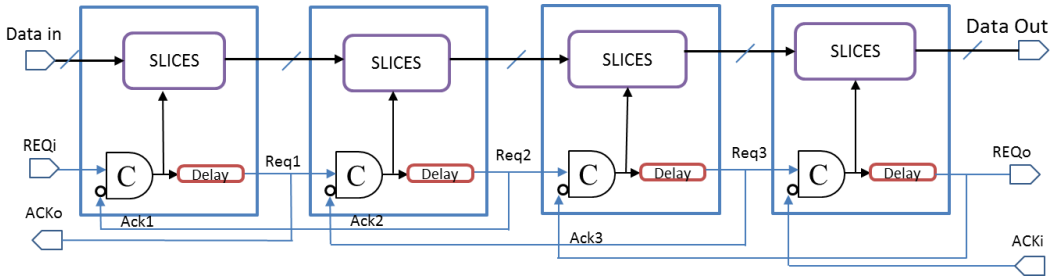

Figure 62 Four Stages implementation of SR-BD circuit.

It is also entirely possible to mix and match these two most popular asynchronous handshaking protocols through one data path (HB-CD), depending on where along that path there may be very long interconnects or where interconnects are compromised by variability. In addition, the global clock could be passed straight through, which basically reverts the CLB back to the conventional synchronous behaviour using the switching resources as shown in Figure 63.

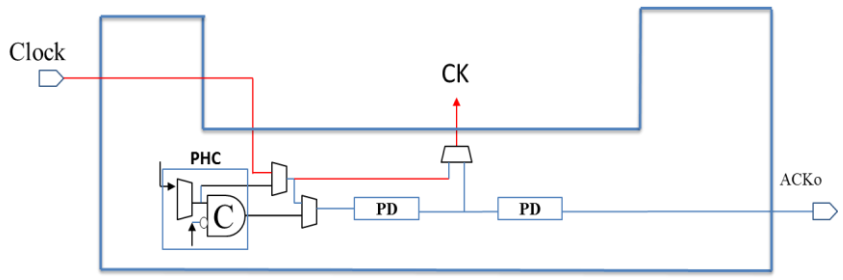

Figure 63: Clock triggers switching.

5.6 Proposed Variation Aware Design Flow

The overall system design approach when the AAL method is used is somewhat different from that for the conventional FPGA architecture. With AAL blocks managing the timing of inter-CLB data communications, place and route is less concerned with ensuring that such data delays are always correct, and therefore chip area utilization and other factors can be optimized with more freedom provided by the additional timing flexibility. The general system design flow is shown in Figure 64.

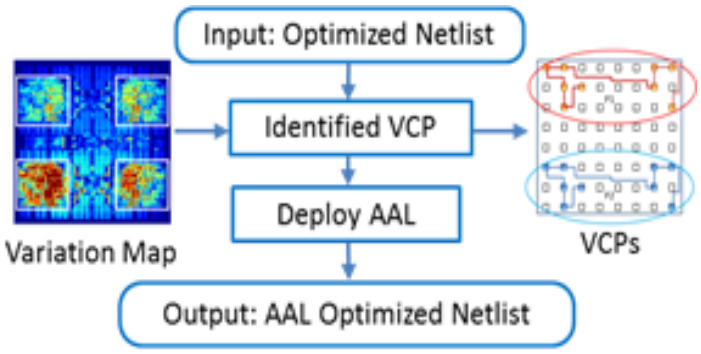

Figure 64: Design flow based on variation map.

5.7 Throughput and Operation Energy Study

The AAL method provides the flexibility of configuring inter-CLB data connections into a full spectrum of different degrees of asynchrony, from completely depending on the global clock, to single-rail asynchrony based on timing assumptions, to fully completion-detected DI. Based on theory they would provide opportunities to trade communication reliability with energy costs. In this section, we attempt to quantitatively study the energy and speed/throughput characteristics on the three styles of asynchrony provided by the AAL method, i.e. everything based on timing assumptions, everything fully completion detected, and a judicious hybrid of the two.

A case study approach is used in this exploration. First, the FPGA logics are configured into a 4-bit ripple-carry-adder (4RCA) and follow by an extended version – a cascade of four 4RCAs (4x4RCA) for a longer critical path. The examples are selected deliberately for the easy identification of critical paths.

5.7.1 Short Critical Path

Figure 65 shows the test setup. Input B of the adder changes (from increment counter) on every complete computation circle based on the valid "Cout" signal - the critical path. A closed loop simulation was run for a fixed amount of time (200ns) and the number of counts from the incremental counter was recorded together with the overall operational energy.

With a single adder and short critical path, the comparative simulation results (at the nominal voltage, 1V) are presented in Table 10. The results show that SR-BD has the highest efficiency (throughput over overall operational energy) compared to the other two setups. SR-BD performance can also be closely benchmarked equivalent to the synchronous design for the reason that matching delay lines were carefully tuned to the data-path. This is similar to the clock frequency setting based on critical-path in typical synchronous system design. Further performance investigations with a supply voltage sweep between 0.4-1.0 volts are shown in Figure 66(a) shows that both (DR-CD) and (HB-CD) consistently produce lower throughput for relying on the slow handshaking protocol. The operation energy graph in Figure 66(b) also indicates, because of the extra dual-rail and completion-detection logics implemented, the circuits are larger and use more power. However, the HB-CD design can improve the efficiency.

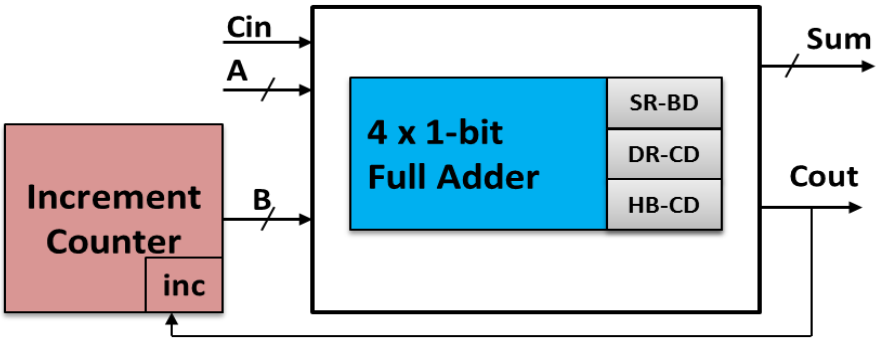

Figure 65: Test setup for 4RCA.

Table 10: Comparison result for short path (4RCA).

Circuits (4RCA)	Throughput (counts)	Operational Energy (pJ)
SR-BD	23	29.49
DR-CD	18	37.28
HB-CD	18	24.64

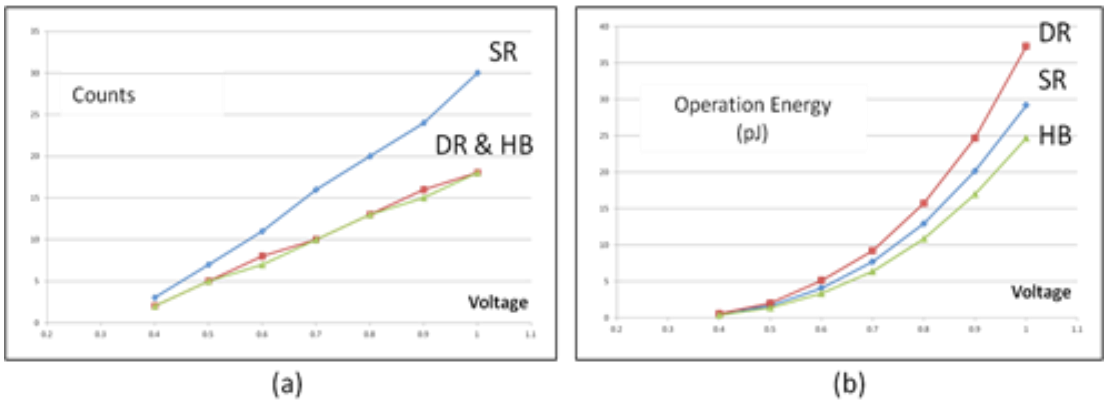

Figure 66: Throughput and energy comparison (Voltage sweep, 0.4 - 1.0v), (a) Throughput (Counts), (b) Operation Energy (pJ).

5.7.2 Long Critical Path

For longer critical path experiment, an an extended version – a cascade of four 4RCAs (4x4RCA) are implemented in four styles. A typical 16-bit ripple-carry-adder (RCA) as a synchronous design is followed by three asynchronous implementations of 4x4-bit (RCA). The experiment setup is shown in Figure 67 including an increment counter that records the loop iterations. Same incremental counter used for input data B. This setup is common to all the four mentioned examples.

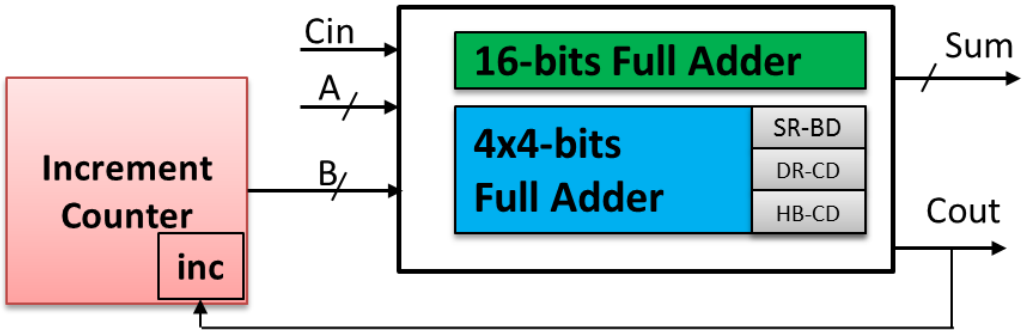

Figure 67: Test setup for 16RCA and 4x4RCA.

The same test vector is applied onto all four designs and fixed time (200ms). Close loop stimulations were run to measure the throughput/counts and average power performances. Results of the simulation are presented in Table 11: Throughput and energy performance. Note that, in the single-rail delay-matching (SR-DM) synchronous 16-bit configuration, the 16-bit RCA's critical path delay line is carefully tuned to match the synchronous clock speed representation.

Table 11: Throughput and energy performance.

no	Circuits	Throughput (Counts)	Operation Energy (pJ)
1.	Single-Rail Delay-Matching (SR-DM) (Non-Pipeline)	6	22.63
2.	Single-Rail Bundle-Data (SR-BD)	15	52.27
3.	Dual-Rail Completion-Detection (DR-CD)	15	81.79

4.	Hybrid Mix-Rail Completion-Detection (HB-CD) (Carry Chain Only)	15	66.53

The maximum count achieved by SR-DM is 6 with an energy consumption of 22.63pJ. In the 4x4-bit configurations, higher throughput was achieved (15 counts). This is due to the pipelined natural of the circuits. DR-CD design used highest energy because of fully dual-rail completion detection scheme and the SR-BD uses much lesser energy for the same throughput. However, this scheme relies more on timing assumption, and may not be as robust as DR-CD.

HB-CD, on the other hand, reduces total operation energy for maintaining the same throughput. In this case, a hybrid approach may be beneficial provided the critical path is carefully determined based on a somewhat accurate variation map – full accuracy is only needed for the data lines covered by timing assumptions. A hybrid asynchronous control of data communication between CLBs is exactly where the AAL method excels.

5.8 Variability Study

In addition to manufacturing process variations, it is also crucial to account for potential FPGA operation mode variations post-configuration such as fluctuations of voltage and temperature. In this section we study how the addition of asynchrony might make FPGA circuits more tolerant to voltage variations.

5.8.1 Global Variability Simulation

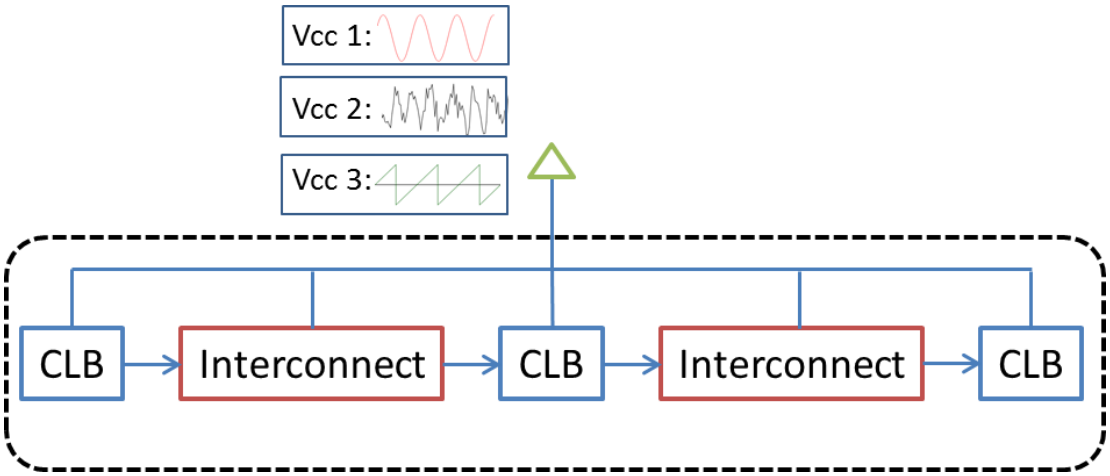

Figure 68: Global Vdd variation simulation setup.

In the previous section, we demonstrated that all three configurations performed correct functions without logic errors under constant Vdds in the range of 0.4V-1.0V in 90nm CMOS technology. Using the DR-CD (dual-rail, most robust) setup in the previous section, we repeat the tests with three dynamic voltage sources as illustrated in Figure 68. The summary of the voltage sources presented in Figure 69 is as follows:

- Vdd 1: Continuously varying voltage (sinusoidal, 0.4-1V, 30MHz).
- Vdd 2: Random varying voltage (Gaussian, $\mu = 0.9$, $\sigma = 0.12$).
- Vdd 3: Switching Capacitor from energy harvesting sources (Saw-tooth, 0.6-1.0V, 50MMz).

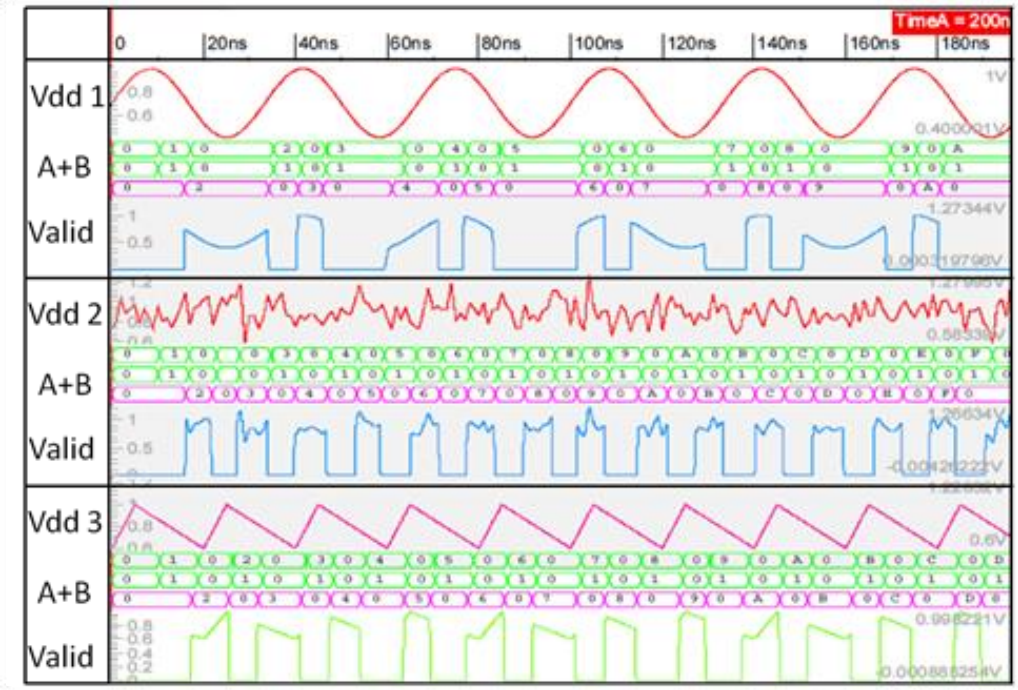

Figure 69: Correct operation under various viable voltage supplies.

Vdd 1 is a relatively slow changing voltage and this can be closely related to correlated process variation and slow aging variation. Delay normally increased with the increase of temperature. Towards lower geometry below 65nm, 45nm, 38nm and beyond at lower threshold voltage, the temperature shows contrarian effects on cell delay [27]. Also within-die variation can be random and fluctuates independently of device location. Therefore Gaussian noises are presented in Vdd 2. Energy harvesters tend to provide variable levels of power. The output waveform of a switching capacitor DC-DC converter in [33] shows in Vdd 3. From these results it can be seen that the circuit works under all three variable sources without errors at every increasing loop on the data value.

5.8.2 Interconnects Variability Simulation

In previous section [145], the robustness of the design with global Vdd variation under three variable power supply sources was demonstrated. In this section, we going to investigate the voltage variability effects on interconnect latency and it's potential impact on the correct operation as illustrated in Figure 70 In FPGAs, a large proportional of the fabric are made of interconnect blocks. Variations in interconnect could dominate the global system performance. This section study the structure performance under gradual and random variable voltages presented in the global interconnect.

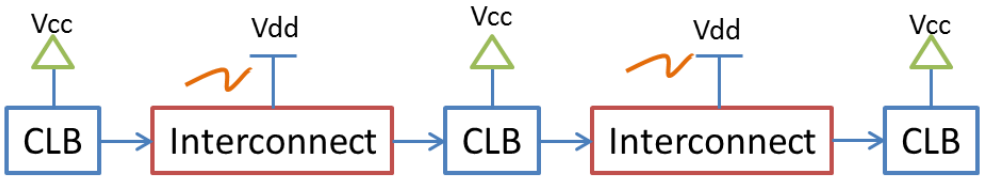

Figure 70: Mixed constant Vcc on CLB and variable Vdd on interconnect simulation.

The most robust DR-CD implementation in the previous section was reused but with all interconnects replaced with analogue models that are made of non-standard cell inverter chains. The simulation was done in the mixed signal mode – all CLBs are using standard cell with fix 1V Vcc supply, while interconnects used custom cells and are powered with variable Vdd supplies. The result in Figure 71 shows the correct operation of adder under two variable voltage sources: Vdd1, a constantly changing voltage between 0.5-1.1V at

25MHz with a sinusoidal shape, and Vdd2, a random variable voltage source with Gaussian distribution ($\mu = 0.9V$, $\sigma = 0.12V$).

Variations in the supply voltage result in timing variations of the interconnect line. Both data and control lines that are connected through the global resources will be affected. However, it can be seen that the circuit works under both variable sources without errors with the correct output sum value on every cycle. The validity of the data was aligned with the "Valid" signal from the output of the dual-rail completion-detection block sampling at the legit output values and not spacers.

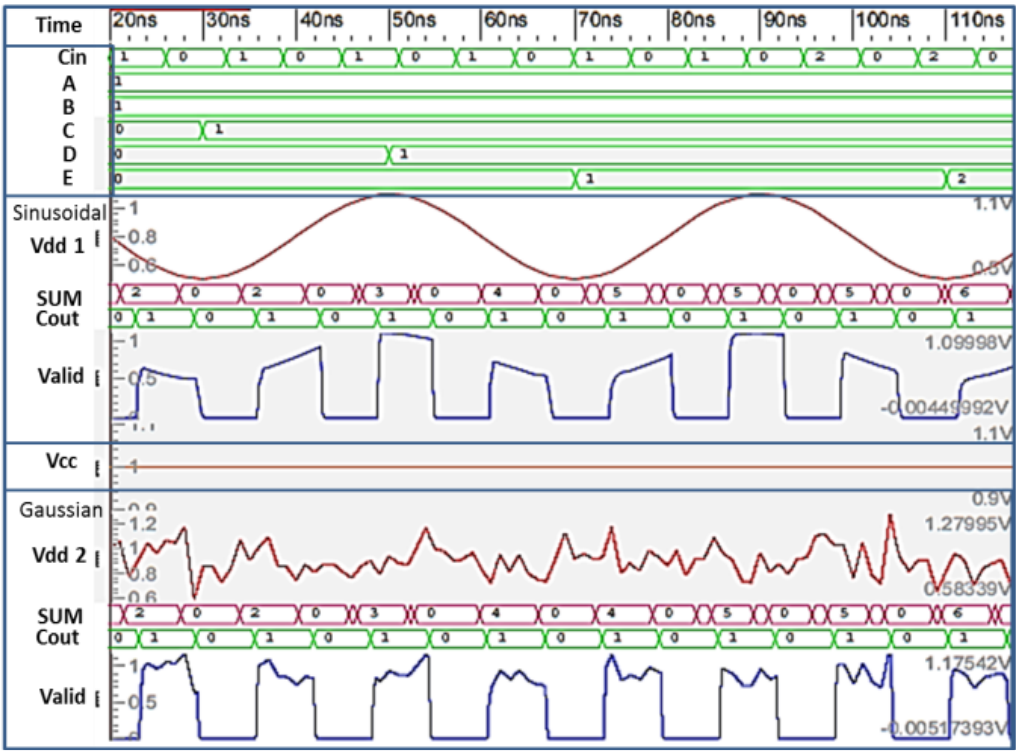

Figure 71: Interconnect variation simulation results

5.9 System Design on AAL structure

This section addresses the implementation of more complex systems using the AAL method.

5.9.1 Handshaking Support for Data Flow Structures

The AAL blocks provide flexibility for implementing various handshaking protocols. A full data flow control structure supports Linear, Fork, Join and Merge elements. These elements allow the construction of more complex system when needed. The 4-Phase Dual-Rail (4P-DR) implementation is slightly different compares to the 4-Phase Bundle-Data (4P-BD) due to part of the control has been embedded in the data line itself.

Table 12: Data flow control elements.

Component	Petri- Net Representation	4-Phase Dual-Rail	4-Phase Bundle-Data
Linear	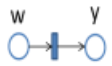	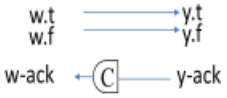	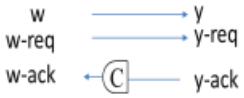
Fork	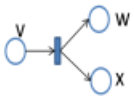	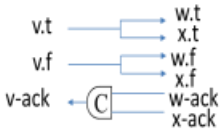	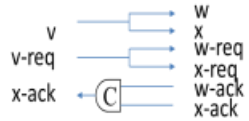
Join	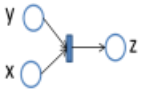	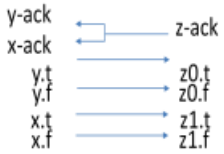	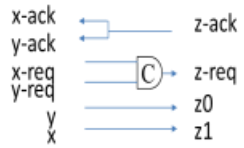
Merge	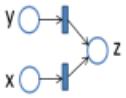	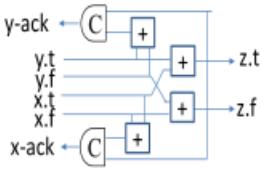	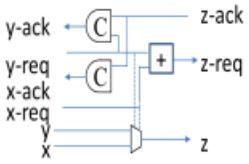

The summaries of implementation elements of both are shown in Table 12 together with their Petri-net (PN) [131, 143] representations. PNs can be graphical and mathematical representations of discrete system. It's the extension of Finite State Machines (FSMs) model for both sequential and concurrent circuits. Therefore it's highly used for modelling asynchronous logics. Table 12 shows that the basic handshaking control for 'linear and fork' are the same for 4P-DR and 4P-BD. For the "join" component, because the dual-rail data itself can carry valid detection for the controller, therefore no extra 'C' element is needed as in the example used in 4P-BD for the "x-req" and "y-req" signals. For similar reasons the merge handshake controller is designed differently between the 4P-DR and 4P-BD.

Following subsection will demonstrate the building of a 4P-BD sub function with most of the components listed in the Table 12

5.9.2 Booth Multiplier Case Study

This section describes a Booth's multiplication algorithm system in the proposed AAL structure with the above-mentioned handshaking components. Figure 72 shows the block diagram of a four by four-signed binary multiplication. This structure is of interest for study because the adder example used for performance study in section IV can be reused with minimum alteration as shown the 9-bit adder in the diagram. Also Booth's multiplier provides balance between speed and area utilization using repetition adding and shifting. The multiplier value is first extended and stored in register "A_reg" and its two's complemented value is stored in "S_reg". Conditioned by the last two bits of the product accumulator register "M", addition or subtraction will be performed between the multiplicand "P_reg" with the "A_reg" or "S_reg" within a set number of iteration controlled by a counter.

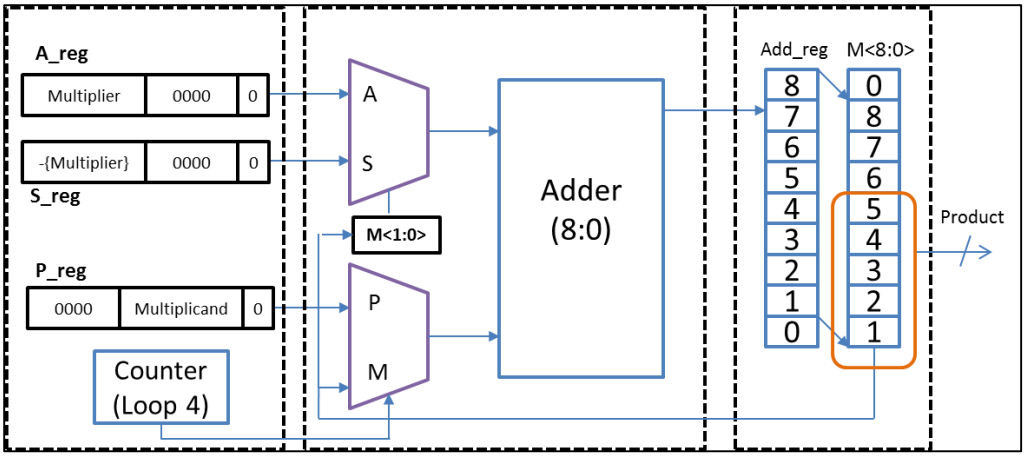

Figure 72: Block diagram of Booth multiplier.

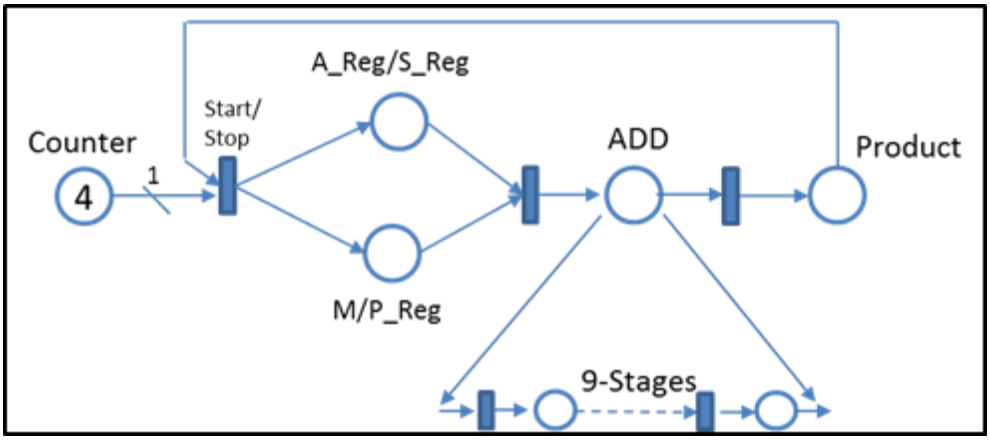

Figure 73 : Petri-net representation of booth multiplier control flow.

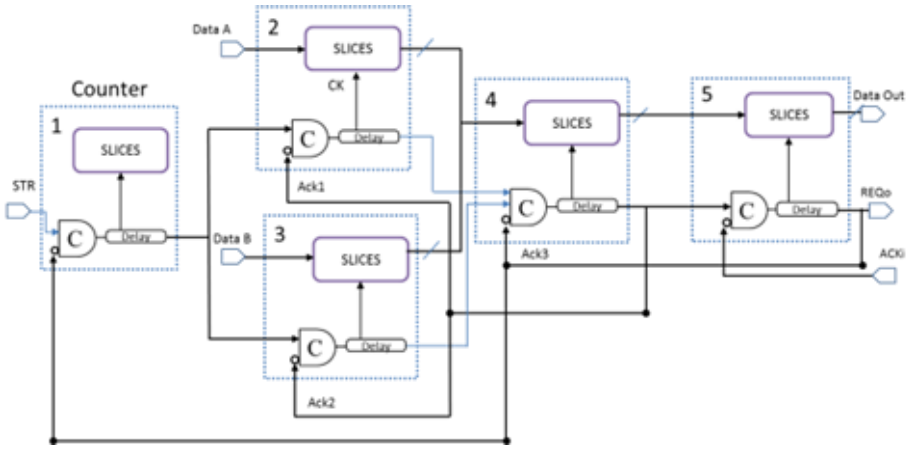

Figure 74: Simplified SR-BD handshaking diagram for Booth multiplier.

Figure 73 shows the data flow diagram using PN representation for the implemented the above Booth's Multiplier and matching with components in Table 12: Data flow control elements, the simplified handshaking building block on CLB with AAL block can easily be constructed as in Figure 74.

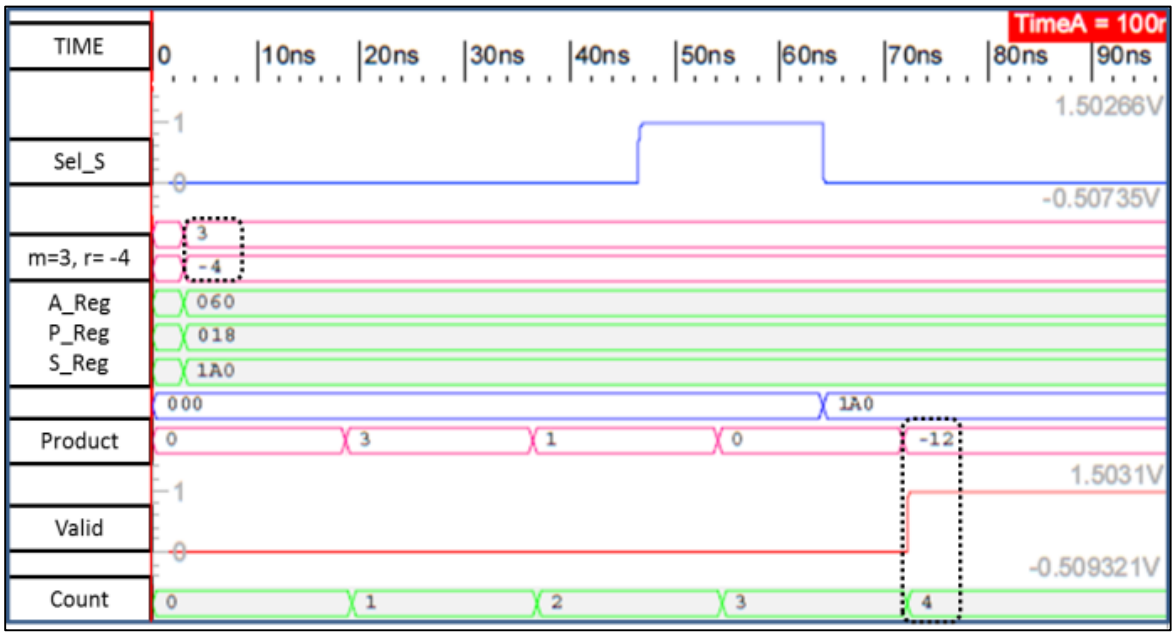

Figure 75: Simulation waveform of Booth multiplier implementations.

The simulation result using Cadence tools is shown in Figure 75. The waveforms show a multiplication of two 4-bit numbers (m = 3 and r = -4). The manipulated equivalent of 'm' and its two's complement value are stored in A_reg and S_reg individually as 9-bit data in hexadecimal format. For 'r', the manipulated value is store in P_reg. The number of iterations loop is determined by the bit length of value 'r'. In this case, after four counts, a correct product value of "-12" is produced demonstrating the correct operation.

5.10 Summary

This chapter aims to present the integration of robust AAL block into existing Xilinx FPGA architecture. The proposed structure does not increase the interconnect resource much as compared to typical asynchronous FPGAs that would at least double the interconnect resources to support dual-rail connection. The die overhead calculation on layout level shows that incorporating AAL into a Xilinx's CLB with SLICEM & SLICEX only incurred 6.3% of die area overhead at the maximum. The AAL design allows the configuration of different styles and degrees of asynchrony for data links between CLBs, depending on specific requirements. Quantitative case studies using a 16-bit RCA also show that potential throughput improvements can be achieved when AAL handshake can be pipelined. In addition, simulations also show that the power efficiency can be improved with the hybrid implantation of DR-CD protocol on critical path only and keeping the rest single-rail. The most robust form of asynchrony is shown to be reliable under radical timing variation caused by varying voltages on interconnects. A case study of Booth's multiplier shows the feasibility of building a more complex system on AAL structure.

With the AAL hardware support and potential variation aware design flow, a more practical and industry acceptable scenario would be more feasible. Standard industrial design flow assumes only one set of bitstream needs to be

generated for a large batch of chips implementation. Thus, compared with traditional variation aware techniques that require expensive computation for re-routing and re-mapping the whole design on the basis of a unique variation map for each chip, AAL technique may avoid this. Summary of such approach will be discussed in the final conclusion chapter.

Chapter 6. Conclusion

6.1 Summary of Thesis

This thesis presents a set of practical techniques for incorporation asynchronous logic into modern FPGAs architectures as a method of dealing with the increasing variability issues face by current and future sub-nanometer technologies.

This approach based on Asynchronously-Assisted Logic (AAL) makes it possible to provide the right degree of asynchronous hard microcircuit while keeping most the conventional FPGA structure intact. The AAL method facilitates the architecture with hard asynchronous components that is distributed around the fabric, thus equips the architecture with robust hardware resources to combat against timing variation. (Traditional methods either modified the architecture greatly for fully asynchronous implementation or betting on P&R tools to impose asynchrony logic on exiting FPGA architecture, which is not ideal).

On the way towards the AAL approach, a hybrid FPGA architecture that wraps conventional synchronous FPGA logic blocks with distributed asynchronous control based on David's cell options was developed. This approach preserves the single-rail data representation of current FPGAs "in the small", it is possible for designers to use existing FPGA logic mapping tools in block design.

By introducing delay-insensitivity “in the large” into the inter-block long data links, the variation tolerance and latency robustness inherent to asynchrony is provided. A number of structural choices were evaluated including the granularity and block structures. This provided the foundation on which the AAL approach was developed.

Several existing solutions to the variability problem exploit the reconfiguration features of FPGAs. For example the late binding techniques suggest performing part of the mapping and routing process as late as possible leveraging the unique variation characterising of each chip. The proposed AAL method provides a complementary solution to existing variation aware late binding approach where delay characterisation is first performed and then techniques such the region relocation, logic replacement and path rerouting techniques can be applied, with AAL it will be reinforcement. The reinforcement strategy suggests retaining the placement and routing and supporting the variation critical regions or paths variation robust hardware components thus minimising the effort for recalculating the new configuration in FPGA.

Implemented on Faraday 90nm standard cell library on Cadence tools, the worst case increase of CLB overhead in the layout level is 6.3% when integrated into Xilinx’s vertex 6 architecture. Considering the interconnect resources that occupy the biggest slice of the FPGA fabric, the overall size

increase for consolidating the AAL block could be significantly lower at around 2%.

Furthermore, the AAL resources support multi-style asynchronous implementation in tolerating wide range of timing variability. As reviewed in chapter 2, the choice of asynchronous implementation style is fixed during the specification process motivated mainly for speed or power performance. This reduced the flexibility for tolerating wide range of variability. For example the bundle data approach is more energy efficient but because it relies heavily on the timing assumption, this makes it not suitable to deal with spatial and random variation. Alternatively, a highly-pipelined 4phase dual-rail (4P-DR) structure choice is made; the robustness of the architecture will be trading-off with the huge area overhead.

The AAL approach avoids the need to globally double the interconnect resources to permit either of these handshaking implementation and combination benefit of SI/DI schemes. The adjustment is made by reduces the logic utilisation of a CLB if AAL is deployed. This is not unreasonable at the assumption that AAL will only be deployed on a few targeted variation-critical paths (VCPs). This technique has been successfully implemented with a case study demonstrated in chapter 5.

6.2 Future Work

This thesis presents an approach for the practical implementation of asynchronous logic to assist with the growing variability issue in digital circuit design. There are several areas in which this approach could be extended.

6.1.1 Variation Aware Design Flow with Consolidated Variation Map

The variability issue will inevitably impact the reliability and timing yield of future generation FPGA. In this thesis a hardware optimized solution has been proposed, however this needs to be supported by a design flow or automated tools. With the assumption of mature off-line and online sensing techniques, each chip can be characterised and treated differently. A few variation aware techniques were discussed in chapter 2, however in all these papers, either only the process variability is considered or in some, the run-time thermal variation. Considering one single variation map may not give a comprehensive view of the variability problem. It is therefore important to develop an algorithm that consolidates both process and run-time variation maps for a more realistic variation aware flow.

6.1.2 Cross Domain and GALS Scheme Study

Proposed AAL technique suggests multiple asynchronous handshaking protocols can be collaboratively worked together. However detail study needs to be performed for seamless integration to avoid complex intermingle of different protocol in a design. Also, data transfer between asynchronous and

synchronous domain would be expected in such implementation. This is in some degree make the system similar to the heterogeneous GALS and multiple-clock-domain system. Mixed timing domain in a system makes the timing-closure and global-clock distribution difficult to achieve. One of the solutions to deal with the global and local communication speed mismatch is to make them insensitive to the latency. The Globally Asynchronous Locally Synchronous (GALS) methodology does not enforce globally synchronized clocks. Instead, communication between modules occurs asynchronously. This approach has been popularly used by industry today to implement large SoC with sub-modules running on different clocks. This trend is expected to extend into future multi-core processors and NoC system. The proposed AAL architecture may fit into this paradigm closely. However, the modification and design of asynchronous and synchronous domain adapter circuits need to be further explored, especially in terms of balancing throughput and size overhead.

6.1.3 Silicon Implementation

The motivation and focus of this work is centred on the practical implementation of FPGA architecture with enhancements for variability. The architecture circuit has been designed and simulated in the Cadence tools environment using both UMC-90nm and Faraday 90nm technology. It would be beneficial, to develop a better sense of context to have the design evaluated in smaller technology nodes such as 45nm or below if the tools and foundry

library are made available. Also, implementation of the developed architecture in silicon for further testing and verification would be a natural next step.

Appendix A: Abbreviations

2P-DR:	2-Phase Dual-Rail
4P-DR:	4-Phase Dual-Rail
ASIC:	Application –Specific Intergraded Circuit
CAD:	Computer-Added-Design
CB:	Connection Block
CD:	Completion Detection
CMP:	Chemical Mechanical Polishing
CPLD:	Complex Programmable Logic Device
DC:	David Cell
DI:	Delay Insensitive
DPA:	Differential Power Analysis
DR-CD:	Dual-Rail Completion-Detection
DR-CD:	Dual-Rail Completion-Detection
DSP:	Digital-Signal-Processing
DUT:	Device-Under-Test
EEPROM:	Electrically Erasable Programmable ROM
EMA:	Electromagnetic Analysis
FSM:	Finite State Machine
FU:	Functional-Unit
GALS:	Global Asynchronous Locally Synchronous
HB-CD:	Hybrid Completion-Detection
HCI:	Hot-Carried-Injection
HDL:	Hardware Description Language
IoT:	Internet-of-Thing
IP:	Intellectual Property

LC:	Logic Cluster
LE:	Logic Element
LEDR:	Level-Encoded Dual-Rail
LER	Line-Edge-Roughness
LUT:	Look-Up Table
NBTI:	Negative Bias-Temperature Instability
NoC:	Network-on-Chip
NRZ:	Non-Return-Zero
P&R:	Placement and Routing
PAL:	Programmable Array Logic
PBTI:	Positive Bias-Temperature Instability
PCB:	Printed Circuit Board
PCD:	Programmable Completion Detection
PD:	Programmable Delay
PL:	Phase Logic
PLA:	Programmable Logic Array
PLD:	Programmable Logic Devices
PLE:	Programmable Logic Elements
PN	Petri-Net
PROM:	Programmable Read-Only Memory
PVT:	Process, Voltage and Temperature
QDI:	Quasi Delay Insensitive
RCA:	Ripple-Carry-Adder
RDF:	Random-Dopant Fluctuation
RO:	Ring oscillator
RTA:	Rapid Thermal Annealing
RZ	Return-to-Zero
SB:	Switching Block
SCA:	Side Channel Attack

SI:	Speed Independent
SoC:	System-on-Chip
SPA:	Simple Power Attack
SRAM:	Atatic-Random-Access-Memory
SR-DM:	Single-Rail Direct-Mapping
SR-DM:	Single-Rail Delay-Matching
SSTA:	Statistical static Timing Analysis
STA:	Static Timing Analysis
TDDB:	Time Dependent Dielectric Breakdown
VCP:	Variation-Critical Path

Appendix B: AAL Implementation

Incorporating AAL into Xilinx's CLB

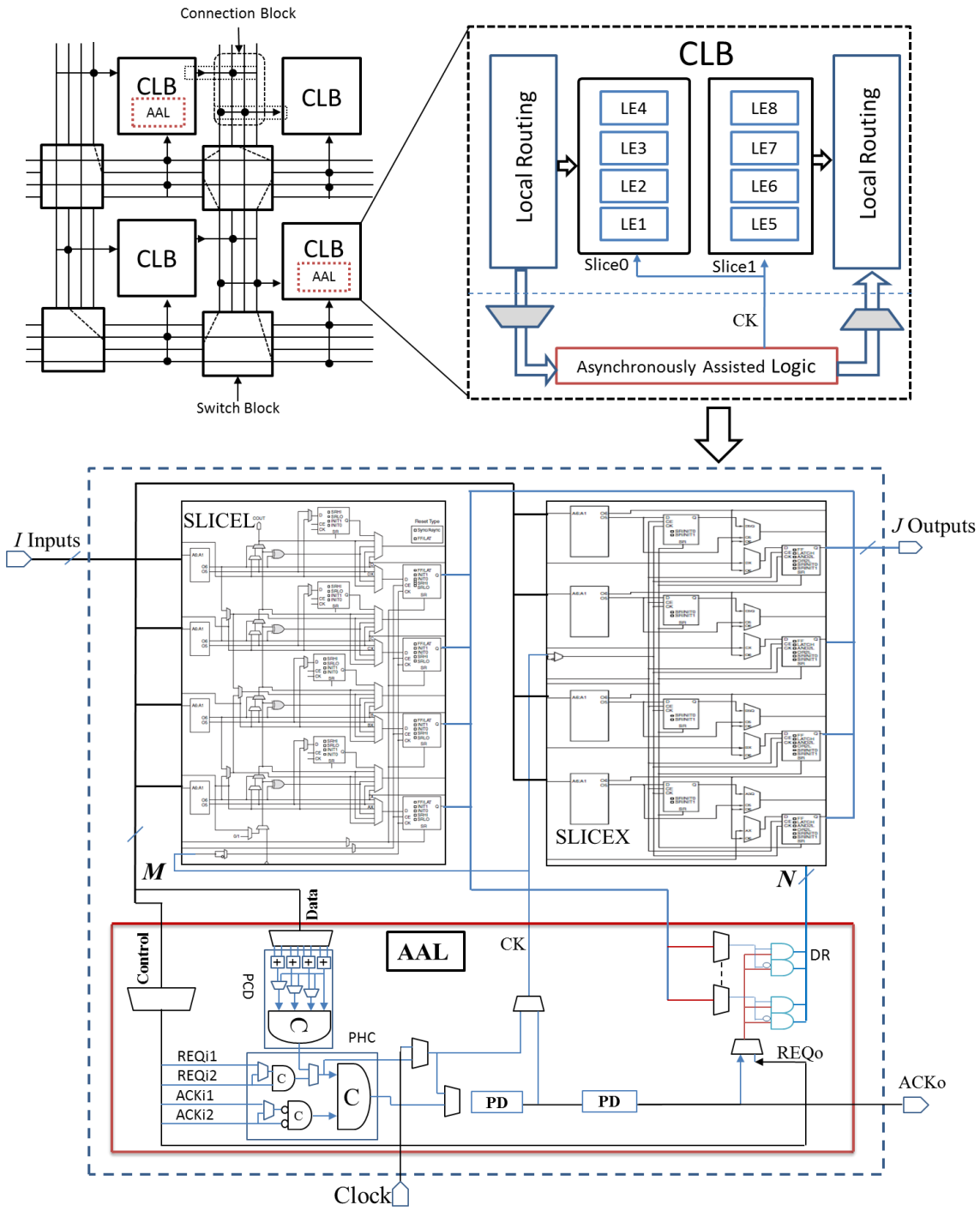

Appendix C: Input Vector for Candence

Input Stimulus “Vector” file sample (Configure LUT as Adder)

```
; PLE cd stimuli
; INPUT & DBUS Use BIG_ENDIAN system (LS byte first 0|1|2|3)
; Address use LITTLE_ENDIAN (MSB fist 3|2|1|0)


Radix 1     1     4444  1     4     1     2     2     2
Io    i     I     iiii  I     I     i     I     I     o
vname start WE DBUS<[15:0]> Sel PCD<[3:0]>  SW PD1<[1:0]> PD2<[1:0]>
sum<[1:0]>


tunit ns
trise 0.1
tfall 0.1
vih 1
vil 0
vol 0
voh 1


;time       start WE    DBUS  Sel   PCD   SW    PD1   PD2   sum
    0       0     0     0000  0     0     0     0     0     0;
   10       0     1     6996  0     0     0     x     x     x; Adder
   20       0     0     6996  0     0     0     x     x     x;
   40       0     0     xxxx  0     0     0     0     0     0; Spacer
   60       1     0     xxxx  1     F     1     2     2     x;
  160       0     0     xxxx  1     F     1     2     2     x;
  180       1     0     xxxx  1     F     1     2     2     x;
```

Appendix D: Sawtooth Vdd Generation

Sawtooth Vdd Input Stimulus File Generation in MATLAB Representing Energy Harvesting Switching Capacitors Supply Sources

```
fid = fopen('sawtooth-pwl.txt','w'); %Create a new txt file

A=0.2;
t = 0:0.0005:1;
x=A*sawtooth(2*pi*40*t,0.25)+0.8; %40 Hertz wave with duty cycle 25%

fprintf(fid,'%1.4fe-3 ',t);
fprintf(fid,'%1.4f\n',x);

plot(t,x);
grid

fclose(fid);
```

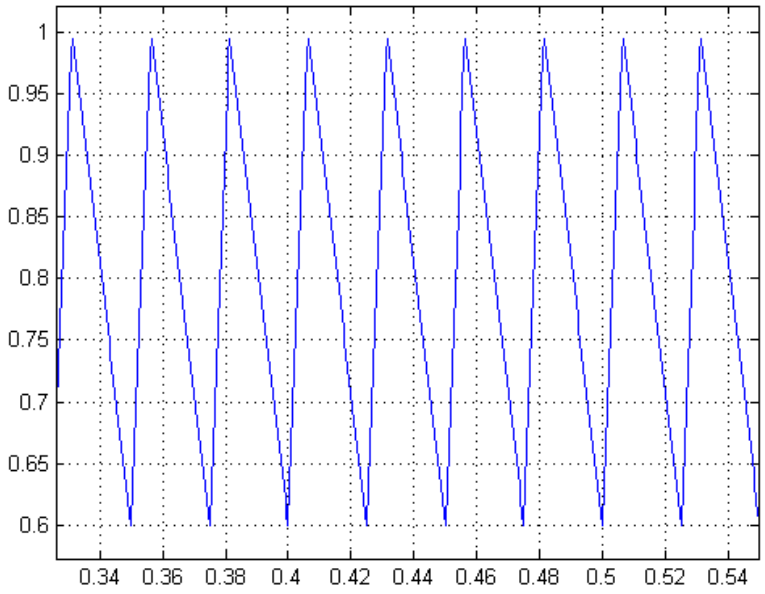

Appendix E: Variation Map Generation

Variation Map Generation in MATLAB

```
%Run in Matlab SimulationTime and TimeIncrement are in
%nanoseconds Mean and StDev of Guassian distribution is in V Nominal
%voltage is in V
% Example m file run code >> VariationMap(0.9, 0.4);

function out = VariationMap(Mean, StDev)

times = zeros(1,201);
xs = zeros(1,201);
for i=0:1:200
time=i;
x=randn(1)*StDev + Mean;
y=randn(1)*StDev + Mean;
z= randn(1);
times(i+1)=time;
xs(i+1)=x;
end

subplot(2,1,1)
plot(times,xs)
subplot(2,1,2)
hist(xs,20)
[X,Y,Z] = peaks(25);
surf(X,Y,Z);
out=1;
end
```

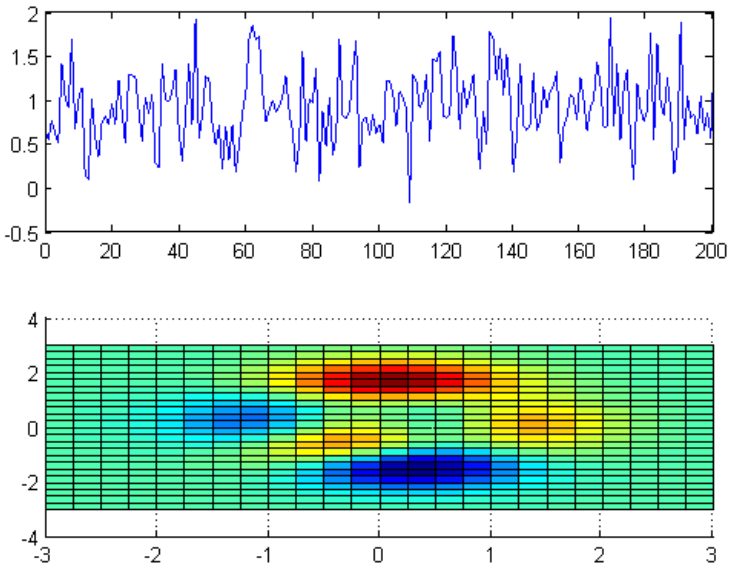

Bibliography

[1] R. Aitken, "Predictive technology for advanced node design exploration," in *Designing with Uncertainty - Opportunities & Challenges, Workshop Invited Speacker*, 2014.

[2] J. M. Levine, E. Stott, and P. Y. K. Cheung, "Dynamic voltage and frequency scaling with online slack measurement," in *Field-Programmable Gate Arrays ACM/SIGDA International Symposium*, Monterey, California, USA, 2014, pp. 109-116.

[3] P. Sedcole and P. Y. K. Cheung, "Within-die delay variability in 90nm FPGAs and beyond," in *International Conference Field Programmable Technology (ICFPT)* 2006, pp. 97-104.

[4] P. Cheung, "Beyond the age of clones," UK Design Forum (UKDF) Workshops 2013.

[5] P. Cheung and P. Sedcole, "Variability & FPGAs - Disaster or Opportunities?," Design, Automation & Test (DATE) Workshop Patent, 2008.

[6] R. Manohar, "Reconfigurable asynchronous logic," in *Custom Integrated Circuits Conference (CICC)*, 2006, pp. 13-20.

[7] K.-L. Chang, J. S. Chang, B.-H. Gwee, and K.-S. Chong, "Synchronous-logic and asynchronous-logic 8051 microcontroller cores for realizing the internet of things: a comparative study on dynamic voltage scaling and variation effects," *IEEE Journal Emerging and Selected Topics in Circuits and Systems,* vol. 3, pp. 23-34, 2013.

[8] M. Jelodari and J. D. Garside, "High level synthesis of GALS systems," in *Designing with Uncertainty - Opportunities & Challenges Workshop* vol. 2014, ed, 2014.

[9] I. Kuon, R. Tessier, and J. Rose, "FPGA Architecture: Survey and Challenges," *Found. Trends Electron. Des. Autom.,* vol. 2, pp. 135-253, 2008.

[10] N. J. Rochelle, "Monolithic Memories announces: a revolution in logic design: Introductory advertisement on PAL (Programmable Array Logic)," 1978.

[11] G. E. Moore, "Cramming more components onto integrated circuits," *Proceedings of the IEEE,* vol. 86, pp. 82-85, 1998.

[12] *Microsemi Antifuse FPGAs*. Available: http://www.microsemi.com/products/fpga-soc/antifuse-fpgas

[13] D. Zacher. Using prescision to design Rad-hard Actel devices [Online]. Available: http://www.pldworld.com/_hdl/2/resources/leo2precision/html/pdfs/actel_rad.pdf

[14] T. R. Kuphaldt, *Lesson In Eletric Circuits* vol. IV-Digital Chapter 16 Principle of Digital Computing, 200-2008.

[15] I. Kuon and J. Rose, "Measuring the gap between FPGAs and ASICs," *IEEE Transactions on Computer-Aided Design of Integrated Circuits and Systems,* vol. 26, pp. 203-215, 2007.
[16] H. Parandeh-Afshar and P. Ienne, "Measuring and reducing the performance gap between embedded and soft multipliers on FPGAs," in *International Conference on Field Programmable Logic and Applications (FPL)*, 2011, pp. 225-231.
[17] *FPGA vs. ASIC*. Available: http://www.xilinx.com/fpga/asic.htm
[18] P. Wilson, *Design recipes for FPGAs*: Newnes, 2007.
[19] S. Borkar, T. Karnik, S. Narendra, J. Tschanz, A. Keshavarzi, and V. De, "Parameter variations and impact on circuits and microarchitecture," in *40th Annual Design Automation Conference*, Anaheim, CA, USA, 2003, pp. 338-342.
[20] A. Bansal and R. M. Rao, "Variations: Sourcecs and characterization," in *Low-Power Variation-Tolerant Design in Nanometer Silicon*, Swarup. Bhunia and Siabal. Mukhopadhyay, Eds., ed: Springer, 2011.
[21] A. Asenov, S. Kaya, and A. R. Brown, "Intrinsic parameter fluctuations in decananometer MOSFETs introduced by gate line edge roughness," *IEEE Transactions on Electron Devices,* vol. 50, pp. 1254-1260, 2003.
[22] S. Ghosh and K. Roy, "Parameter variation tolerance and error resiliency: New design paradigm for the nanoscale Era," *Proceedings of the IEEE,* vol. 98, pp. 1718-1751, 2010.
[23] S. Bhunia and S. Mukhopadhyay, *Low-Power Variation-Tolerant Design in Nanometer Silicon*: Springer, 2011.
[24] J. A. Walker, M. A. Trefzer, S. J. Bale, and A. M. Tyrrell, "PAnDA: A reconfigurable architecture that adapts to physical substrate variations," *IEEE Transactions on Computers,* vol. 62, pp. 1584-1596, 2013.
[25] S. K. Saha, "Modeling process variability in scaled CMOS technology," *IEEE Design & Test of Computers,* vol. 27, pp. 8-16, 2010.
[26] A. Asenov, "Random dopant induced threshold voltage lowering and fluctuations in sub-0.1um MOSFET's: A 3-D "atomistic" simulation study," *Electron Devices, IEEE Transactions,* vol. 45, pp. 2505-2513, 1998.
[27] M. Ruben. (2012). *How to close timing with hundreds of multi-mode/multi-corner views*. Available: http://www.eejournal.com/archives/articles/20121206-cadence/
[28] S. Herbert and D. Marculescu, "Variation-aware dynamic voltage/frequency scaling," in *IEEE 15th International Symposium on High Performance Computer Architecture (HPCA)*, 2009, pp. 301-312.
[29] M. Wirnshofer, *Variation-aware adaptive voltage scaling for digital CMOS circuits*: Springer Dordrecht Heidelberg New York London, 2013.
[30] A. Nahapetian, P. Lombardo, A. Acquaviva, L. Benini, and M. Sarrafzadeh, "Dynamic reconfiguration in sensor networks with regenerative energy sources," in *Design, Automation & Test in Europe Conference & Exhibition (DATE)*, 2007, pp. 1-6.
[31] *ARVENI*. Available: http://www.arveni.fr/en/

[32] A. Yakovlev. Energy-modulated computing [Online]. Available: http://async.org.uk/tech-reports/NCL-EECE-MSD-TR-2010-167.pdf

[33] X. Zhang, D. Shang, F. Xia, H. S. Low, and A. Yakovlev, "A hybrid power delivery method for asynchronous loads in energy harvesting systems," in *IEEE 10th International New Circuits and Systems Conference (NEWCAS)*, 2012, pp. 413-416.

[34] F. Xia, A. Mokhov, A. Yakovlev, A. Iliasov, A. Rafiev, and A. Romanovsky, "Adaptive resource control in multi-core systems," Newcastle University NCL-EEE-MICRO-TR-2013-183, 2013.

[35] A. Mokhov, D. Sokolov, and A. Yakovlev, "Adapting Asynchronous Circuits to Operating Conditions by Logic Parametrisation," in *Asynchronous Circuits and Systems (ASYNC), 2012 18th IEEE International Symposium on*, 2012, pp. 17-24.

[36] F. Xia, A. Mokhov, Y. Zhou, Y. Chen, I. Mitrani, D. Shang*, et al.*, "Towards power-elastic systems through concurrency management," *Computers & Digital Techniques, IET,* vol. 6, pp. 33-42, 2012.

[37] A. Mokhov, M. Rykunov, D. Sokolov, and A. Yakovlev, "Design of Processors with Reconfigurable Microarchitecture," *Low Power Electronics and Applications,* pp. 26-43, 2014.

[38] M. Rykunov, "Design of asynchronous microprocessor for power proportionality," PhD, School of Electrical and Electronic Engineering, Newcastle University, 2014.

[39] T. Mizuno, J. Okumtura, and A. Toriumi, "Experimental study of threshold voltage fluctuation due to statistical variation of channel dopant number in MOSFET's," *Electron Devices, IEEE Transactions,* vol. 41, pp. 2216-2221, 1994.

[40] K. Agarwal, F. Liu, C. McDowell, S. Nassif, K. Nowka, M. Palmer*, et al.*, "A test structure for characterizing local device mismatches," in *Symposium on VLSI Circuits, Digest of Technical Papers*, 2006, pp. 67-68.

[41] F. Stellari, P. Song, A. J. Weger, and D. L. Miles, "Mapping systematic and random process variations using Light emission from Off-State Leakage," in *IEEE International Reliability Physics Symposium* 2009, pp. 640-649.

[42] A. N. Nowroz and S. Reda, "Thermal and power characterization of field-programmable gate arrays," in *Proceedings of the 19th ACM/SIGDA international symposium on Field programmable gate arrays*, Monterey, CA, USA, 2011, pp. 111-114.

[43] M. Bhushan, M. B. Ketchen, S. Polonsky, and A. Gattiker, "Ring oscillator based technique for measuring variability statistics," in *IEEE International Conference on Microelectronic Test Structures (ICMTS)*, 2006, pp. 87-92.

[44] I. A. K. M. Mahfuzul, A. Tsuchiya, K. Kobayashi, and H. Onodera, "Variation-sensitive monitor circuits for estimation of Die-to-Die process variation," in *IEEE International Conference on Microelectronic Test Structures (ICMTS)*, 2011, pp. 153-157.

[45] K. M. Zick and J. P. Hayes, "On-line sensing for healthier FPGA systems," in *Proceedings of the 18th Annual ACM/SIGDA International Symposium*

on Field Programmable Gate Arrays, Monterey, California, USA, 2010, pp. 239-248

[46] W. Xiaoxiao, M. Tehranipoor, and R. Datta, "Path-RO: A novel on-chip critical path delay measurement under process variations," in *IEEE/ACM International Conference on Computer-Aided Design (ICCAD)* 2008, pp. 640-646.

[47] S. Lopez-Buedo, J. Garrido, and E. Boemo, "Thermal testing on programmable logic devices," in *IEEE International Symposium on Circuits and Systems (ISCAS)*, 1998, pp. 240-243 vol.2.

[48] N. Dahir, G. Tarawneh, T. Mak, R. Al-Dujaily, and A. Yakovlev, "Design and implementation of dynamic thermal-adaptive routing strategy for networks-on-chip," in *22nd Euromicro International Conference on Parallel, Distributed and Network-Based Processing (PDP)*, 2014, pp. 384-391.

[49] G. Tarawneh, T. Mak, and A. Yakovlev, "Intra-chip physical parameter sensor for FPGAS using flip-flop metastability," in *International Conference on Field Programmable Logic and Applications (FPL)*, 2012, pp. 373-379.

[50] P. Y. K. Cheung. On-silicon instrumentation - An approach to alleviate the variability problem [Online]. Available: http://www.panda.ac.uk/workshop/

[51] S. Mukhopadhyay, K. Keunwoo, K. A. Jenkins, C. Ching-Te, and K. Roy, "An On-Chip test structure and digital measurement method for statistical characterization of local random variability in a process," *IEEE Journal of Solid-State Circuits,* vol. 43, pp. 1951-1963, 2008.

[52] R. Rao, K. A. Jenkins, and J.-J. Kim, "A completely digital on-chip circuit for local-random-variability measurement," in *IEEE International Solid-State Circuits Conference (ISSCC), Digest of Technical Papers*, 2008, pp. 412-623.

[53] R. Rao, K. A. Jenkins, and J.-J. Kim, "A local random variability detector with complete digital On-Chip measurement circuitry," *IEEE Journal of Solid-State Circuits,* vol. 44, pp. 2616-2623, 2009.

[54] S. Lopez-Buedo, J. Garrido, and E. Boemo, "Thermal testing on reconfigurable computers," *IEEE Design & Test of Computers,* vol. 17, pp. 84-91, 2000.

[55] Haile. Yu, Qiang. Xu, and P. H. W. Leong, "Fine-grained characterization of process variation in FPGAs," in *International Conference on Field-Programmable Technology (FPT)*, 2010, pp. 138-145.

[56] E. Stott, A, J. S. J. Wong, P. Sedcole, and P. Y. K. Cheung, "Degradation in FPGAs: measurement and modelling," in *Proceedings of the 18th Annual ACM/SIGDA International Symposium on Field Programmable Gate Arrays*, Monterey, California, USA, 2010, pp. 229-238

[57] S. Reda, R. J. Cochran, and A. N. Nowroz, "Improved thermal tracking for processors using hard and soft sensor allocation techniques," *IEEE Transactions on Computers,* vol. 60, pp. 841-851, 2011.

[58] J. S. J. Wong, P. Sedcole, and P. Y. K. Cheung, "Self-Measurement of combinatorial circuit delays in FPGAs," *ACM Trans. Reconfigurable Technol. Syst.,* vol. 2, pp. 1-22, 2009.

[59] J. S. J. Wong and P. Y. K. Cheung, "Improved delay measurement method in FPGA based on transition probability," in *Proceedings of the 19th ACM/SIGDA international symposium on Field programmable gate arrays*, Monterey, CA, USA, 2011, pp. 163-172

[60] J. S. J. Wong and P. Y. K. Cheung, "Timing measurement platform for arbitrary black-box circuits based on transition probability," *IEEE Transactions on Very Large Scale Integration (VLSI) Systems,* vol. 21, pp. 2307-2320, 2013.

[61] N. Mehta and A. DeHon, "Variation and aging tolerance in FPGAs," in *Low-Power Variation-Tolerant Design in Nanometer Silicon*, S. Bhunia and S. Mukhopadhyay, Eds., ed: Springer US, 2011, pp. 365-380.

[62] Ho-Yan. Wong, Lerong. Cheng, Yan. Lin, and Lei. He, "FPGA device and architecture evaluation considering process variations," in *IEEE/ACM International Conference on Computer-Aided Design (ICCAD)* 2005, pp. 19-24.

[63] J. S. J. Wong, P. Sedcole, and P. Y. K. Cheung, "A transition probability based delay measurement method for arbitrary circuits on FPGAs," in *ICECE Technology, 2008. FPT 2008. International Conference on*, 2008, pp. 105-112.

[64] I. Kuon and J. Rose, "Automated transistor sizing for FPGA architecture exploration," in *45th ACM/IEEE Design Automation Conference (DAC)*, 2008, pp. 792-795.

[65] J. Sparsø and S. Furber, *Principles of asynchronous circuit design*, 1st ed.: Springer, 2002.

[66] A. J. Martin, "Compiling communicating processes into delay-insensitive VLSI circuits," *Distributed Computing,* vol. 1, pp. 226-234, 1986/12/01 1986.

[67] T.-A. Chu, "Synthesis of self-timed VLSI circuits from graph-theoretic specifications," PhD, Massachusetts Institute of Technology. Dept. of Electrical Engineering and Computer Science., Massachusetts Institute of Technology, 1987.

[68] D. Shang, F. Xia, and A. Yakovlev, "Asynchronous FPGA architecture with distributed control " in *IEEE International Symposium Proceedings of Circuits and Systems*, 2010, pp. 1436-1439.

[69] H. S. Low, D. Shang, F. Xia, and A. Yakovlev, "Variation tolerant AFPGA architecture," presented at the 17th IEEE International Symposium Asynchronous Circuits and Systems, Ithaca, NY, 2011.

[70] P. Sedcole and P. Y. K. Cheung, "Parametric yield in FPGAs due to within-die delay variations: a quantitative analysis," in *Proceedings of the 2007 ACM/SIGDA 15th international symposium on Field programmable gate arrays*, Monterey, California, USA, 2007.

[71] M. Yohei, H. Masakazu, K. Takashi, T. Toshiyuki, N. Tadashi, S. Toshihiro*, et al.*, "Performance and yield enhancement of FPGAs with within-die variation using multiple configurations," in *Proceedings of the 2007 ACM/SIGDA 15th international symposium on Field programmable gate arrays*, Monterey, California, USA, 2007.

[72] L. Cheng, J. Xiong, L. He, and M. Hutton, "FPGA performance optimization via chipwise placement considering process variations," in *International Conference on Field Programmable Logic and Applications (FPL)*, 2006, pp. 1-6.

[73] Y. Lin, M. Hutton, and L. He, "Placement and timing for FPGAs considering variations," in *International Conference on Field Programmable Logic and Applications (FPL)*, 2006, pp. 1-7.

[74] Y. Lin, L. He, and M. Hutton, "Stochastic physical synthesis considering prerouting interconnect uncertainty and process variation for FPGAs," *IEEE Transactions on Very Large Scale Integration (VLSI) Systems,* vol. 16, pp. 124-133, 2008.

[75] A. Kumar and M. Anis, "FPGA design for timing yield under process variations," *IEEE Transactions on Very Large Scale Integration (VLSI) Systems,* vol. 18, pp. 423-435, 2010.

[76] S. Sivaswamy and K. Bazargan, "Statistical analysis and process variation-aware routing and skew assignment for FPGAs," *ACM Transactions on Reconfigurable Technology System,* vol. 1, pp. 1-35, 2008.

[77] P. Sedcole and P. Y. K. Cheung, "Parametric yield modeling and simulations of FPGA circuits considering within-die delay variations," *ACM Transactions on Reconfigurable Technology System,* vol. 1, pp. 1-28, 2008.

[78] V. Betz, J. Rose, and A. Marquardt, *Architecture and CAD for deep-submicron FPGAs*. Boston: Kluwer Academic, 1999.

[79] E. Stott and P. Y. K. Cheung, "Improving FPGA reliability with wear-levelling," in *International Conference on Field Programmable Logic and Applications (FPL)*, 2011, pp. 323-328.

[80] S. Srinivasan, P. Mangalagiri, Y. Xie, N. Vijaykrishnan, and K. Sarpatwari, "FLAW: FPGA lifetime awareness," in *43rd Annual Design Automation Conference*, San Francisco, CA, USA, 2006, pp. 115-127.

[81] P. Sedcole, E. Stott, and P. Y. K. Cheung, "Compensating for variability in FPGAs by re-mapping and re-placement," in *International Conference on Field Programmable Logic and Applications (FPL)*, 2009, pp. 613-616.

[82] M. Ashouei, J. Hulzink, M. Konijnenburg, Z. Jun, F. Duarte, A. Breeschoten*, et al.*, "A voltage-scalable biomedical signal processor running ECG using 13pJ/cycle at 1MHz and 0.4V," in *IEEE International Solid-State Circuits Conference Digest of Technical Papers (ISSCC)*, 2011, pp. 332-334.

[83] J. Sparsø and S. Furber, *Principles of asynchronous circuit design - A systems perspective*: Kluwer Academic Publishers, 2001.

[84] T. Verhoeff, "Delay-insensitive codes - an overview," *Distributed Computing,* vol. 3, pp. 1-8, 1988/03/01 1988.

[85] T. Beyrouthy, A. Razafindraibe, L. Fesquet, M. Renaudin, S. Chaudhuri, S. Guilley*, et al.*, "A novel asynchronous e-FPGA architecture for security applications," in *International Conference on Field-Programmable Technology (ICFPT)* 2007, pp. 369-372.

[86] S. Hauck, "Asynchronous design methodologies: An overview," in *Proceedings of the IEEE*, 1995, pp. 69-93.

[87] J. M. Alain, "The limitations to delay-insensitivity in asynchronous circuits," presented at the Proceedings of the sixth MIT Conference on Advanced Research in VLSI, Boston, Massachusetts, USA, 1990.
[88] A. Martin, J. , "Compiling communicating processes into delay-insensitive VLSI circuits," California Institute of Technology, 1986.
[89] M. B. Josephs, S. M. Nowick, and C. H. Van Berkel, "Modeling and design of asynchronous circuits," *Proceedings of the IEEE,* vol. 87, pp. 234-242, 1999.
[90] S. Hauck, S. Burns, G. Borriello, and C. Ebeling, "An FPGA for implementing asynchronous circuits," *IEEE Design & Test of Computers,* vol. 11, p. 60, 1994.
[91] K. Maheswaran, *Implementing self-timed circuits in field programmable gate arrays*: University of California Davis, 1995.
[92] R. Payne, *Asynchronous FPGA architectures* vol. 143, 1996.
[93] D. H. Linder and J. C. Harden, "Phased Logic: supporting the synchronous design paradigm with delay-insensitive circuitry," *IEEE Transactions on Computers,* vol. 45, pp. 1031-1044, 1996.
[94] J. Teifel and R. Manohar, "Programmable asynchronous pipeline arrays," in *Proceedings of International Conference on Field Programmable Logic and Applications*, 2003.
[95] J. Teifel and R. Manohar, "An asynchronous dataflow FPGA architecture," *IEEE Transactions on Computers,* vol. 53, pp. 1376-1392, 2004.
[96] J. Teifel and R. Manohar, "Highly pipelined asynchronous FPGAs," in *Proceedings of the ACM/SIGDA 12th International Symposium on Field programmable Gate Arrays*, Monterey, California, USA, 2004.
[97] S. Peng, D. Fang, J. Teifel, and R. Manohar, "Automated synthesis for asynchronous FPGAs," presented at the Proceedings of the ACM/SIGDA 13th international symposium on Field-Programmable Gate Arrays, Monterey, California, USA, 2005.
[98] J. Teifel and R. Manohar, "Programmable asynchronous pipeline arrays," US Patent, 2007.
[99] A. Royal and P. Cheung, "Globally asynchronous locally synchronous FPGA architectures," in *Field-Programmable Logic and Applications*. vol. 2778, ed: Springer Berlin / Heidelberg, 2003, pp. 355-364.
[100] C. G. Wong, A. J. Martin, and P. Thomas, "An architecture for asynchronous FPGAs," in *Proceedings of IEEE International Conference on Field-Programmable Technology (FPT)*, 2003, pp. 170-177.
[101] X. Jia and R. Vemuri, "A novel asynchronous FPGA architecture design and its performance evaluation," in *International Conference on Field Programmable Logic and Applications*, 2005, pp. 287-292.
[102] X. Jia and R. Vemuri, "CAD tools for a globally asynchronous locally synchronous FPGA architecture," presented at the 19th International Conference on VLSI Design, Held jointly with 5th International Conference on Embedded Systems and Design 2006.
[103] K. M. Fant and S. A. Brandt, "NULL Convention Logic: a complete and consistent logic for asynchronous digital circuit synthesis," in *Proceedings*

of International Conference on Application Specific Systems, Architectures and Processors (ASAP) 1996, pp. 261-273.

[104] M. Mishra, T. J. Callahan, T. Chelcea, G. Venkataramani, S. C. Goldstein, and M. Budiu, "Tartan: Evaluating spatial computation for whole program execution," *SIGPLAN Not.,* vol. 41, pp. 163-174, 2006.

[105] M. Mishra and S. C. Goldstein, "Virtualization on the tartan reconfigurable architecture," in *International Conference on Field Programmable Logic and Applications (FPL)*, 2007, pp. 323-330.

[106] *Achronix Semiconductor Corporation*. Available: http://www.achronix.com/

[107] R. Payne, "Self-timed FPGA systems," in *Field-programmable logic and applications*. vol. 975, W. Moore and W. Luk, Eds., ed: Springer Berlin Heidelberg, 1995, pp. 21-35.

[108] I. E. Sutherland. (1989) Micropipelines. *Communications of the ACM*. 720-738.

[109] R. Manohar and C. W. Kelly, "Reconfigurable logic fabrics for integrated circuits and systems and methods for configuring reconfigurable logic fabrics," 2013.

[110] V. Ekanayake, C. W. Kelly, and R. Manohar, "Programmable crossbar structures in asynchronous systems," ed: Google Patents, 2012.

[111] R. Manohar, G. Martin, and J. L. Holt, "Synchronous to asynchronous logic conversion," ed: Google Patents, 2012.

[112] K. Morris, "Fast. very, very fast. Achronix introduces Speedster," *Electronic Engineering Journal,* September 16, 2008 2008.

[113] E. D. Mark, E. W. Ted, and L. D. David, "Efficient self-timing with level-encoded 2-phase dual-rail (LEDR)," in *Proceedings of the 1991 University of California/Santa Cruz conference on Advanced research in VLSI*, 1991.

[114] M. Aydin and C. Traver, "Implementation of a programmable phased logic cell [FPGA]," presented at the 45th Midwest Symposium on Circuits and Systems (MWSCAS) 2002.

[115] R. B. Reese, M. A. Thornton, and C. Traver, "A fine-grain Phased Logic CPU," in *Proceedings of IEEE Computer Society Annual Symposium on VLSI*, 2003, pp. 70-79.

[116] C. Traver, R. B. Reese, and M. A. Thornton, "Cell designs for self-timed FPGAs," in *Proceedings of 14th Annual IEEE International ASIC/SOC Conference*, 2001, pp. 175-179.

[117] A. Mitra, W. F. McLaughlin, and S. M. Nowick, "Efficient asynchronous protocol converters for two-phase delay-insensitive global communication," presented at the 13th IEEE International Symposium on Asynchronous Circuits and Systems (ASYNC), 2007.

[118] Y. Komatsu, S. Ishihara, M. Hariyama, and M. Kameyama, "An implementation of an asychronous FPGA based on LEDR/four-phase-dual-rail hybrid architecture," presented at the 16th Asia and South PacificDesign Automation Conference (ASP-DAC), 2011.

[119] C. LaFrieda, B. Hill, and R. Manohar, "An asynchronous FPGA with two-phase enable-scaled routing," presented at the IEEE Symposium on Asynchronous Circuits and Systems (ASYNC), 2010.

[120] R. B. Reese, M. A. Thornton, and C. Traver, "A coarse-grain phased logic CPU," *IEEE Transactions on Computers,* vol. 54, pp. 788-799, 2005.
[121] D. M. Chapiro, "Globally-asynchronous locally-synchronous systems (performance, reliability, digital)," Stanford University, 1985.
[122] S. W. Moore, G. S. Taylor, P. A. Cunningham, R. D. Mullins, and P. Robinson, "Self calibrating clocks for globally asynchronous locally synchronous systems," in *Proceedings International Conference on Computer Design*, 2000, pp. 73-78.
[123] A. Sheibanyrad, A. Greiner, and I. Miro-Panades, "Multisynchronous and fully asynchronous NoCs for GALS architectures," *IEEE Design & Test of Computers,* vol. 25, pp. 572-580, 2008.
[124] M. N. Horak, S. M. Nowick, M. Carlberg, and U. Vishkin, "A low-overhead asynchronous interconnection network for GALS chip multiprocessors," *IEEE Transactions on Computer-Aided Design of Integrated Circuits and Systems,* vol. 30, pp. 494-507, 2011.
[125] A. Yakovlev, P. Vivet, and M. Renaudin, "Advances in asynchronous logic: From principles to GALS & NoC, recent industry applications, and commercial CAD tools," in *Design, Automation & Test in Europe Conference & Exhibition (DATE)*, 2013, pp. 1715-1724.
[126] *Theseuse research - NULL Convention Logic*. Available: http://www.theseusresearch.com/
[127] S. C. Smith, "Design of an FPGA Logic Element for Implementing Asynchronous NULL Convention Logic Circuits," *IEEE Transactions on Very Large Scale Integration (VLSI) Systems,* vol. 15, pp. 672-683, 2007.
[128] I. P. Dugganapally, W. K. Al-Assadi, V. Pillai, and S. Smith, "Design and implementation of FPGA configuration logic block using asynchronous semi-static NCL circuits," presented at the IEEE Region 5 Conference 2008.
[129] N. Huot, H. Dubreuil, L. Fesquet, and M. Renaudin, "FPGA architecture for multi-style asynchronous logic," in *Proceedings of Design, Automation and Test in Europe (DATE)*, 2005, pp. 32-33 Vol. 1.
[130] T. Beyrouthy and L. Fesquet, "An asynchronous FPGA block with its tech-mapping algorithm dedicated to security applications," *International Journal of Reconfigurable Computing,* vol. 2013, p. 12, 2013.
[131] R. David, "Modular design of asynchronous circuits defined by graphs," *IEEE Transactions on Computers,* vol. C-26, pp. 727-737, 1977.
[132] J. Rose, A. El Gamal, and A. Sangiovanni-Vincentelli, "Architecture of field-programmable gate arrays," *Proceedings of the IEEE,* vol. 81, pp. 1013-1029, 1993.
[133] V. Betz and J. Rose, "How much logic should go in an FPGA logic block," *IEEE Design & Test of Computers* vol. 15, pp. 10-15, 1998.
[134] V. Betz, J. Rose, and A. Marquardt, *Architecture and CAD for deep-submicron FPGAs*: Kluwer Academic Publishers, 1999.
[135] D. Shang, "Asynchronous communication circuits: Design, test, and synthesis.," PhD Thesis, University of Newcastle upon Tyne, 2003.

[136] E. Ahmed and J. Rose, "The effect of LUT and cluster size on deep-submicron FPGA performance and density," *IEEE Transactions of Very Large Scale Integrated (VLSI) System,* vol. 12, pp. 288-298, 2004.
[137] T. Behne. (2003). *FPGA Clock Schemes*. Available: http://www.design-reuse.com/articles/4854/fpga-clock-schemes.html
[138] *XILINX Spartan-3 FPGA Family Data sheet. available online.* Available: http://www.xilinx.com/support/documentation/data_sheets/ds099.pdf
[139] S. Borkar, T. Karnik, S. Narendra, J. Tschanz, A. Keshavarzi, and V. De, "Parameter variations and impact on circuits and microarchitecture," in *Proceedings of Design Automation Conference*, Anaheim, CA, USA, 2003, pp. 338-342.
[140] A. Baz, D. Shang, F. Xia, and A. Yakovlev, "Self-Timed SRAM for energy harvesting Systems," in *Integrated Circuit and System Design. Power and Timing Modeling, Optimization, and Simulation*. vol. 6448, R. Leuken and G. Sicard, Eds., ed: Springer Berlin Heidelberg, 2011, pp. 105-115.
[141] D. Sokolov, "Automated synthesis of asynchronous circuits using direct mapping for control and data paths," PhD Thesis, School od Electrical, Electronic and Computer Engineering, University of Newcastle Upon Tyne, 2006.
[142] A. Bystrov and A. Yakovlev, "Asynchronous circuit synthesis by direct mapping: interfacing to environment," in *Proceedings of Eighth International Symposium Asynchronous Circuits and Systems*, 2002, pp. 127-136.
[143] D. Shang, F. Burns, A. Koelmans, A. Yakovlev, and F. Xia, "Asynchronous system synthesis based on direct mapping using VHDL and Petri nets," in *IEE Proceedings of Computers and Digital Techniques*, 2004, pp. 209-220.
[144] "Spartan-6 FPGA Configurable Logic Block," XILINX, Ed., ed, 2010.
[145] H. S. Low, D. Shang, F. Xia, and A. Yakovlev, "Asynchronously assited FPGA for variability," in *Field Programmable Logic and Applications* Munich, Germany, 2014, pp. 1-4.